DRONES FOR CONSERVATION: INTEGRATING UAVS WITH FIELD METHODS TO CLASSIFY SATELLITE IMAGERY TO MAP PLANT COMMUNITIES – A CASE STUDY OF DRENTSCHE AA, THE NETHERLANDS

RHEA SINGH CHIB

August, 2021

SUPERVISORS:
Dr. P. Nyktas
Dr.ir. W. Bijker

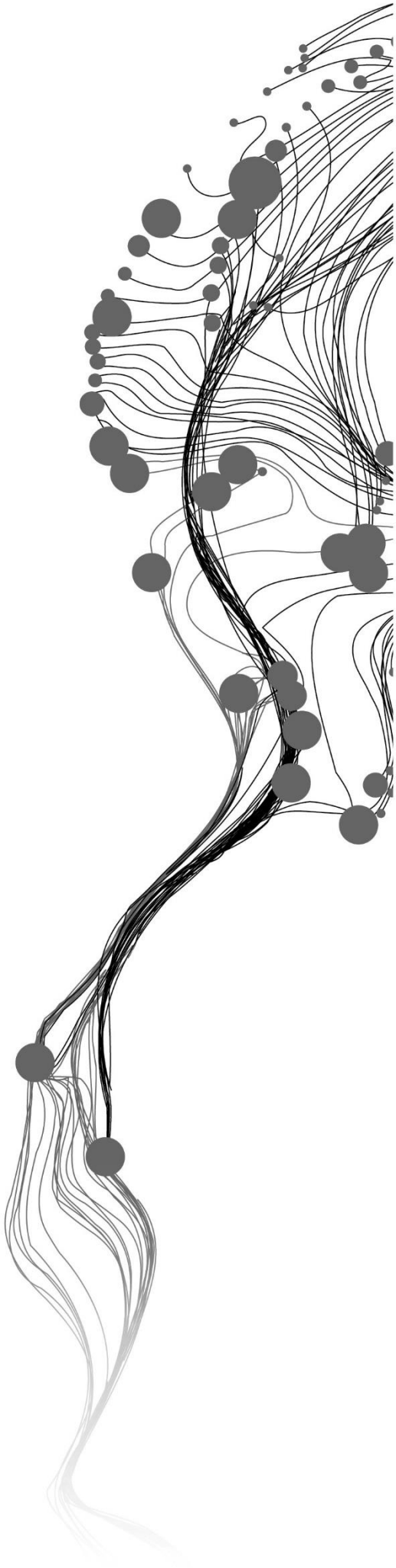

DRONES FOR CONSERVATION: INTEGRATING UAVS WITH FIELD METHODS TO CLASSIFY SATELLITE IMAGERY TO MAP PLANT COMMUNITIES – A CASE STUDY OF DRENTSCHE AA, THE NETHERLANDS

RHEA SINGH CHIB

Enschede, The Netherlands, August, 2021

Thesis submitted to the Faculty of Geo-Information Science and Earth Observation of the University of Twente in partial fulfilment of the requirements for the degree of Master of Science in Geo-information Science and Earth Observation.
Specialization: Geoinformatics (GFM)

SUPERVISORS:
Dr. P. Nyktas
Dr.ir. W. Bijker

THESIS ASSESSMENT BOARD:
Dr.ir. T.A. Groen (Chair)
Dr.ir. C.A. Mücher (External Examiner, Wageningen University & Research, The Netherlands)

ABSTRACT

Plant Communities are the rudimentary unit of natural habitats and have high ecological importance. With the increasing rate of biodiversity loss, vulnerable plant communities and associated species are at higher risk. Hence, mapping their extent becomes important to assess the conservation status of an area. The traditional method of ground survey is the most precise, but laborious and expensive, restricting it to smaller areas. On the other hand, satellite imagery can cover larger areas, but the spatial resolution of freely available imageries does not allow detailed mapping. UAVs have several advantages over these methods like very high spatial resolution, being more cost-efficient and allowing flexible data collection, but limitations of lower spatial coverage and restrictive flying regulations. Hence, all these three methods have their advantages and disadvantages but integrating them could result in a promising approach to precisely map plant communities. This study proposes a method to integrate UAVs with ground surveys to improve the classification results of the satellite imagery. It aims to combine the benefits of high spatial resolution of the UAV imagery with the high spatial coverage of satellite imagery, to produce detailed maps on a larger scale. The National Park of Drentsche Aa, the Netherlands is used as a case study area to test this approach. The results show that OBIA efficaciously classifies the UAV imagery and produces detailed maps, with an accuracy of 87% for the classes of interest i.e., plant communities (different from the overall accuracy). The UAV imagery was then used to create additional samples to train RF to classify the satellite imagery; SuperView-1 and Sentinel-2 were used for the analysis. It produced better results in comparison to using only field samples (64% for Sentinel-2 and 67% for SuperView-1). The results did not have high accuracy as the spatial resolution of the satellite imageries did not allow clear separation of some classes. However, to make the classified maps more comparable to the broader scale of the existing vegetation map, the classes were systematically merged. It resulted in an increase in the accuracy (92% for Sentinel-2 and 93% for SuperView-1), though the level of detail was reduced. Nevertheless, this approach with some further improvements can emerge as a promising technique to precisely map plant communities on a larger scale for conservation.

Keywords: UAVs, Plant Communities, Conservation, Object-Based Image Analysis (OBIA), Random Forest, Sentinel-2, SuperView-1

ACKNOWLEDGEMENTS

The process undertaken to complete this research required sincere and continuous efforts, along with assistance, guidance and motivation from a whole lot of people. Having successfully completed this research, I would like to use this opportunity to thank all, who have directly or indirectly helped me in this journey.

First and foremost, I would like to thank my supervisors, Dr. P. Nyktas and Dr.ir. W. Bijker for their constant guidance, encouragement, supervision and support throughout my research period. I would also like to thank them for making time for the weekly meetings, which not only helped me track my progress but the relentless feedback and discussions helped me improve my work.

I would further like to extend my gratitude to the drone pilots that is my first supervisor, Dr. P. Nyktas and Mr. T.M.R. Roberts for helping me collect the UAV data and Dr. P. Nyktas again for guiding me during the field work and making the necessary arrangements.

I would like to offer my special thanks to the management of the National Park, Drentsche Aa (Staatsbosbeheer) for granting us permission to fly the drone and collect the data. I highly acknowledge and appreciate Mrs. Judith Bosman for organizing it all for us and accompanying us in the field to give a general idea about the area and plant communities present in it.

I would also like to express my gratitude to Drs. P.E. Budde for assisting me with the satellite data and downloading the SuperView-1 imagery for me, Dr. M. Belgiu for her valuable suggestions and guidance with the Random Forest classification, Dr.ir. R.A. de By, my mentor during my first year of study, for his support and encouragement, Drs. J.P.G. Bakx, the specialization coordinator for GFM (Geoinformatics) for encouraging me to pick a topic from another specialization and apply my GFM skills to solve an NRM (Natural Resources Management) problem, and Dr.ir. T.A. Groen, the Chair of the Assessment Board for his insightful comments and suggestions during the proposal defense and the mid-term presentation.

At the same time, I would like to extend my sincere indebtedness to the Faculty of Geo-Information Science and Earth Observation (ITC), for awarding me the ITC Excellence Scholarship and for giving me the opportunity to pursue this course and for providing me with all the resources to complete my studies. I would also like to thank the GFM staff and my colleagues for their help and support and, Student Affairs to ensure I had a comfortable stay.

My deepest gratitude goes to my family and friends for providing me with the emotional and moral support to be able to finish my studies. I am extremely grateful for their unwavering encouragement and belief in me. I would especially like to thank my parents and my brother for encouraging me to follow my dreams and make use of this opportunity to study abroad.

Last but not the least, I would like to thank God for keeping me healthy and giving me the strength to go through these tough times.

TABLE OF CONTENTS

LIST OF FIGURES

LIST OF TABLES

LIST OF ABBREVIATIONS

2D	2-Dimensional
3D	3-Dimensional
ACoI	Accuracy for Classes of Interest
CSV	Comma-Separated Values
ESP	Estimation of Scale Parameter
EVI	Enhanced Vegetation Index
GCP	Ground Control Point
GNDVI	Green Normalized Difference Vegetation Index
GRVI	Green-Red Vegetation Index
GSD	Ground Sampling Distance
H	Hypothesis
MDA	Mean Decrease Accuracy
MDG	Mean Decrease Gini
ML	Machine Learning
MS	Multi-Spectral
MTP	Manuel Tie Point
NDVI	Normalized Difference Vegetation Index
NDWI	Normalized Difference Water Index
NIR	Near-Infrared
OBIA	Object-Based Image Analysis
PA	Producer's Accuracy
RF	Random Forest
RGB	Red Green Blue
RO	Research Objective
RQ	Research Question
SfM	Structure from Motion
spp.	species pluralis
SPU	Service Providing Unit
SVM	Support Vector Machine
UA	User's Accuracy
UAV	Unmanned Aerial Vehicle

1. INTRODUCTION

1.1. Background & Motivation

Plant Communities are an assemblage of plant species growing together within a local area, showing a definite affinity with each other (Kent, 2012). They are the rudimentary unit of natural habitats and provide the structural and functional basis to the ecosystem, which in turn provides the fundamental support to life on earth (Corlett, 2016). With the increasing rate of climate change, half of the world's plant species are at risk of extinction (Román-Palacios & Wiens, 2020). We are in the midst of biodiversity loss and plant conservation is an urgent task. Plant Communities are considered a powerful indicator to assess the conservation status of an area (Rapinel et al., 2019). They are regarded as Service Providing Units (SPUs) which are of high ecological importance (Villoslada et al., 2020). Identifying the extent and location of these communities can give major insights about an area. They can even indicate the soil properties and habitat conditions that influence and get influenced by plant communities (Fischer et al., 2019).

One way to observe the occurrence, distribution and status of plant communities is via mapping. Personnel involved in the field of conservation, especially for mapping plant communities, have traditionally relied on ground surveys, aerial photographs and/or satellite imagery (Koh & Wich, 2012; Tay et al., 2018). These methods have several drawbacks in comparison to what can be accomplished with the current technological advancement. Ground surveys can be significantly expensive, time-consuming, laborious and pragmatically challenging in inaccessible landscapes (Koh & Wich, 2012). Some areas are so large that it is practically not possible to collect data to map the location & extent of all the plant communities (Villoslada et al., 2020). Moreover, ground surveys can also have a direct negative impact on plants, as some habitats are so delicate that they can even be damaged by foot (Rominger & Meyer, 2019). On the other hand, the development in Remote Sensing techniques made it possible to map large areas in a more time and cost-efficient manner, with additional spectral information (Rocchini et al., 2016). However, the spatial resolution of freely available satellite data is still considered coarse to be used for some applications dealing with fine-scale plant species (Manfreda et al., 2018). While using time-series or multi-temporal data to map plant communities based on their phenological behaviour has produced better results than single-date images, it remains challenging for certain landscapes (Rapinel et al., 2020). For instance, grasslands, where species are highly mixed, have a fine-grained pattern and similar phenology, satellite imagery fails to precisely capture their spatial variability, as coarse spatial resolution tends to smoothen the spectral differences between them (Rocchini et al., 2013; Strong et al., 2017). Moreover, for conservation, it is essential to discriminate species at a finer scale with high accuracy. The European Biodiversity Conservation Policy requires the production of detailed maps in which even small-scale plant communities can be distinguished, to precisely monitor the change and conservation status of a protected area (Pesaresi et al., 2020).

This gap due to spatial comparability issues makes it difficult to integrate fine-scaled ground survey data with satellite imagery (Reinke & Jones, 2006). The collection of the ground survey data is often not designed to be

combined with remote sensing data (Rocchini et al., 2013). It creates a problem when the size of the pixel is much bigger than the field sampling units which itself might consist of several species (Rocchini et al., 2010). Therefore, data at a finer spatial scale is required to precisely map plant communities for conservation. Whereas, for very high-resolution satellite imagery, the cost can again be a major barrier (Zweig et al., 2015). Besides, issues like persistent cloud cover can hamper the analysis (Baena et al., 2017).

Of course, there is nothing that can replace good scientists, but drones also referred to as Unmanned Aerial Vehicles (UAVs), have the potential to fill the above-mentioned gap and assist them to easily carry out conservation projects. They can systematically observe natural phenomena at high spatio-temporal resolution and can be coupled with lightweight cameras and multispectral sensors at a lower cost (Assmann et al., 2019). Besides, as they fly at low altitudes they do not have many cloud cover constraints (Sibaruddin et al., 2018). Though rain and strong wind conditions pose some constraints, the flexibility to plan the UAV flight when the weather conditions are suitable is an advantage. In recent years, drones have progressively been used in many aspects of ecosystem management, monitoring and mapping (Rominger & Meyer, 2019). They have successfully demonstrated the potential to produce highly precise vegetation maps, which could differentiate plants at the community level (Kaneko & Nohara, 2014). There has also been an increase in the overall accuracy when UAV imagery was used to classify vegetation on species-level (Manfreda et al., 2018). The level of detail in UAV imagery is so high that even individual plant species can be identified, which makes it comparable to field observations (Baena et al., 2017; Manfreda et al., 2018). Due to this, some recent studies have even proposed using UAVs as an alternative to ground surveys (Kattenborn et al., 2019; Hegarty-Craver et al., 2020).

However, the precision of field methods cannot be completely replicated by drones yet (Zhang et al., 2020). UAV imagery is only restricted to the visible plant communities from an aerial view. Some plant species might be covered under tree canopies or other bigger plants. Moreover, sole reliance on UAVs could result in classification and interpretation problems, as remote pilots might be lacking the basic understanding of the ecosystem and the plant communities present in it, due to a lack of direct interaction with the habitat (Gray et al., 2018). Some species which are so small that differences between them can only be observed by a magnifying glass might never be identified. Therefore, with the current UAV technology, ground surveys cannot be completely eradicated. They still play a vital role to validate and measure the accuracy for both the UAV and Satellite Imagery. The idea should be to minimize the area/extent of the ground survey, to make it as little invasive as possible. This becomes extremely important when the area is sensitive or unsafe to access, where a group of surveyors and scientists trekking through these landscapes would not only be at risk but also could disturb the habitat over time. Therefore, drones have the potential to complement ground surveys, as they offer a relatively risk-free, non-hazardous and reliable monitoring technique to collect ecological data (Jiménez-López & Mulero-Pázmány, 2019). However, this benefit is only restricted to areas having a relatively small extent. Economically drones work best for areas preferably less than 20 hectares (Manfreda et al., 2018). Whereas protected areas usually refer to much larger areas. Moreover, the overly restrictive regulatory framework still limits the application of drones in the field of conservation, despite following guidelines to

minimize its impact on the natural environment. Some authors even argue that it can have disturbance effects on birds and mammals (Jiménez López & Mulero-Pázmány, 2019). Besides, the issue of privacy and safety further restricts the application of drones (Duffy et al., 2018). Therefore, to cover large-protected areas, one still has to rely on satellite imagery as drones cannot compete with it in terms of spatial coverage. Whereas to map fine-scale plant communities satellite imagery has several limitations, as discussed earlier. Hence, all these three methods have their advantages and disadvantages but integrating them could result in a promising approach to precisely map plant communities.

1.2. Problem Statement & Justification

To assess the conservation status of plant communities, it is essential to have accurate detailed maps. Field methods are most precise but are restricted to smaller areas. While satellite imagery can cover larger areas, but the coarser spatial resolution doesn't allow detailed mapping. A method to produce accurate maps on a larger spatial scale is needed. Therefore, this research intends to investigate the potential of UAVs to bridge the gap between field methods and satellite imagery to map plant communities for conservation; by using an approach to integrate UAVs with ground surveys to improve the classification results of the Satellite Imagery.

For this, ground surveys can be conducted in smaller sample areas to obtain the ground truth, instead of intruding the whole area, which can be covered using a drone. When the protected area is too large to be mapped using drones or some regulations might restrict the area it can cover, then drones can be deployed on the smaller sensitive terrains of that area, where it is possible to fly or where signs of disturbances have already been detected using satellite imagery (Jiménez-López & Mulero-Pázmány, 2019). The UAV imagery can then be classified and used to create additional samples to classify the satellite imagery, covering the whole area. Drones have the same bird's eye perspective as the satellite imagery which makes it more comparable and easier to match in terms of spatial scale to collect additional samples. Furthermore, some of the advanced classifiers perform better and produce more stable results with an increase in sample size (Shang et al., 2018). Therefore, these additional samples could help to improve the satellite classification results, making them closer to the field observations. This would not only minimize the invasion of the landscape but also result in reliable data covering a larger area, in a more cost-efficient way. Therefore, the benefits of high spatial resolution in the UAV imagery can be directed towards the satellite imagery with high spatial coverage. This would improve the remote sensing techniques to accurately map plant communities in a way that ground surveys alone can never replicate (Manfreda et al., 2018). Such analysis could be used as a tool to assess the conservation status of an area, which could expose the state of plant communities, which can further serve as a basis for improving adaptive community-based conservation and restoration of an area (Baena et al., 2017). It would help the management to amend the protocols, to ensure the survival of rare or diminishing plant communities. It will further spread more awareness about the need for conservation and the importance plant communities hold. Therefore, drones have so much potential, and this research aims to further explore their use in the field of conservation of critical and vulnerable plant communities and associated species.

1.3. Research Identification

The overall aim of the proposed research is to assess the efficacy of drones, to bridge the gap between field methods and satellite imagery to map plant communities for conservation. The research objectives (RO), research questions (RQ) and their subsequent hypotheses (H) are as follows: -

RO1. To assess the ability of drones to map plant communities, based on the visibly dominant species and to evaluate the effect of different seasons and dominant plant life-form on the classification results.

RQ1.1. What is the accuracy of classifying UAV imagery to map plant communities?

H1.1. The high-resolution UAV imagery would lead to a precise classification of plant communities and high overall accuracy.

RQ1.2. What is the effect of different seasons on the classification accuracy?

H1.2. The seasons would affect the overall and the individual accuracies of plant communities.

RQ1.3. Does combining images from different seasons improve the classification results?

H1.3. Combining images from different seasons will yield higher classification accuracy than single-season imagery.

RQ1.4. What is the effect of dominant plant life-forms on the classification accuracy?

H1.4. The communities dominated by larger plant species like trees and shrubs will be classified with higher accuracy than those of smaller plants, like dwarf shrubs and grasses.

RO2. To assess the effect of using additional UAV obtained samples on the accuracy of satellite image classification of various spatial and spectral resolutions, to map plant communities.

RQ2.1. How do the additional UAV obtained samples affect the classification results of satellite imagery in comparison to using only field samples?

H2.1. Additional samples obtained from visual interpretation of the UAV imagery will result in higher accuracy than the classification with only field samples.

RQ2.2. What is the effect of different spatial and spectral resolutions on the satellite image classification results?

H2.2. The spatial resolution would be more important for accurate classification of smaller plant life-forms like grasses, whereas the spectral resolution would be more important for classifying plants with similar phenology and spectral properties.

RO3. To qualitatively compare the classification results with existing vegetation surveys aiming to assess the conservation status of plant communities.

RQ3.1. What differences can be observed between the classified maps and the existing vegetation survey maps?

H3.1. Integrating UAVs with field methods will improve the quality of the satellite classification results and the classified maps will have more information than the vegetation survey maps.

2. MATERIALS AND METHODS

The methodology followed for this research consists of four main parts: (i) Selection of a case study area (ii) Data collection – primary and secondary data, (iii) Data processing, classification & accuracy assessment and (iv) Comparison of the results, with each other and with the existing map(s). A detailed description of the steps is mentioned in the subsequent sections. The overview of the methodology is shown in the flow chart below (*Figure 1*).

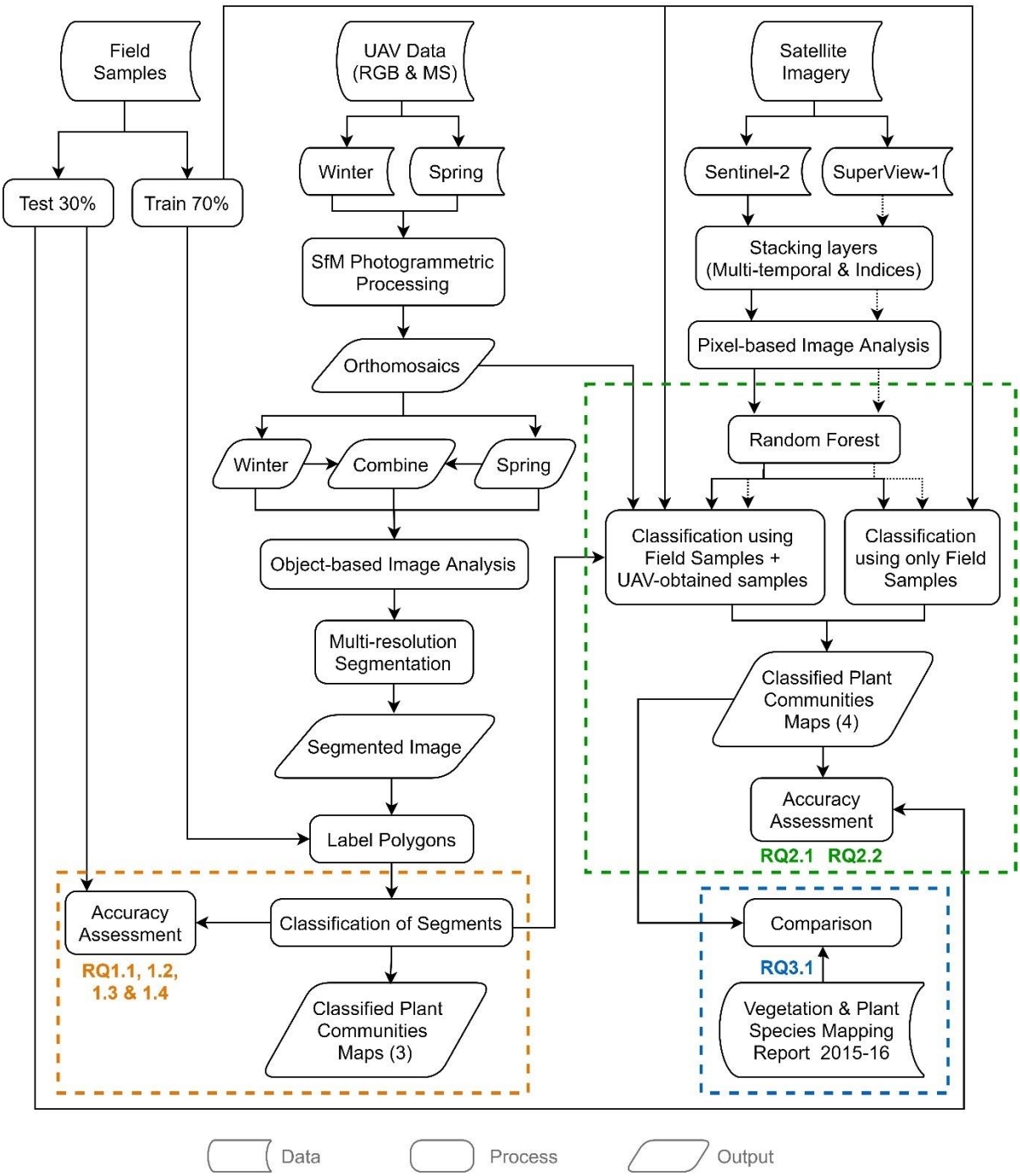

Figure 1. Flow chart showing the methodology used for this research

2.1. Overview of Study Area

The study area is located in the National Park Drentsche Aa, in the province of Drenthe, in the North of the Netherlands. The area has been among the most beautiful landscapes in the Netherlands and the best-preserved village landscape of Western Europe. It is a wooded wetland region with river valley grasslands, green villages, and agricultural heathlands. The landscape is nearly the same as it was a hundred years ago, and the streams still follow their natural meandering course. Nature, water and agriculture are the defining characteristics of the landscape, and the streams are its lifelines (National Park Drentsche Aa, n.d.a).

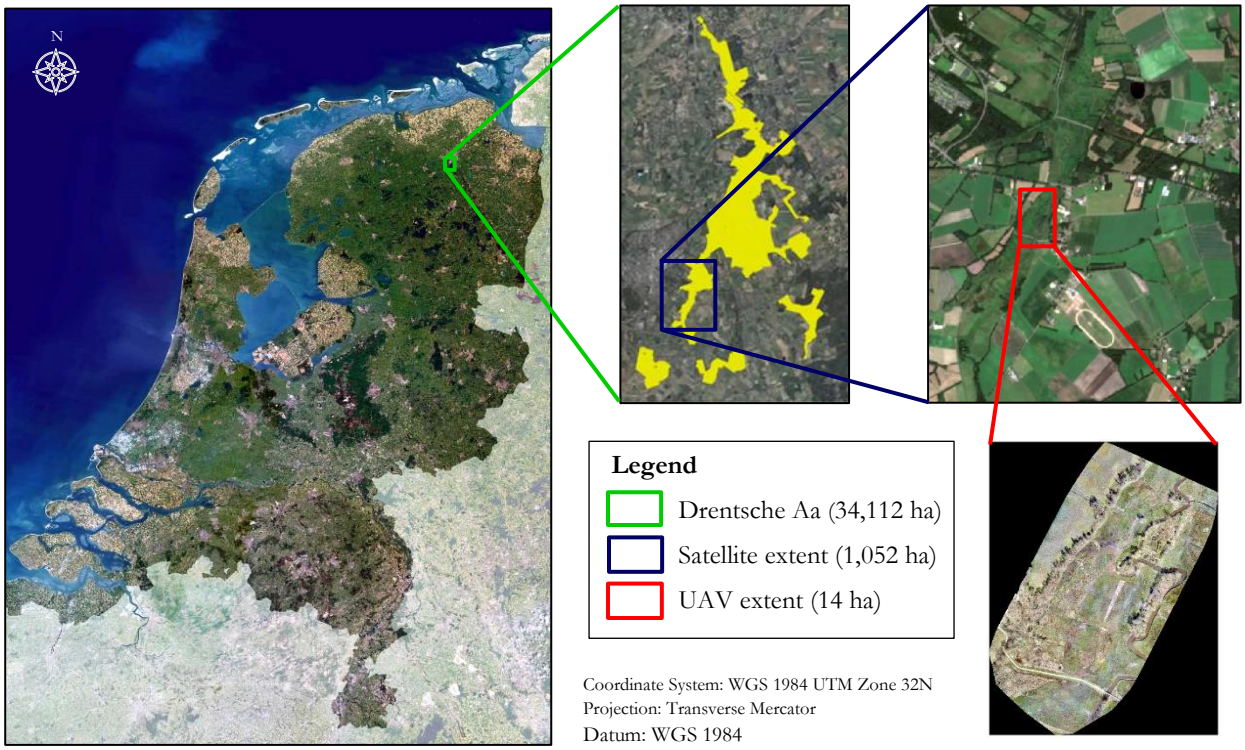

Figure 2. Location and extent of the Drentsche Aa, along with specific study area for the satellite and the UAV

At present, the area is predominantly agricultural, and the remaining is forest and natural area. The area is one of the ecological gems of the country with a variety of plant and animal species. Moreover, the cultural and historical importance adds to the landscape. In terms of natural wealth, approximately 3900 hectares of the area falls under Natura 2000, which mainly consists of the catchment area of the stream valleys. Important parts of the area, such as the narrow strips along the streams and the river valley grasslands are protected areas, with some rare plant species too. The area has around 850 plant species, which is almost half of the plant species in the Netherlands (National Park Drentsche Aa, n.d.b). The ground and surface water system and the soil highly influence the distribution of plant species in the area. Some of these areas are sensitive and not easy to access due to seasonal flooding, which allows exploring the potential of UAVs to collect data. Moreover, the plant communities present in the area allow addressing the research problem and further investigating the RQs. Besides, the UAV flight restrictions, breeding and migration seasons of birds also influenced the selection of the site; *Figure 2* shows the location and extent of the study area.

2.2. Data Collection

The data was collected between December 2020 and April 2021. Multiple field visits were made to collect the data. It mainly consists of two parts, the field observations, and the UAV image acquisition.

2.2.1. Field Observations

For the field observations, plant communities were identified via the dominant species. Observations were made following the Purposive Sampling approach at points (Wulfsohn, 2010). Samples were collected based on prior knowledge of the study area with a focus on specific communities representing different plant life-forms, to fulfil the objectives of this study. Approximate centres (points-x,y) of the representative patches of plant communities were recorded, which were covering a minimum of roughly 1-meter area around the centre. The field survey forms (Appendix I) were filled, noting down all the necessary information and photographs were taken for reference. *Figure 3* illustrates the photographs of the dominant species representing the plant communities selected for this study. The non-biotic components were recorded as well, as they also contribute to the spectral signature representing a certain plant community (*Figure 3*d). These samples were used as ground truth. A part of these observations was used for classification, while the rest was used for the accuracy assessment.

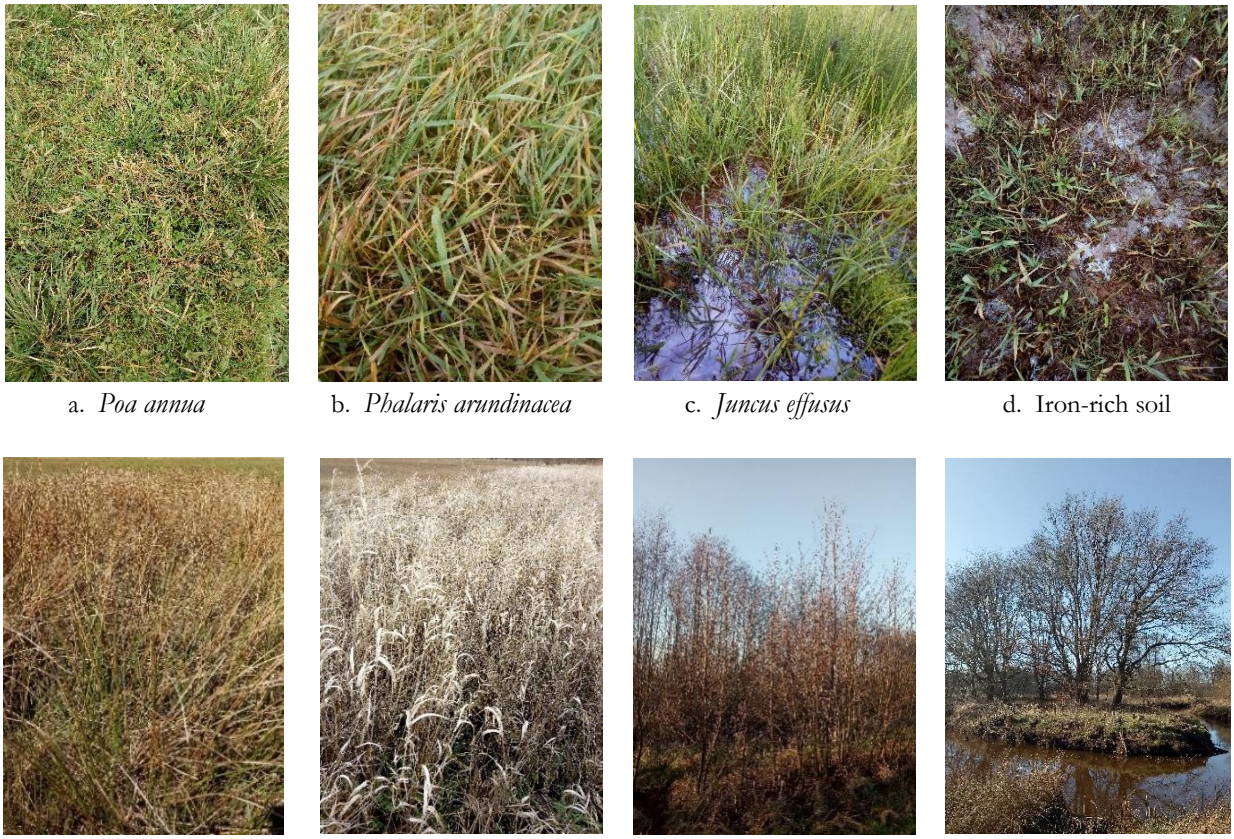

a. *Poa annua* b. *Phalaris arundinacea* c. *Juncus effusus* d. Iron-rich soil

e. *Phragmites australis* f. *Carex* spp. g. *Salix* spp. h. *Alnus glutinosa*

Figure 3. Field Photographs from winter with the scientific names of the dominant species representing the plant communities, along with a photograph of the iron-rich soil (d) representing the habitat in which Juncus effusus (c) usually grows

- *Poa annua* known as Straatgras in Dutch and Annual meadow grass in English is the most common grass which can be found everywhere from lawns to in between paving stones. It grows all year round and is very short and grows close to the ground, almost like creepers. The colour ranges from light green to yellow (Flora of the Netherlands, n.d.a).
- *Phalaris arundinacea* known as Rietgras in Dutch and Reed canary grass in English is usually found along streams in wet soils with blade-like flat long leaves (Flora of the Netherlands, n.d.b). In the study area, it was found growing together with *Juncus effusus* in several spots.
- *Juncus effusus* known as Pitrus in Dutch and Soft rush in English, is a grass-like plant with needle-shaped erect stems, without any knots (Flora of the Netherlands, n.d.c). In the study area, it was found in wet iron-rich soil in temporarily flooded areas (grasslands).
- *Phragmites australis* known as Gewoon riet in Dutch and Common reed in English is an erect plant with long stems and a hairy top. It is predominant on waterfronts and wet soils of river valleys (Flora of the Netherlands, n.d.d). In the study area, it was maintained in geometric patches by the management.
- *Carex* known as Zegge in Dutch and Sedge in English is a plant with solid stems. Their leaves are similar to grasses, though the exact shape can vary between species (Lizzie Harper, 2018). In the study area, it could be either *Carex acuta* (Scherpe zegge in Dutch and Sharp sedge in English) or *Carex nigra* (Zwarte zegge in Dutch and Black sedge in English). The exact species could not be identified; therefore, for this study, they are referred to as *Carex* spp. (where spp. stands for species pluralis i.e., multiple species).
- *Salix* known (Wilg in Dutch and Willow in English) is a deciduous tree species chiefly found in wet soils of cold and temperate regions (New World Encyclopedia, n.d.). In the study area, it can either be *Salix repens* (Kruipwilg in Dutch and Creeping willow in English) or *Salix alba* (Schietwilg in Dutch and White willow in English); as the exact species could not be confirmed they are referred to as *Salix* spp. for this study.
- *Alnus glutinosa* (Zwarte els in Dutch and Black Alder in English) is a common tree species of the Birch family. It prefers soils with sufficient moisture like along riverbanks, wetlands, etc. It is a multi-stemmed tree with dark coloured branches and small pine-like buds (Flora of the Netherlands, n.d.e).

These species are indicative of plant communities that are named after them. They are further categorized according to their main plant life-form, based on their general physical characteristics and height during their vegetation period (Einar & Rietz, 1931). The types used for this study are Trees (plants with a distinct main trunk), Dwarf-shrubs (smaller bushy woody plants) and Herbaceous plants (herbs and grasses). For simplicity, these are referred to as trees, shrubs and grasses for this study. Hence, the community of *Poa annua*, *Phalaris arundinacea* and *Juncus effusus* are categorized as grasses, *Phragmites australis* and *Carex* spp. as shrubs and *Salix* spp. and *Alnus glutinosa* as trees.

Most observations were made in winter as the communities in focus are more visible in that season. During the field visit in spring, the same locations were revisited. It was observed that the extent of the

communities did not change, allowing for the same dataset to be used for spring as well. Moreover, some additional samples were collected in spring from previously inaccessible, flooded areas due to higher water levels in winter. Likewise, the plant and the site description were added for spring in the field survey forms and more photographs were taken. There were also some new species that emerged in spring, but their extent did not meet the minimum requirement for this research, the patches were so tiny to even be recorded. These species could possibly grow and spread out more in summer, but for this research due to time constraints, these new species could not be added.

2.2.2. UAV Image Acquisition

For the UAV image acquisition, a pre-flight site visit was made to assess the site and choose a suitable area considering various factors like the plant communities present to investigate the RQs, legal restrictions to fly, breading seasons of birds, etc. After the area was finalized, permission to fly a drone was sought from the authority. Then the pre-flight preparations were made and test flights were conducted, where the different parameters were adjusted and the most suitable specifications were used for the final acquisition.

The winter images were acquired on 22 December 2020 (10:30 to 14:00). The weather conditions were good enough to fly but due to the season, it had a grey sky and scattered clouds resulting in low lighting conditions. Whereas the spring images were acquired on 26 April 2021 (9:45 to 12:00) where the weather conditions were better, with a higher solar incidence angle and a clear sky.

A multi-spectral sensor was considered to be most suitable for this research, as the prime focus was on vegetation. It can measure the surface reflectance for two or more specific wavelengths, which allows the calculation of various vegetation indices, which further helps in a more detailed spectral differentiation among plants (Assmann et al., 2019). Therefore, Parrot Sequoia multispectral sensor was used. It captures images across four spectral bands (Red, Green, Red Edge & Near Infrared) plus RGB imagery. It also comes with a sunshine sensor, which records the incoming radiation and automatically calibrates the captured images. (Parrot Sequoia, n.d.) Their specifications are shown in *Figure 4*.

a. Specifications of Parrot Sequoia b. Sunshine sensor

Figure 4. General specifications of Parrot Sequoia multispectral sensor and the sunshine sensor (Parrot Sequoia, n.d.)

The sequoia was mounted at the bottom of a quadcopter - DJI Phantom 4, whereas the sunshine sensor on the top as can be seen in *Figure 5*(a, b). DJI Phantom 4 is operated via a remote controller, which can be connected to either a tablet or a smartphone where the flight can be planned (*Figure 6*). It also comes with an intelligent flight battery (*Figure 5*c), which prompts the pilot when it reaches the minimum distance required to come back to the take-off point.

a. Parrot Sequoia b. Sunshine Sensor c. Battery

Figure 5. Parrot Sequoia and sunshine sensor mounted on DJI Phantom 4, along with its battery, in the field

Figure 6. DJI Phantom 4 with Parrot Sequoia and sunshine sensor, the controller connected to a tablet and the calibration plate in the field

Then a flight plan was created using Pix4D capture (*Figure 7*a). A single grid mission was sufficient for this research as the terrain was relatively flat and the focus was to only generate a 2D output i.e. an orthomosaic. The flying height was set to 60m to acquire the Ground Sampling Distance (GSD) of 2.62 cm and the speed was set to slow, to avoid any blurry images. The camera specifications were set using the Parrot Sequoia app on a smartphone using its Wi-Fi hotspot, which can be seen in *Figure 7*b. Furthermore, GCPs (Ground Control Points) were not used for these missions as the area being a flat grassland region, did not have many well distributed natural intersections or conspicuous points. Additionally, as the first UAV dataset was acquired in winter, the area was flooded not only making it harder to access but also not making it possible to place artificial points using checkboards.

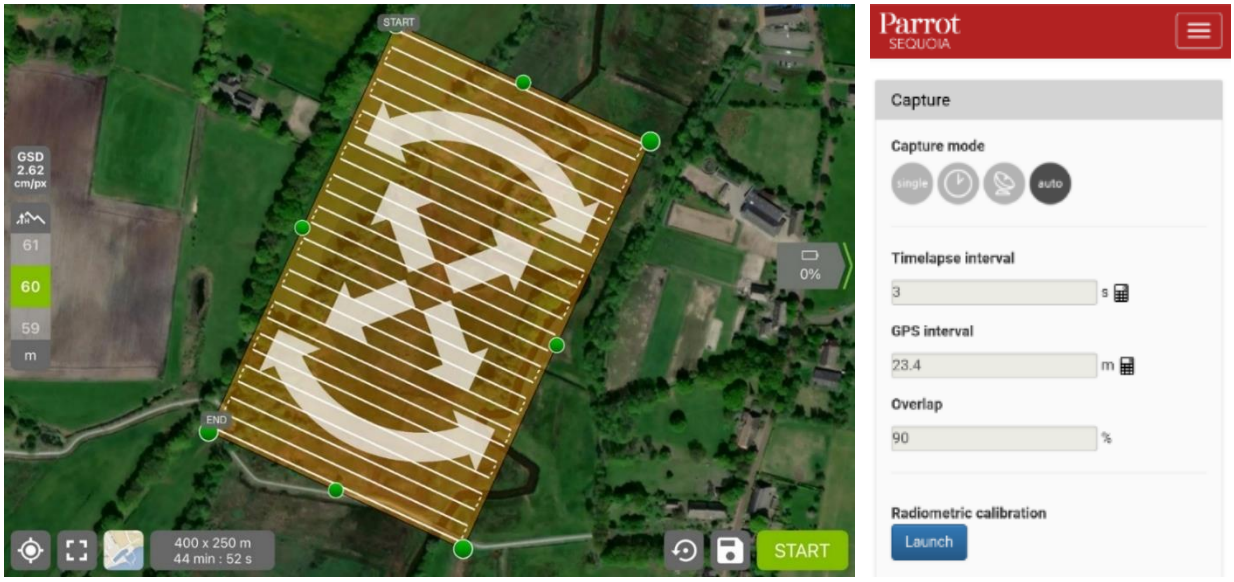

a. Flight plan in Pix4D capture b. Camera settings

Figure 7. Flight plan in Pix4D capture and Parrot sequoia settings in the Parrot Sequoia app

Then finally radiometric calibration was done using the calibration plate (*Figure 8*). The drone needs to be held perpendicular over the plate for it to automatically capture the images for calibration. It took a total of 5 flights to cover the entire area as the battery had to be changed after every 6 to 7 flight lines. Hence, radiometric calibration was done before every flight.

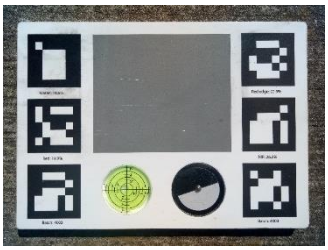

Figure 8. Calibration Plate

2.3. Data

The data used for this study includes the primary data i.e., the field samples and the UAV acquired data, as well as some secondary data like the satellite imagery and the reference map from the Vegetation and Plant Species Mapping Report.

2.3.1. Field samples

A total of 298 points were collected in winter for 10 classes. A few additional points were collected in Spring, resulting in a total of 310 points for Spring along with an additional class, making the total number of classes 11. Moreover, the field photographs along with the details recorded on the field survey forms served as additional information.

2.3.2. UAV acquired data

A total number of approximately 2,500 images were acquired for each season, including both the RGB and MS images. The images from each flight as well as the calibration images for each one of them were stored in separate folders in the internal memory of parrot sequoia.

2.3.3. Satellite Data

Two different Satellite images were used for this research i.e., Sentinel-2 and SuperView-1. These imageries have different spatial and spectral resolutions, but the temporal dimension was kept the same to have the same multi-temporal dimension to have a basis for comparison.

Sentinel-2 imagery was selected due to its wide range of spectral resolution. It has 13 spectral bands, including three red-edge bands, which are very helpful for calculating various vegetation indices (Rapinel et al., 2019). Clear cloud-free imageries were downloaded from Copernicus Open Access Hub. The specifications of the imagery are shown in *Table 1*, and the details of the images used for this research, along with their description in *Table 2* and *Table 3*, respectively.

Bands	Spatial Resolution (m)	Central Wavelength (nm)	
		S-2A	S-2B
B1 - Coastal aerosal	60	443.9	442.3
B2 - Blue	10	496.6	492.1
B3 - Green	10	560.0	559
B4 - Red	10	664.5	665
B5 - Vegetation Red Edge	20	703.9	703.8
B6 - Vegetation Red Edge	20	740.2	739.1
B7 - Vegetation Red Edge	20	782.5	779.7
B8 - NIR	10	835.1	833
B8A - Narrow NIR	20	864.8	864
B9 - Water Vapour	60	945.0	943.2
B10 - SWIR - Cirrus	60	1373.5	1376.9
B11 - SWIR	20	1613.7	1610.4
B12 – SWIR	20	2202.4	2185.7

Table 1. Sentinel-2 specifications: Band names and numbers, spatial resolution in meters, central wavelength in nano-meters for both Sentinel-2A and Sentinel-2B (Earth Observing System, n.d.a)

Date	Product Identifier
22-04-2020	S2B_MSIL2A_20200422T103619_N0214_R008_T32ULD_20200422T140230
26-06-2020	S2A_MSIL2A_20200626T104031_N0214_R008_T32ULD_20200626T135731
03-11-2020	S2A_MSIL2A_20201103T104221_N0214_R008_T32ULD_20201103T133056

Table 2. Sentinel-2 data used for this research along with its acquisition date and product identifier (Copernicus Sentinel Data, 2020)

Columns and Rows	10980, 10980
XY Coordinate System	WGS_1984_UTM_Zone_32N
Datum	D_WGS_1984
Format	TIFF

Table 3. Description of the downloaded Sentinel-2 data used for this study

SuperView-1 was selected due to its high spatial resolution and data availability for at least three seasons. The imagery was downloaded from Satellite Data Portal. The specifications of the imagery are shown in *Table 4* and the details of the images used for this research in *Table 5*.

Bands	Spatial Resolution (m)	Spectral Resolution (µm)
PAN	0.5	0.45 - 0.89
B1 - Blue	2	0.45 - 0.52
B2 - Green	2	0.52 - 0.59
B3 - Red	2	0.63 - 0.69
B4 - NIR	2	0.77 - 0.89

Table 4. SuperView-1 specifications: Band names and numbers, spatial resolution in meters, and spectral resolution in micro-meters (Earth Observing System, n.d.b)

Date	Product Identifier
04-04-2020	20200404_103926_SV1-01_SV_RD_11bit_RGBI_50cm_Assen
23-06-2020	20200623_111355_SV1-02_SV_RD_11bit_RGBI_50cm_Assen
06-11-2020	20201106_105752_SV1-04_SV_RD_11bit_RGBI_50cm_Assen

Table 5. SuperView-1 data used for this research along with its acquisition date and product identifier (Beijing Space View Technology Co. Ltd., China, 2020)

SuperView-1 offers a pan-sharpened imagery as well, therefore it was used for this research to get even a higher resolution. *Table 6* provides a description of the data.

Columns and Rows	31520,32344
Cell Size (X,Y)	0.5, 0.5
XY Coordinate System	RD_New
Datum	D_Amersfoort
Format	TIFF

Table 6. Description of the downloaded SuperView-1 data used for this study

2.3.4. Vegetation Report

To compare the results produced for this study, the already mapped data by Staatsbosbeheer for the Vegetation and Plant Species Mapping Report, Drentsche Aa 2015-16 was used. For the report, the quality and distribution of the vegetation types and specific plant species have been mapped, where communities are also distinguished based on the level of associations. The area was mapped using digital true colour aerial photographs. The level of detail was on a coarser level, with the scale being 1:5,000 and the minimum mapping unit as 25 by 25 m (10 by 50 m for elongated surfaces). Only in exceptional cases for valuable vegetation, this was adjusted (Ecologengroep Groningen, 2017). The report also has a detailed description of all the plant species along with the communities they represent or are a part of. Moreover, the report document was in Dutch and hence was translated to English. The plant communities that correspond to the area where the data was collected are mentioned as follows.

As per the report, *Poa annua* is found with other grasses like *Juncus bufonius* (Greppelrus in Dutch and Toad rush in English) and *Polygonum aviculare* (Gewoon varkensgras/Common pig grass), forming a community represented by the code 12A1-1. The community of *Phalaris arundinacea* is represented by the codes 08-16, 08-17 and 08-18. The community of *Juncus effusus* is denoted by the code 16-32. It is also found with some other plants like *Holcus lanatus* (Gestreepte witbol/Yorkshire-fog) and *Lotus uliginosus* (Moerasrolklaver/Swamp roll clover). *Holcus lanatus* is a soft grassy erect plant with a hairy top, which flowers between May to September (Flora of the Netherlands, n.d.f). While *Lotus uliginosus* is a leafy plant with tiny yellow flowers which flowers between June to August (Flora of the Netherlands, n.d.g). These three together represent a community which is denoted by the codes 16-1, 16-2, 16-6 and 16B-7. *Phragmites australis* is found growing with *Juncus articulates* (Zomprus) and *Mentha Aquatica* (Water Mint), represented by the code 08A-2. The area also consists of various species of *Carex* like *Carex acuta* (Scherpe zegge/Sharp sedge), *Carex nigra* (Zwarte zegge/Black sedge) denoted by the codes 08C2-1, 08C2-2, 09A-2, 09A-3 and 09A3-5. *Carex nigra* also grows together with *Equisetum fluviatile* (Holpijp/Hollow) represented by the code 09A3-2. As the English name suggests, *Equisetum fluviatile* is a hollow pipe that almost looks like bamboo with knots dividing each section (code: 09-2) which flowers between April and July (Flora of the Netherlands, n.d.h). Some of these species' flower in the summer months like *Holcus lanatus*, *Lotus uliginosus,* etc., while the last field data for this study was collected in spring. Therefore, these species could not be recorded, as they had just started to flourish and their extent did not match the minimum area requirement for this study; some of them are shown in *Figure 9*. The report also mentions some more grass species, which could not be seen in the study area yet, possibly because they grow later in the year. Hence, for comparison, these species are collectively referred to as 'Other grasses' for this study.

a. *Holcus lanatus* b. *Lotus uliginosus* c. *Equisetum fluviatile* d. Unidentified species

Figure 9. Field photographs of the plant species that started to flourish in spring, but could not be recorded as their cover didn't meet the minimum area requirement for this study

For the trees, a species of *Salix, Salix repens* (Kruipwilg/Creeping willow) was found with other tree species like *Quercus robur* (Zomereik/English oak), *Corylus avellana* (Hazelaar/Hazel), etc. denoted by the code 43-1. While *Alnus glutinosa* is represented by the code 39A-5 in the report. Lastly, the other classes were treated as one, which includes river, road, bare soil, etc., denoted by the codes 50C-1, 50C-4 and 50A-2.

2.4. Software

Table 7 presents the software used for this study. It mainly consists of the UAV flight planning and data processing software, image analysis and visualization software and finally the ones used for report writing.

Software	Use
ArcGIS 10.8.1	Pre-Processing & Visualization
eCoginition 10.0.2	Object-Based Image Analysis
ERDAS Imagine 2018	Pre-Processing
Google Earth Pro 7.3	Site Inspection & Pre-flight planning
Mendeley 1.19.8	Citation and referencing
Microsoft Office 365	Analysis, Data entry, Presentation & Writing
Pix4D Capture 4.12.1(1)	UAV Flight Planning
Pix4D Mapper 4.6.4	UAV Image Processing
Parrot Sequoia 1.4.1	Radiometric Calibration & Camera Settings
QGIS 3.16.0	Field Data Processing & Visualization
RStudio 1.2.5033	Random Forest Classification

Table 7. Software used for this study along with the tasks they were used for

2.5. Data Processing, Classification & Accuracy Assessment

For the data processing, the field samples, UAV data and satellite data were processed. The field data processing mainly consists of splitting the samples for training and testing. While the UAV data processing consists of photogrammetric processing to generate orthomosaics, classification, and accuracy assessment. Whereas the satellite data processing consists of pre-processing, classification, and accuracy assessment.

2.5.1. Field Samples Processing

The field samples were stored in a CSV (Comma-Separated Values) file with a unique ID for each class. After that, the samples were prepared for classification by using the train-test split procedure. It is used to evaluate the performance of the classification algorithm, by making predictions on the test set which is not used to train the algorithm (Brownlee, 2020). Adelabu et al. (2015) concluded that Random Forest resulted in the lowest error rate and highest accuracy with a 70-30% split. Therefore, this split was used for this research, where roughly 70% of the sample points were used for training and 30% for testing. Then these CSV files were converted to shapefiles; the points were visually inspected to make sure that for each class the validation points were spatially independent of the training points.

Samples for a new community or a class were not collected in spring, only additional samples of the same communities were added, however, some alterations were still made in the already existing samples. For

instance, there were areas which were completely flooded in winter but not so much in spring (*Figure 10*). Therefore, samples in the areas which were not flooded anymore were removed and samples only for the patches that were still wet were kept and called 'Iron-rich water'. For the combined images, where the samples from the two seasons were merged, these two classes were treated separately. The area flooded only in winter (Flooded area) was labelled as 'Periodically Flooded' and the area that was flooded or wet in both seasons (Iron-rich water) was labelled as 'Permanently Flooded'.

a. Area in winter (22 Dec 2020) b. Area in spring (26 April 2021)

Figure 10. The difference in the level of flooding at a site in the study area between the two seasons

2.5.2. UAV Data Processing

The UAV data processing involves photogrammetric processing to generate orthomosaics, segmenting and classifying these orthomosaics, accuracy assessment and finally visualizing the results to produce classified maps of plant communities.

a. Orthomosaic Generation

The UAV data was processed by applying Structure from Motion (SfM), using the software 'Pix4D Mapper'. It processes the sequence of overlapping drone images and extracts the 3D & 2D structure of the scene along with its camera positions (Alsadik & Nex, 2020). First, the UAV data was cleaned, and the RGB & MS images were separated for easy processing as Pix4D has different templates to process the RGB & MS images ('3D Maps' for RGB images and 'Ag Multispectral' MS images). The coordinate system was automatically detected as WGS_1984 (UTM Zone 32N). Then for processing, Pix4D consists of 3 steps i.e., 1. Initial Processing, 2. Point Cloud and Mesh and 3. DSM, Orthomosaic and Index. The second step was skipped for this study to save time and storage space as a point cloud was not required and the prime focus was to generate an orthomosaic.

Most of the default settings were used except for one, where for initial processing, the 'Internal Parameters Optimization' was set to 'All Prior' (Appendix II), without which the images were not properly aligned or geo-located and there were false height differences as well. This issue seems to occur in the case

of perfectly nadir flights over flat terrains (Pix4D Community, n.d.), therefore, changing this setting is extremely important to ensure good quality of the orthomosaics.

To generate the RGB orthomosaic, images from all the flights were processed together. Whereas to generate the MS orthomosaic, each flight was processed separately as the radiometric calibration was done before each flight. It is important to make sure that the images are properly calibrated for each flight. Once the flights were processed individually, then all of them were merged using Manual Tie Points (MTPs). For an MS project, MTPs must be marked in all the bands, in a minimum of 3 sets of images (Pix4D, n.d.). In this case, as there were 4 bands, therefore at least 12 MTPs were marked. Both the winter & spring datasets were processed in the same manner, except for an additional step for the spring dataset, where GCPs were used for the generation of the orthomosaic. They were created by taking measurements from the winter orthomosaic, to make sure that both the orthomosaics overlap perfectly.

b. Object-Based Image Analysis (OBIA)

OBIA was used to classify the orthomosaics. Based on the literature, for high-resolution imagery, OBIA performs better than the pixel-based classification (Makinde et al., 2016; Sibaruddin et al., 2018). A pixel-based approach is substantially limited for very high-resolution imagery, as it does not consider the rich spatial information which results in low accuracy with the salt and pepper effect (Blaschke et al., 2000; Zhang et al., 2020). Whereas OBIA can delineate ecologically meaningful objects by aggregating homogeneous groups of pixels, instead of classifying single pixels (Ventura et al., 2018). Along with the spectral information, it takes into consideration the spatial and contextual (shape & texture) properties as well. Moreover, it is closer to human visual perception as humans see objects in space, not pixels (Blaschke & Strobl, 2001; Belgiu, 2020). A study by Lu & He (2017) even demonstrates its effectiveness in classifying species in heterogeneous grasslands.

The typical OBIA workflow involves two steps, first is image segmentation and then the classification of these segments (Ventura et al., 2018). The software 'eCognition' was used for this purpose.

i. Pre-processing/Index Calculation

In addition to the RGB and MS layers, some additional indices were also created in eCognition itself. They include Normalized Difference Vegetation Index (NDVI), Normalized Difference Water Index (NDWI), Enhanced Vegetation Index (EVI) & Green-Red Vegetation Index (GRVI). A total of 11 layers were used for the following steps i.e., 3 from RGB, 4 from MS and 4 indices.

ii. Segmentation

To delineate plant communities, multi-resolution segmentation was used. It is a bottom-up approach that starts with a single pixel and iteratively merges similar neighbouring pixels into bigger objects. It works based on the homogeneity criteria, which is determined by certain parameters like Scale Parameter (SP),

Shape, Compactness, etc. Some of these parameters need to be fine-tuned and are usually determined by a trial-and-error process (Belgiu, 2020). Segmentation results are sensitive to these parameters; therefore, they were visually inspected before moving to the next step. A rough guideline one can use is that the image objects should be considerably larger than the size of noise relative to texture, which would ensure that meaningful segments are created (Blaschke et al., 2000). Moreover, attention should be paid to areas with shadows as they can be treated as separate objects and cause problems (Lechner et al., 2012).
Keeping these things in mind, the following parameters were selected as they seemed to work well for the given dataset: Scale Parameter (SP) was set as 900, Shape as 0.1 and Compactness as 0.3. Moreover, different weights were assigned to the layers; more weight was assigned to the indices, NIR and red layers, whereas less to the RGB layers (Appendix III).

iii. Classification

The segments were classified following a supervised approach. It was trained using 70% of the field samples i.e., the training points. The points (shapefile) were added as a thematic layer and segments (objects) were assigned to the corresponding classes, which resulted in labelled segments. 'Random trees' algorithm was used for classification as it resulted in slightly better accuracy in comparison to Decision Trees (DT) and Support Vector Machine (SVM).

iv. Accuracy Assessment

Finally, the validation points i.e., 30% unused observations were added in the same manner as the training points (as a thematic layer). Then an error matrix was generated and the classes that are not in focus i.e., river, road, etc. were merged as 'others' to present the final results. Along with the overall, producer's and user's accuracy, the accuracy for only the classes of interest i.e., plant communities were also presented.

Both the winter and spring data were processed in the same manner, with the winter and spring samples respectively, using the same weights, parameters, and classification algorithm.

c. Combining the two seasons.

For combining the two seasons the same workflow was followed. Here the orthomosaics from both seasons were added as layers in eCognition and used for OBIA. First the pre-processing was done, where the four indices were calculated for each season, resulting in a total of 22 layers (11 from each season), followed by a multi-resolution segmentation, with the same parameters, weights and specifications. Then the merged samples (winter + spring) were used for both classification and accuracy assessment.

Finally, all the classification results were exported and visualized in ArcGIS and three classified maps for plant communities were produced for winter, spring and combination of the two seasons. Consistent colours were assigned to the classes, throughout the analysis.

2.5.3. Satellite Data Processing

The satellite data processing mainly consists of pre-processing, which involves preparing the satellite imagery for classification, the accuracy assessment of the classification results and finally visualization of the results to produce classified maps for plant communities.

a. Pre-processing

For Sentinel-2, the following bands were used for the analysis: band 2 (blue), band 3 (green), band 4 (red), band 5 (vegetation red edge), band 6 (vegetation red edge), band 7 (vegetation red edge) and band 8 (NIR). The bands 2, 3, 4 and 8 are of 10m resolution, whereas bands 5, 6 and 7 are 20m. Therefore, the 20m bands were resampled to 10m resolution using the nearest neighbour interpolation. Then the following indices were calculated:

Index	Equation	Reference
Normalized Difference Vegetation Index (NDVI)	(NIR – Red)/(NIR + Red)	Tucker & Sellar (1986)
Green Normalized Difference Vegetation Index (GNDVI)	(Green – Red)/(Green + Red)	Tucker (1979)
Normalized Difference Water Index (NDWI)	(Green – NIR)/(Green + NIR)	McFeeters (1996)

Table 8. Equations to calculate the vegetation indices used for the analysis of Sentinel-2 for this study

This was done for all three images individually. All the layers (7 bands + 3 indices for each image) were then stacked together, resulting in stack of 30 layers. Finally, a subset was created to match the extent of the study area. *Table 9* presents a summary of the processed Sentinel-2 data.

Columns and Rows	293, 364
Number of bands	30
Cell Size (X,Y)	10, 10
XY Coordinate System	WGS_1984_UTM_Zone_32N
Datum	D_WGS_1984
Format	TIFF

Table 9. Description of the processed Sentinel-2 data used for this study

For SuperView-1, all four bands (of the three images) were used for the analysis. Then these images were stacked together, resulting in a stack of 12 layers. This stack was then reprojected into the same coordinate system as of the Sentinel-2, i.e., from RD_New to WGS_1984. Finally, a subset was created of the same extent as the Sentinel-2; *Table 10* presents its description.

Columns and Rows	6591, 7870
Number of bands	12
Cell Size (X,Y)	0.5, 0.5
XY Coordinate System	WGS_1984_UTM_Zone_32N
Datum	D_WGS_1984
Format	TIFF

Table 10. Description of the processed SuperView-1 data used for this study

b. Classification

A pixel-based classification approach was used to classify the satellite imagery as it seemed more suitable considering the spatial resolution of the imageries. For the classifier, Random Forest (RF) was selected as based on literature it has previously performed well to classify plant communities (Rapinel et al., 2019; Villoslada et al., 2020). It is a supervised Machine Learning (ML) algorithm, which is an ensemble of decision trees created by a bootstrap aggregation approach, to make a prediction (Belgiu & Drăgu, 2016). It runs efficiently on large data sets, is computationally efficient and resists overfitting (Gislason et al., 2006; Sabat-Tomala et al., 2020). It is also a good choice when there are sufficient training samples (Shang et al., 2018) Additionally, it rates the variables based on their importance or contribution in classifying the data. Moreover, as the same classification algorithm was used for OBIA in eCognition, it became a more preferred choice. Therefore, the satellite imageries were classified using RF in RStudio. Besides, the RF results are sensitive to the parameters like the number of trees (ntree), number of variables randomly selected to split the tree nodes (mtry), etc. These parameters can be fine-tuned to ensure that the results are a good representative of the characteristics of the data. For this study, the most suitable value for ntree was 500, while mtry was set as default i.e., square root of total number of input parameters.

The merged samples were used for classification as the satellite imagery was a multi-temporal stack consisting of both seasons. The satellite imagery was classified in two different ways, mentioned as follows: -

(i) Using only field samples (239 training points)

(ii) Using additional UAV-obtained samples, along with the field samples. The orthomosaic and the UAV classified image was used to create these additional samples. These samples were only added to the training points, as they cannot serve as the ground truth yet. Therefore, an additional 148 samples were collected, which resulted in the total number of training points being 387.

Another point to be noted is that RF produces slightly different results each time as it uses a random subset of the training data, which could make it hard to decide which result to report in the end. Therefore, the function 'set.seed' was used to ensure that the same results were produced each time.

Both the satellite imageries i.e., Sentinel-2 and SuperView-1 were classified in the same manner. Finally, the results were exported and visualized in ArcGIS and four classified maps were produced (two for each satellite imagery i.e., one with only field samples and one with additional UAV obtained samples).

c. Accuracy Assessment

The accuracy assessment was done in RStudio as well, by producing an error matrix by using the same validation points for both classifications. Then similar to the UAV, the classes that were not in focus i.e., non-plant communities were merged as others. Along with the overall, user's and producer's accuracies, the accuracy for only plant communities was also reported.

d. Variable Importance

The variable importance plots were also generated in R (ggplot), to assess the importance of each variable or layer in classifying the data. The sole purpose was to analyse the importance of the variables and not to select the most important ones for classification, also known as variable selection. The code consists of two measures, one is 'Mean Decrease Accuracy' which illustrates the importance of the variables on the accuracy i.e., how much the accuracy would decrease if a variable is discarded or excluded. The second is 'Mean Decrease Gini' which measures the importance of a variable based on the Gini impurity index. The variables are ranked based on how much they contribute to the homogeneity of the nodes and leaves in building the RF model (Martinez-Taboada & Redondo, 2020).

Additional Analysis

A brief analysis was done for Sentinel-2 to further investigate the effect of additional information layers on the classification results. The aim was to explore the possibilities of improving the classification results with additional temporal and spectral information, which could not be done for SuperView-1 due to limited data availability and spectral resolution. Moreover, this is referred to as additional analysis as it is not the main focus of this study and is not used to investigate any of the RQs. The sole purpose is to support certain statements to explain and critically reason the classification results.

Therefore, to do so, three more Sentinel-2 imageries were added to the stack. i.e., from March (23-03-2020), May (07-05-2020) and September (14-09-2020). The same pre-processing steps were followed where the same number of bands and indices were added (10 per image), which resulted in a stack of 60 layers (30 additional information layers). Then using RF, the imagery was classified in the same manner, first using only field samples and then with additional UAV obtained samples. Finally, the accuracy was assessed using the validation points and error matrices were generated. In this case, classified maps and variable importance graphs were not produced as the aim was to assess the accuracies, mainly the accuracy for the classes of interest (plant communities) and the overall accuracy.

2.6. Comparison of Results

The classified maps produced for this study i.e., UAV and satellite were compared amongst each other and finally, the satellite classified maps were compared with the existing map produced for the vegetation report.

2.6.1. Comparison of UAV and Satellite classification results

To compare the classification results, the differences in the classification approach i.e., OBIA for UAV and pixel-based for the satellite, were kept in mind. The focus was more on comparing the level of detail achieved by each method and the quality of the classified maps. Therefore, the classified maps were visually compared. For this, all the four satellite classified maps were zoomed in to the same extent as the

UAV for a direct visual evaluation. This was done to examine how close the satellite results are to the UAV and the effect of different spatial and spectral resolutions on the classification results. For the UAV part, the results for the merged orthomosaic were used for this purpose as the processed satellite imagery was a multi-temporal stack, consisting of both seasons. Moreover, as the same samples and classes were used for classification and the same colours were assigned to the corresponding classes, it ensured an easy and fair comparison.

2.6.2. Comparison of Satellite Classified maps and Vegetation Report map

This comparison is done assuming that the extent and composition of the plant communities did not change in these 4-5 years and the differences would only be due to the difference in data, field sampling technique, spatial and temporal scales, mapping methods, etc. Moreover, to make the satellite classification results and the vegetation report map comparable, the classes in the classified maps were merged to make them closer to the ones in the report. This was done by analysing the error matrices to observe overlapping classes; alongside the vegetation report was also used as a reference. Finally, the classes were merged based on their main life-forms. The results were only visually compared and to do so, the same area as of the UAV was zoomed-in both the satellite results and the vegetation report map. This was done to make the maps readable and ensure a more detailed comparison. Lastly, the maps were visualized with the new classes and the same colours were assigned to corresponding classes. Additionally, the error matrices for the satellite classification results were also merged to see how the new classes affect the accuracy.

3. RESULTS

The first part of this section consists of the UAV results, the second part consists of the satellite results and the final part consists of a comparison of these results with each and with the existing map from the vegetation report.

3.1. UAV Results

The UAV results consist of the orthomosaics, classified maps and their error matrices for winter, spring and the combination of the two seasons.

3.1.1. Orthomosaics

The orthomosaics generated in the SfM photogrammetric processing of the UAV data in Pix4D are shown in the following figures. The RGB orthomosaics for both the seasons are shown in *Figure 11* and the four MS orthomosaics (Green, NIR, Red Edge & Red) for winter and spring in *Figure 12* & *Figure 13*, respectively.

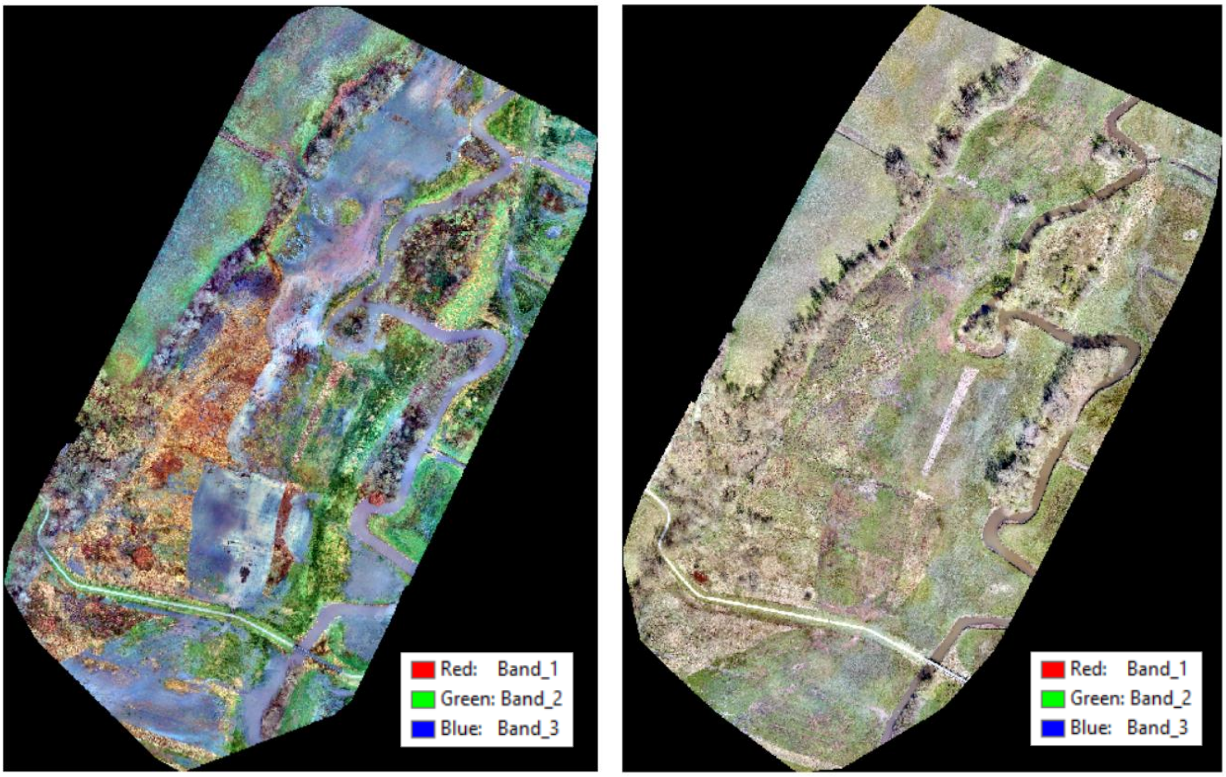

a. Winter RGB orthomosaic b. Spring RGB orthomosaic

Figure 11. RGB orthomosaics for Winter & Spring along with a legend representing the colour in which the bands are displayed

The orthomosaics cover an area of approximately 13.50 ha/0.135 km²/0.05 sq. mi./33.390 acres. For the RGB orthomosaics, 98% images were calibrated and all images were enabled; while for the MS

orthomosaics 99% images were calibrated and a few were disabled. All the orthomosaics have a very good overlap, where most of the area has more than 5 overlapping images for every pixel (Appendix IV).

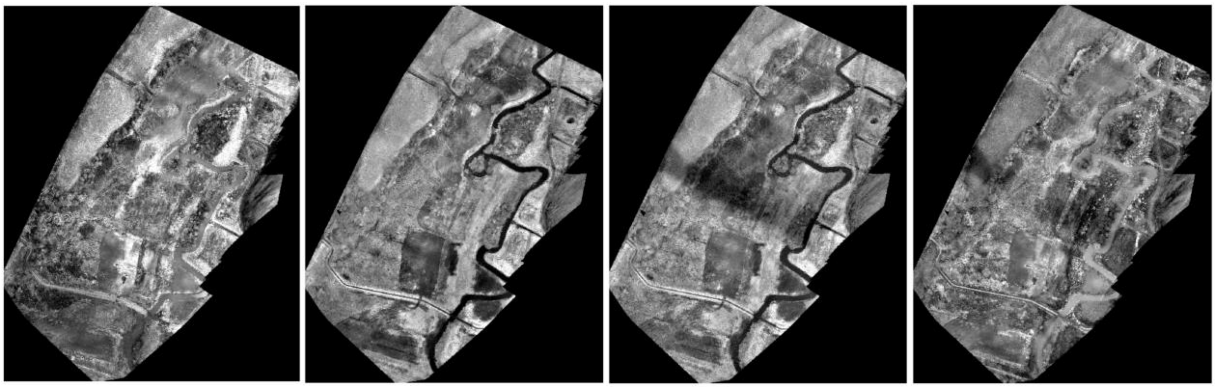

a. Green b. NIR c. Red Edge d. Red

High: 65472 Low: 0

Figure 12. Winter MS orthomosaics along with their value scale bar

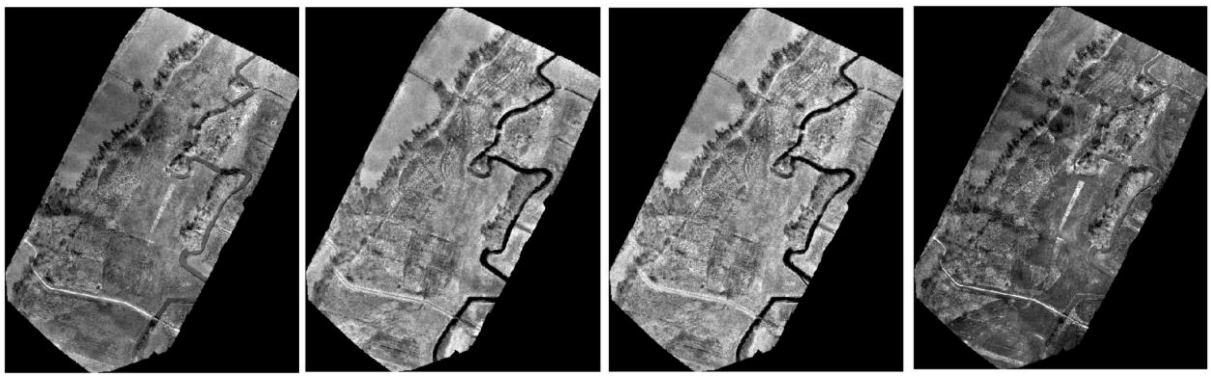

a. Green b. NIR c. Red Edge d. Red

High: 65472 Low: 0

Figure 13. Spring MS orthomosaics along with their value scale bar

3.1.2. Classification

The classification results for the orthomosaics produced using OBIA in eCognition are presented in the following figures. The results for the winter, spring & combined (winter + spring) orthomosaic are shown in *Figure 14*, *Figure 15* & *Figure 16* respectively.

A total of seven classes were created for plant communities, representing different plant-life forms i.e., grasses, shrubs, and trees. The communities of *Poa annua*, *Phalaris arundinacea* and *Juncus effusus* represent grasses, *Phragmites australis* and *Carex* spp. represent shrubs, and *Salix* spp. and *Alnus glutinosa* represent trees. The classes for plant communities remain consistent for all three UAV classifications, the only changes were made in the class 'Others' due to the seasonal differences, as has been explained in section 2.5.1. For the winter orthomosaic (*Figure 14*), the 'Others' consists of three classes - River, Road and

Flooded area, resulting in a total of 10 classes (7 for plant communities and 3 for others). Whereas, for the spring orthomosaic (*Figure 15*), the class 'Flooded area' was replaced by 'Iron-rich water', as the area was not as flooded in spring and only had some wet patches of iron-rich water. However, for the combined orthomosaic (winter + spring), these two classes were treated separately, resulting in a total of 11 classes for classification (7 for plant communities and 4 for others). The class 'Flooded area' was referred to as 'Periodically Flooded' and 'Iron-rich water' as 'Permanently Flooded' as can be seen in *Figure 16*.

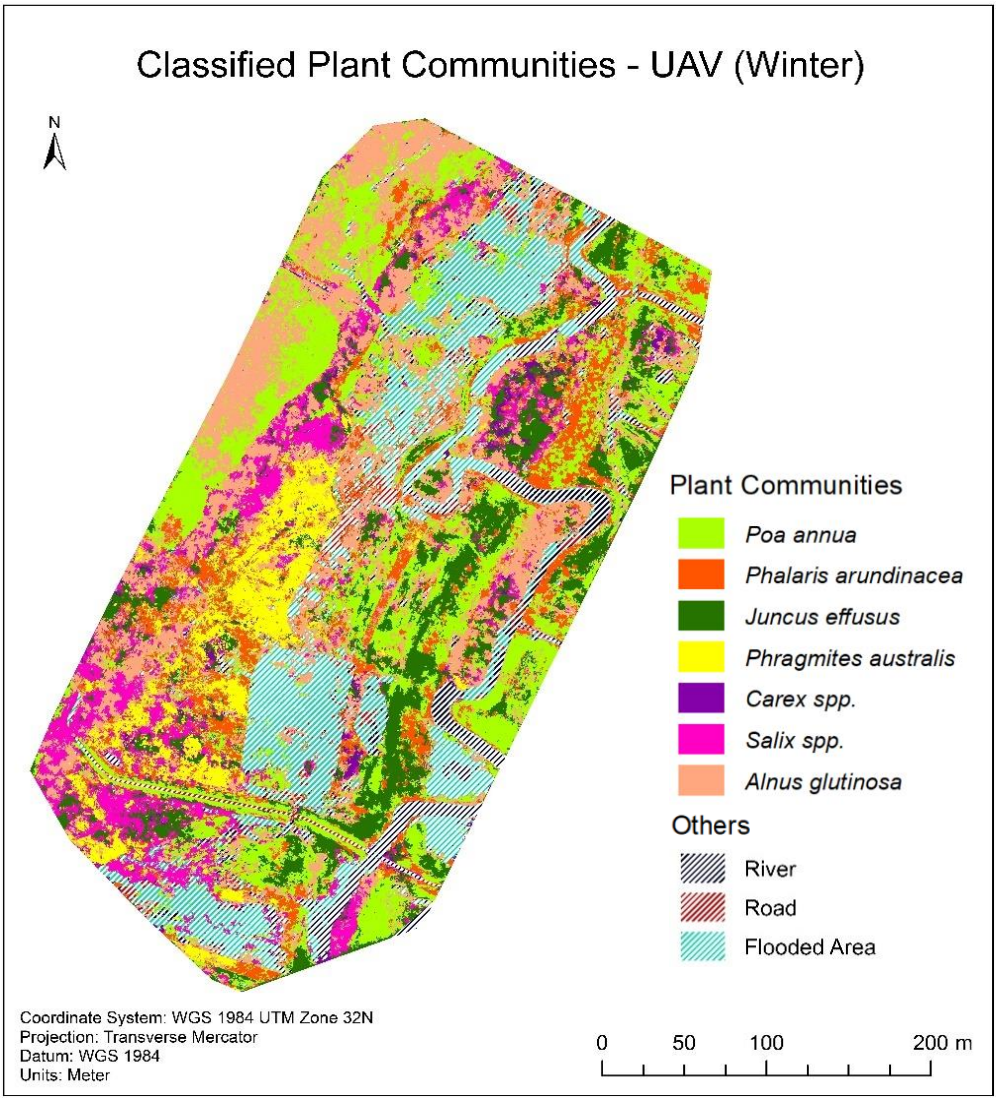

Figure 14. Classified plant communities map for the winter orthomosaic

The winter classification results when visually compared with the orthomosaic (*Figure 11*a), it can be observed that most of the area seems to be correctly classified, except for the upper left corner. A lot of that area has been misclassified as *Alnus glutinosa* (tree) whereas in reality it is majorly dominated by *Poa annua* (grass). Besides that, though the other class is not a focus for this study, some parts of the river have been misclassified as flooded area.

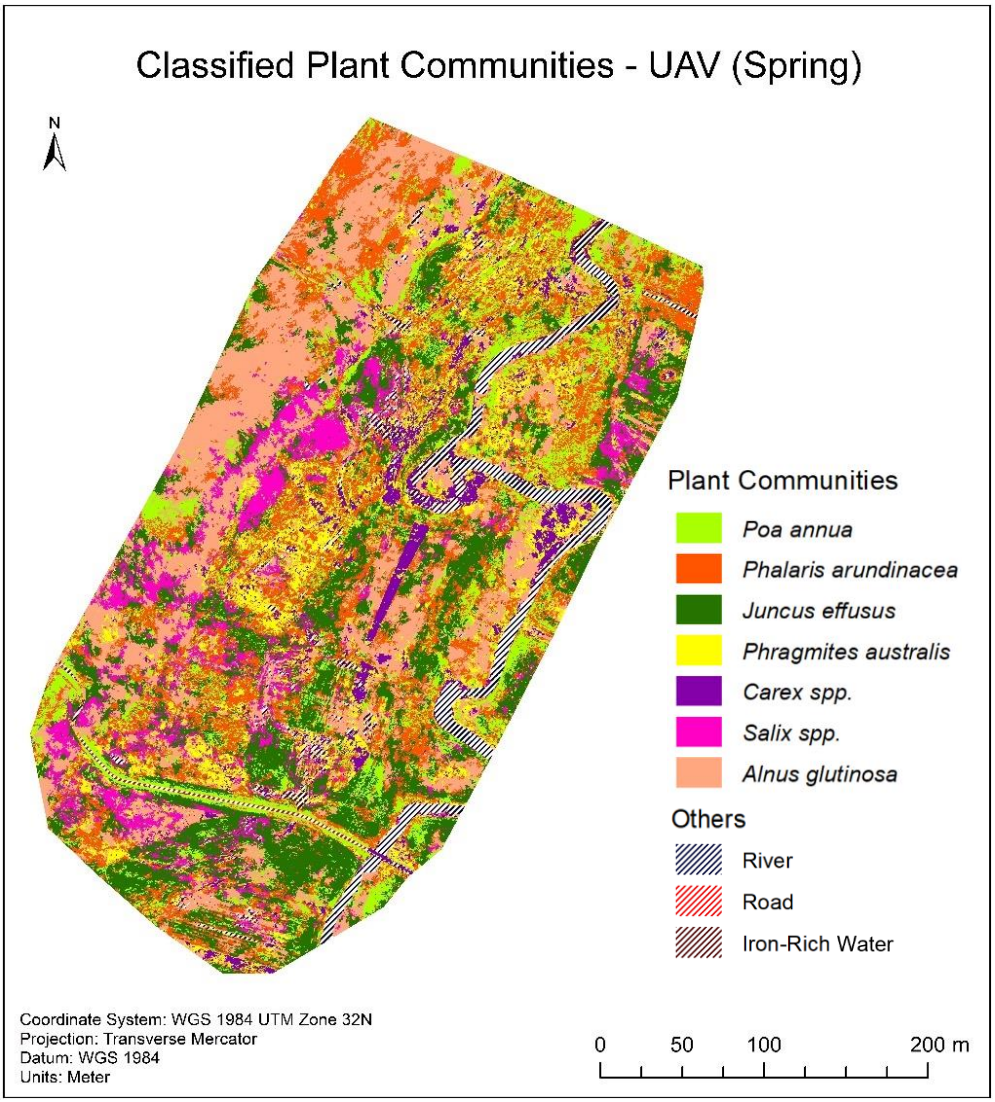

Figure 15. Classified plant communities map for the spring orthomosaic

For the spring classification results (*Figure 15*), the same issue can be observed with the upper left corner. Here, more area is misclassified, not only as *Alnus glutinosa* but also as *Phalaris arundinacea* and a little as *Juncus effusus*. Other than that, not many differences can be visually spotted within plant communities. However, concerning the other class, a positive difference can be seen, where the river now seems to be perfectly classified as there is no flooded area to be confused with.

Lastly, the combined classification results (*Figure 16*) visually seem to be more dominated by the winter image. The problem with the misclassification of the upper left area is still there; it seems like a difference between the two seasons, where it is slightly more misclassified than in winter, but less than that in spring. Nevertheless, the rest of the area looks fine. Moreover, here there is no confusion between the river and the flooded area; the river is nicely classified. Therefore, combining the images from the two seasons visually improves the overall classification results.

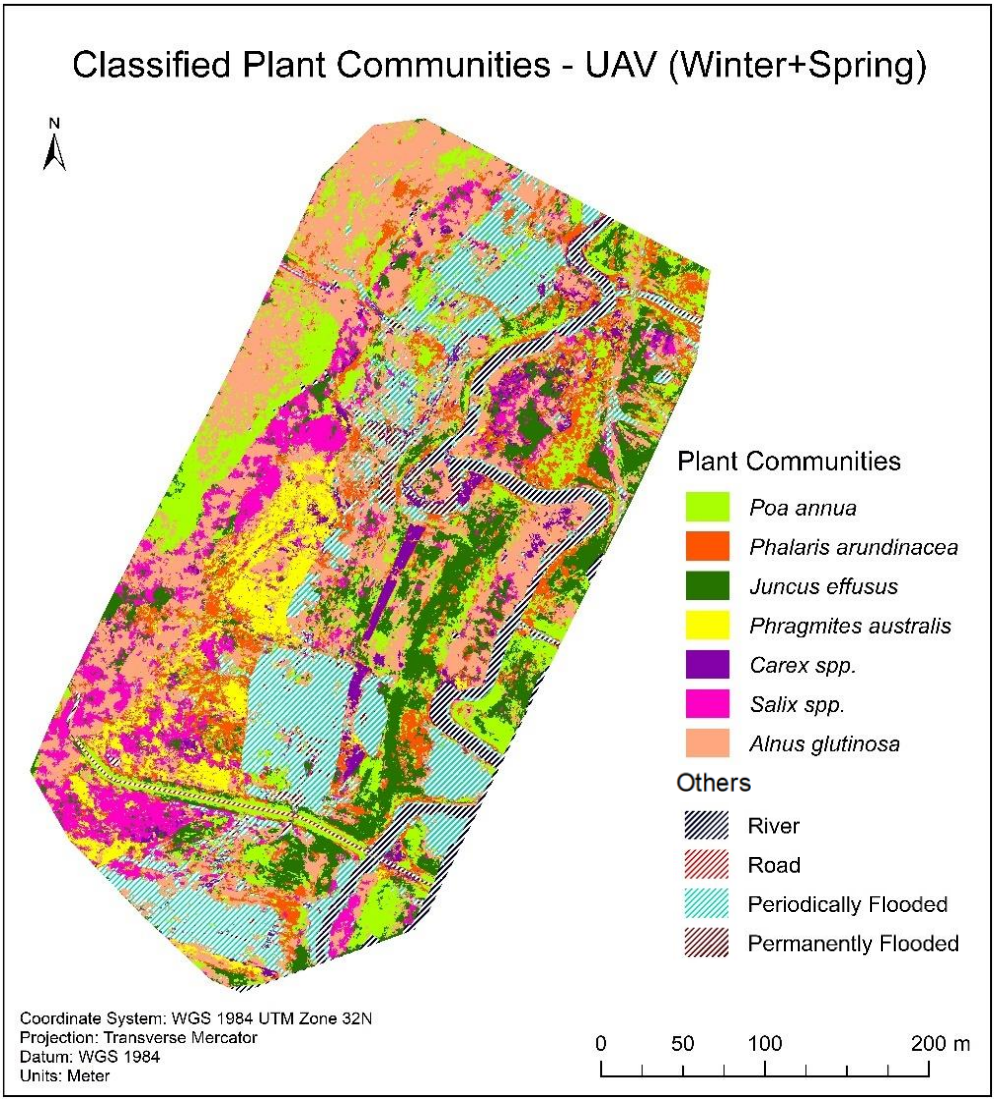

Figure 16. Classified plant communities map for the combined orthomosaic (winter + spring)

3.1.3. Accuracy Assessment

The following figures present the error matrices for the classification results of the orthomosaics. The values in the error matrices were rounded off for easy interpretation and the classes that are not of interest were merged as 'Others'. The actual classes along with their original values can be found in Appendix V.

As can be seen in *Table 11*, the Accuracy for the Classes of Interest (ACoI) and the Overall Accuracy (OA) of the winter orthomosaic in classifying plant communities is 84% and 86%, respectively. The community of *Carex* spp. (shrub) and *Salix* spp. (tree) have the highest Producer's Accuracy (PA) i.e., 100%. Whereas the community of *Phragmites australis* (shrub) has the lowest PA, i.e., 70%. In terms of the User's Accuracy (UA), shrubs consisting of the communities of *Phragmites australis* and *Carex* spp. have the highest accuracy i.e., 100%, whereas the community of *Salix* spp. (tree) has the lowest i.e., 67%.

User Class/Samples	*Poa an.*	*Phal. au.*	*Juncus e.*	*Phra. as.*	*Carex* s.	*Salix* s.	*Alnus g.*	Others	Sum
Poa annua	11	1	0	0	0	0	0	0	12
Phalaris arundinacea	0	10	0	3	0	0	1	0	14
Juncus effusus	1	1	12	0	0	0	0	0	14
Phragmites australis	0	0	0	7	0	0	0	0	7
Carex spp.	0	0	0	0	1	0	0	0	1
Salix spp.	0	0	0	0	0	4	1	1	6
Alnus glutinosa	0	1	1	0	0	0	9	0	11
Others	0	0	0	0	0	0	0	14	14
Sum	12	13	13	10	1	4	11	15	79
Classes of Interest	84%								
Overall Accuracy	86%								
Producer's Accuracy	92%	77%	92%	70%	100%	100%	82%	93%	
User's Accuracy	92%	71%	86%	100%	100%	67%	82%	100%	

Table 11. Error matrix produced for the accuracy assessment of the classification results for the winter orthomosaic, where the shades of green from light to dark indicate grass, shrub and tree life forms respectively

For the spring error matrix (*Table 12*), the ACoI is 60% and the OA is 65%, which is the lowest out of the three classifications. Both the PA and UA are the highest for the class 'Others', but as the focus of this study is on plant communities, this class is not considered in the following description. Therefore, the community of *Alnus glutinosa* (tree) has the highest PA i.e., 82%, whereas *Poa annua* (grass) has the lowest PA i.e., 42%. In terms of the UA, *Phragmites australis* (shrub) has the highest (75%) while *Phalaris arundinacea* (grass) has the lowest (45%).

User Class/Samples	*Poa an.*	*Phal. au.*	*Juncus e.*	*Phra. as.*	*Carex* s.	*Salix* s.	*Alnus g.*	Others	Sum
Poa annua	5	2	0	1	0	0	1	0	9
Phalaris arundinacea	5	8	1	2	0	1	1	0	18
Juncus effusus	0	1	8	0	0	3	0	0	12
Phragmites australis	0	1	0	6	1	0	0	0	8
Carex spp.	0	0	0	1	3	0	0	2	6
Salix spp.	0	0	3	0	0	3	0	0	6
Alnus glutinosa	2	1	1	0	0	0	9	0	13
Others	0	0	0	0	0	0	0	13	13
Sum	12	13	13	10	4	7	11	15	85
Classes of interest	60%								
Overall Accuracy	65%								
Producer's Accuracy	42%	62%	62%	60%	75%	43%	82%	87%	
User's Accuracy	56%	45%	67%	75%	50%	50%	69%	100%	

Table 12. Error matrix produced for the accuracy assessment of the classification results for the spring orthomosaic, where the shades of green from light to dark indicate grass, shrub and tree life forms respectively

As can be seen in *Table 13*, both the ACoI and OA for the combined orthomosaic are 87%. In terms of the PA, the community of *Carex* spp. (shrub) and *Salix* spp. (tree) have the highest i.e., 100%, while the lowest i.e., 70% is for the community of *Phragmites australis* (shrub). Whereas, the UA is the highest for the community of *Phragmites australis* (shrub) and *Poa annua* (grass) i.e., 100% and lowest for the community of *Carex* spp. (shrub) i.e., 67%.

User Class/Samples	*Poa an.*	*Phal. au.*	*Juncus e.*	*Phra. as.*	*Carex* s.	*Salix* s.	*Alnus g.*	Others	Sum
Poa annua	11	0	0	0	0	0	0	0	11
Phalaris arundinacea	1	10	0	3	0	0	0	0	14
Juncus effusus	0	2	11	0	0	0	0	0	13
Phragmites australis	0	0	0	7	0	0	0	0	7
Carex spp.	0	0	0	0	4	0	1	1	6
Salix spp.	0	0	0	0	0	7	1	1	9
Alnus glutinosa	0	0	1	0	0	0	10	0	11
Others	0	1	0	0	0	0	0	18	19
Sum	12	13	12	10	4	7	12	20	90
Classes of interest	87%								
Overall Accuracy	87%								
Producer's Accuracy	92%	77%	92%	70%	100%	100%	83%	90%	
User's Accuracy	100%	71%	85%	100%	67%	78%	91%	95%	

Table 13. Error matrix produced for accuracy assessment of the classification results for the combined orthomosaic, where the shades of green from light to dark indicate grass, shrub and tree life forms respectively

In conclusion, the combined orthomosaic results in the highest accuracy (both ACoI and OA), followed by the winter and the spring orthomosaic.

3.2. Satellite Results

The results for Satellite Imagery include the classified maps and their error matrices for both Sentinel-2 and Superview-1 and their variable importance graphs.

3.2.1. Classification

The classification results for the Satellite Imagery produced using Random Forest in R, are presented in the following figures. The classified plant communities map for Sentinel-2 produced using only field samples is presented in *Figure 17*, whereas the one produced using additional UAV-obtained samples is in *Figure 18*. The classified maps for SuperView-1 are presented in *Figure 19* & *Figure 20*, with only field samples and with additional UAV-obtained samples, respectively. As the Satellite Imagery is a multi-temporal stack, the combined samples with 11 classes (7 for plant communities and 4 for others) were used for the classification. The additional UAV samples were also collected for these 11 classes. Moreover, in the following description, the abbreviation FS is used to refer to the classified maps produced using only field samples, whereas FAS is used to refer to the classified maps produced using the additional UAV obtained samples i.e., Field samples + UAV obtained samples.

In the case of Sentinel-2, the visual comparison of the classification results show significant differences between the two maps. A lot of the area classified as *Salix* spp. in the FS (*Figure 17*), is classified as *Alnus glutinosa* in FAS (*Figure 18*), both are trees. The same difference can be observed where a lot of areas classified as *Phalaris arundinacea* and *Juncus effusus* in FS are classified as *Poa annua* in FAS (all three are grasses). Lastly, the class 'Periodically Flooded' is more visible in the FAS roughly in the centre, whereas in the FS it is comparatively not.

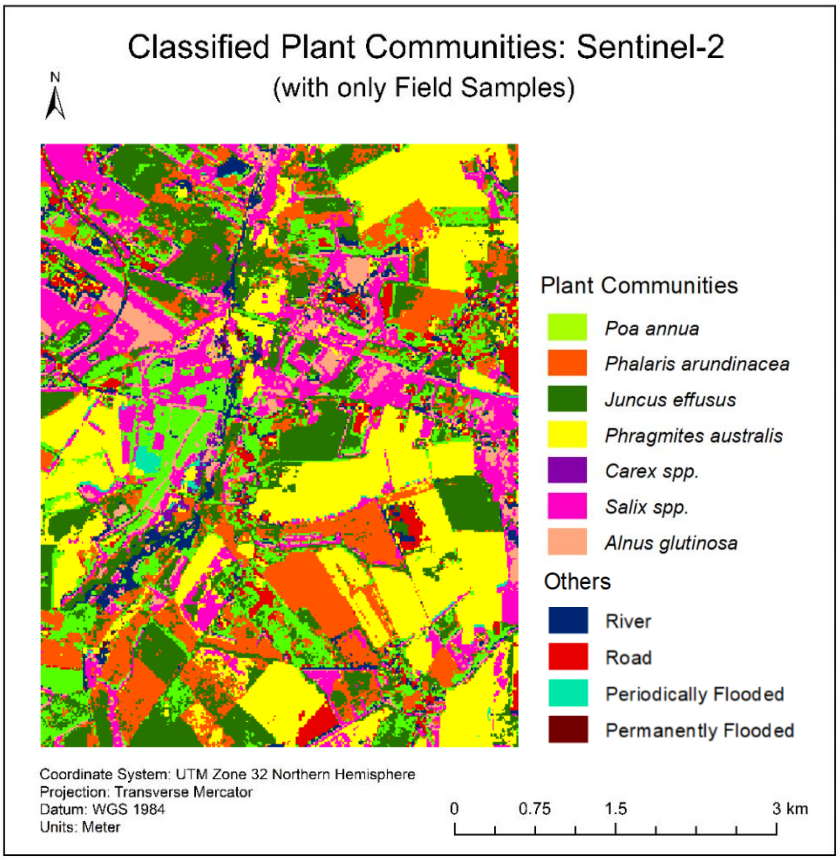

Figure 17. Classified Plant Communities Map: Sentinel-2 produced using only field samples

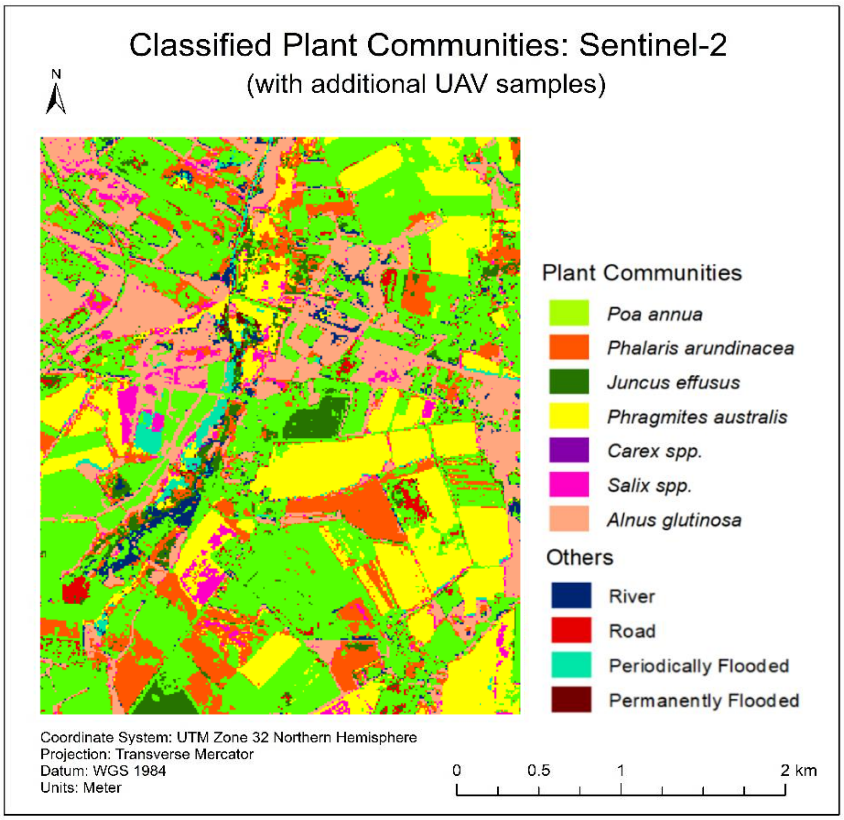

Figure 18. Classified Plant Communities Map: Sentinel-2 produced using additional UAV samples

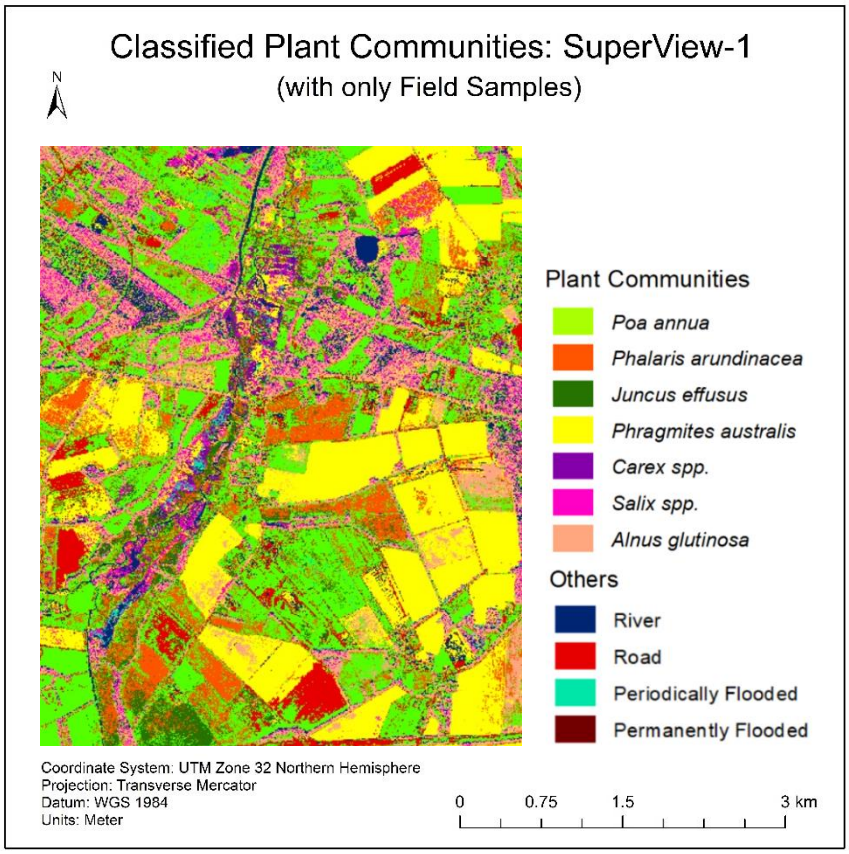

Figure 19. Classified Plant Communities Map: SuperView-1 produced using field only samples

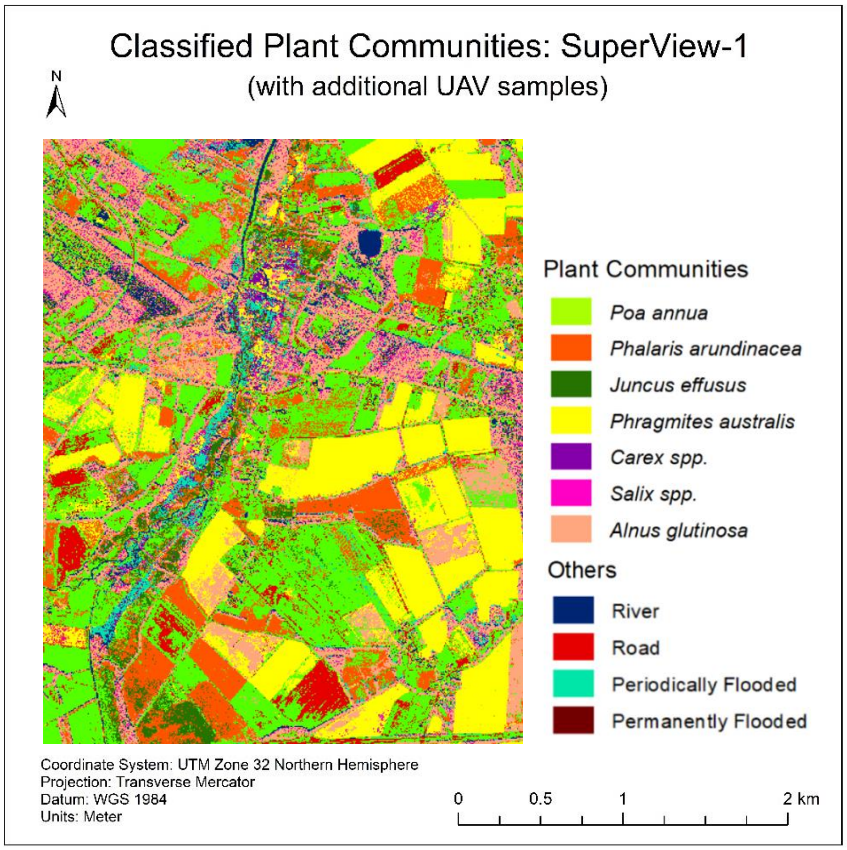

Figure 20. Classified Plant Communities Map: SuperView-1 produced using additional UAV samples

In the case of SuperView-1, there is not as much visible difference between the two classification results at the given scale. However, some similar differences as were in the case of Sentinel-2, can be observed, though they cover a comparatively smaller area in this case. One is with trees, where the area classified as *Salix* spp. in the FS (*Figure 19*), is classified as *Alnus glutinosa* in FAS (*Figure 20*). Another difference can be observed along the stream, which is classified as 'River' in FS (*Figure 19*) but as 'Periodically Flooded' in FAS (*Figure 20*). Moreover, the maps also look a bit speckled and have more noise as compared to Sentinel-2, which could be due to the difference in spatial resolutions.

3.2.2. Accuracy Assessment

This section consists of the error matrices produced for the accuracy assessment of the satellite classification results. The error matrices for the classification results of Sentinel-2 with only field samples and with additional UAV obtained samples are presented in *Table 14* and *Table 15*, respectively. Whereas the ones for SuperView-1 with only field samples and with additional UAV obtained samples are presented in *Table 16* and *Table 17*, respectively. Here also the classes that are not of interest have been merged as 'Others' and the values have been rounded off. The error matrices with the original values for all 11 classes can be found in Appendix VI.

User Class/Samples	*Poa an.*	*Phal. au.*	*Juncus e.*	*Phra. as.*	*Carex* s.	*Salix* s.	*Alnus g.*	Others	Sum
Poa annua	4	3	0	0	0	0	7	8	22
Phalaris arundinacea	2	3	2	0	0	1	0	0	8
Juncus effusus	3	4	10	0	0	0	0	0	17
Phragmites australis	1	0	0	10	0	2	0	3	16
Carex spp.	0	0	0	0	4	0	0	4	8
Salix spp.	0	0	0	0	0	4	0	0	4
Alnus glutinosa	0	2	0	0	0	0	5	0	7
Others	2	1	1	0	0	0	0	5	9
Sum	12	13	13	10	4	7	12	20	91
Classes of interest	60%								
Overall Accuracy	49%								
Producer's Accuracy	33%	23%	77%	100%	100%	57%	42%	25%	
User's Accuracy	18%	38%	59%	63%	50%	100%	71%	56%	

Table 14. Error matrix produced for accuracy assessment of the classification results of Sentinel-2 using only field samples, where the shades of green from light to dark indicate grass, shrub and tree life forms respectively

As can be seen in *Table 14*, for Sentinel-2, the classification using only the field samples resulted in the ACoI of 60% and OA of 49%. The community of shrubs *Phragmites australis* and *Carex* spp. have the highest PA of 100%, whereas the community of *Phalaris arundinacea* (grass) has the lowest of 23%. For the UA, the community of *Salix* spp. (tree) has the highest accuracy of 100%, while *Poa annua* (grass) has the lowest of 18%.

User Class/Samples	*Poa an.*	*Phal. au.*	*Juncus e.*	*Phra. as.*	*Carex* s.	*Salix* s.	*Alnus g.*	Others	Sum
Poa annua	5	5	1	0	0	0	1	0	12
Phalaris arundinacea	1	3	3	0	0	1	0	1	9
Juncus effusus	2	5	9	0	3	0	0	0	19
Phragmites australis	0	0	0	6	0	0	0	2	8
Carex spp.	0	0	0	0	1	0	0	0	1
Salix spp.	0	0	0	0	0	4	0	0	4
Alnus glutinosa	0	0	0	0	0	0	11	0	11
Others	4	0	0	4	0	2	0	17	27
Sum	12	13	13	10	4	7	12	20	91
Classes of interest	64%								
Overall Accuracy	62%								
Producer's Accuracy	42%	23%	69%	60%	25%	57%	92%	85%	
User's Accuracy	42%	33%	47%	75%	100%	100%	100%	63%	

Table 15. Error matrix produced for accuracy assessment of the classification results of Sentinel-2 using additional UAV samples, where the shades of green from light to dark indicate grass, shrub and tree life forms respectively

The classification using additional UAV obtained samples (*Table 15*) increases the ACoI by 4% and the OA by 13%. In this case, the community of *Alnus glutinosa* (tree) has the highest PA i.e., 92%, while the community of *Phalaris arundinacea* (grass) has the lowest i.e., 23%. In the case of the UA, three communities have 100% accuracy i.e., *Carex* spp. (shrub), *Salix* spp. (tree) and *Alnus glutinosa* (tree), while the lowest is for the community of *Phalaris arundinacea* (grass) i.e., 33%.

For SuperView-1 as can be seen in *Table 16*, the classification results using only field samples resulted in the ACoI of 64% (same as the one for Sentinel-2 classified using additional UAV samples) and the OA of 87%. Here the community of *Alnus glutinosa* (tree), has the highest PA of 83%, while the lowest is of *Phalaris arundinacea* (grass) i.e., 23%. In the case of the UA, the community of *Phragmites australis* (shrub) has the highest i.e., 88%, while *Phalaris arundinacea* (grass) has the lowest i.e., 38%.

User Class/Samples	*Poa an.*	*Phal. au.*	*Juncus e.*	*Phra. as.*	*Carex* s.	*Salix* s.	*Alnus g.*	Others	Sum
Poa annua	8	3	1	0	0	0	0	2	14
Phalaris arundinacea	2	3	3	0	0	0	0	0	8
Juncus effusus	0	7	9	0	1	1	1	1	20
Phragmites australis	1	0	0	7	0	0	0	0	8
Carex spp.	0	0	0	1	3	0	0	0	4
Salix spp.	0	0	0	1	0	5	1	1	8
Alnus glutinosa	1	0	0	0	0	1	10	0	12
Others	0	0	0	1	0	0	0	16	17
Sum	12	13	13	10	4	7	12	20	91
Classes of interest	64%								
Overall Accuracy	87%								
Producer's Accuracy	67%	23%	69%	70%	75%	71%	83%	80%	
User's Accuracy	57%	38%	45%	88%	75%	63%	83%	94%	

Table 16. Error matrix produced for accuracy assessment of the classification results of SuperView-1 using only field samples, where the shades of green from light to dark indicate grass, shrub and tree life forms respectively

For SuperView-1, the classification using additional UAV-obtained samples (*Table 17*) increases the ACoI by 3%, whereas it reduces the OA by 19%. The communities of *Alnus glutinosa* (tree) and *Poa annua* (grass) have the highest PA i.e., 92%, while the lowest is for *Phragmites australis* (shrub) i.e., 40%. However, in the case of the UA, *Phragmites australis* (shrub) has the highest accuracy of 100%, while the community of *Carex* spp. (shrub) has the lowest i.e., 33%.

User Class/Samples	*Poa an.*	*Phal. au.*	*Juncus e.*	*Phra. as.*	*Carex* s.	*Salix* s.	*Alnus g.*	Others	Sum
Poa annua	11	2	0	0	0	0	0	2	15
Phalaris arundinacea	1	6	4	0	0	0	0	1	12
Juncus effusus	0	5	9	0	1	1	1	1	18
Phragmites australis	0	0	0	4	0	0	0	0	4
Carex spp.	0	0	0	4	2	0	0	0	6
Salix spp.	0	0	0	1	0	3	0	0	4
Alnus glutinosa	0	0	0	0	1	2	11	0	14
Others	0	0	0	1	0	1	0	16	18
Sum	12	13	13	10	4	7	12	20	91
Classes of interest	67%								
Overall Accuracy	68%								
Producer's Accuracy	92%	46%	69%	40%	50%	43%	92%	80%	
User's Accuracy	73%	50%	50%	100%	33%	75%	79%	89%	

Table 17. Error matrix for accuracy assessment of classification results of SuperView-1 using additional UAV samples, where the shades of green from light to dark indicate grass, shrub and tree life forms respectively

In conclusion, SuperView-1 classified using additional UAV-obtained samples has the highest ACoI and Sentinel-2 with only field samples has the lowest. In the case of the OA, SuperView-1 with only field samples has the highest and Sentinel-2 with only field samples has the lowest.

Therefore, based on this analysis it can be concluded that SuperView-1 results in higher ACoI and OA than Sentinel-2. Moreover, the additional UAV-obtained samples improve ACoI for both Sentinel-2 and SuperView-1, however it does not improve the OA for SuperView-1.

3.2.3. Variable Importance

The Variable Importance plots generated during the Random Forest classification for the satellite imagery are presented in the figures below. It consists of two plots - the Mean Decrease Accuracy (MDA) and Mean Decrease Gini (MDG). The variables are presented in descending order, from the highest importance to the lowest (top to bottom). The variables are denoted in the format of 'XDate_Month_Year_Layer/Band/Index'.

As can be seen in *Figure 21*, for Sentinel-2 classified using only field samples, the green layer of the 26-06-2020 imagery has the highest Mean Decrease Accuracy (MDA), very closely followed by the red layer of 03-11-2020. While in the case of Mean Decrease Gini (MDG) the red layer of 03-11-2020 has the highest, very closely followed by the green layer of the 26-06-2020 imagery. Whereas band 5 (Vegetation Red Edge) of the 22-04-2020 imagery has both the lowest MDA and MDG.

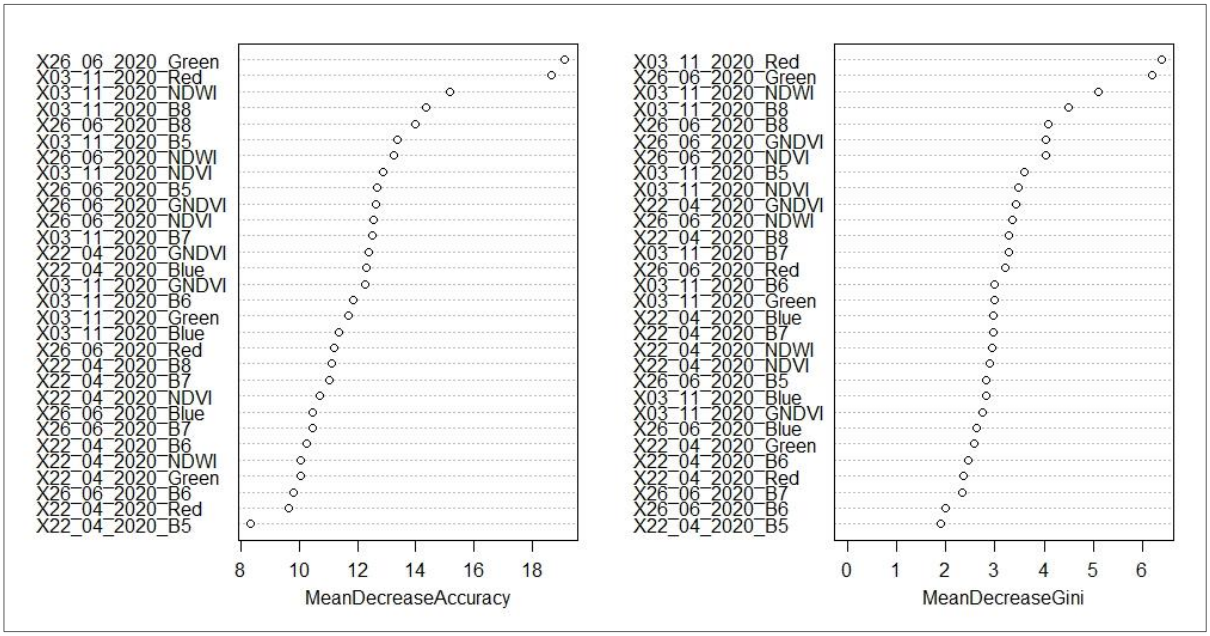

Figure 21. Variable Importance plot for Sentinel-2, produced while using only field samples to classify the imagery using RF

In the case of Sentinel-2 with additional UAV samples (*Figure 22*), again the green layer for 26-06-2020 has both the highest MDA and MDG, closely followed by the NDWI layer of the 03-11-2020 imagery. Whereas band 7 (Vegetation Red Edge) for 26-06-2020 has the lowest MDA and band 6 (Vegetation Red Edge) for the same date has the lowest MDG value.

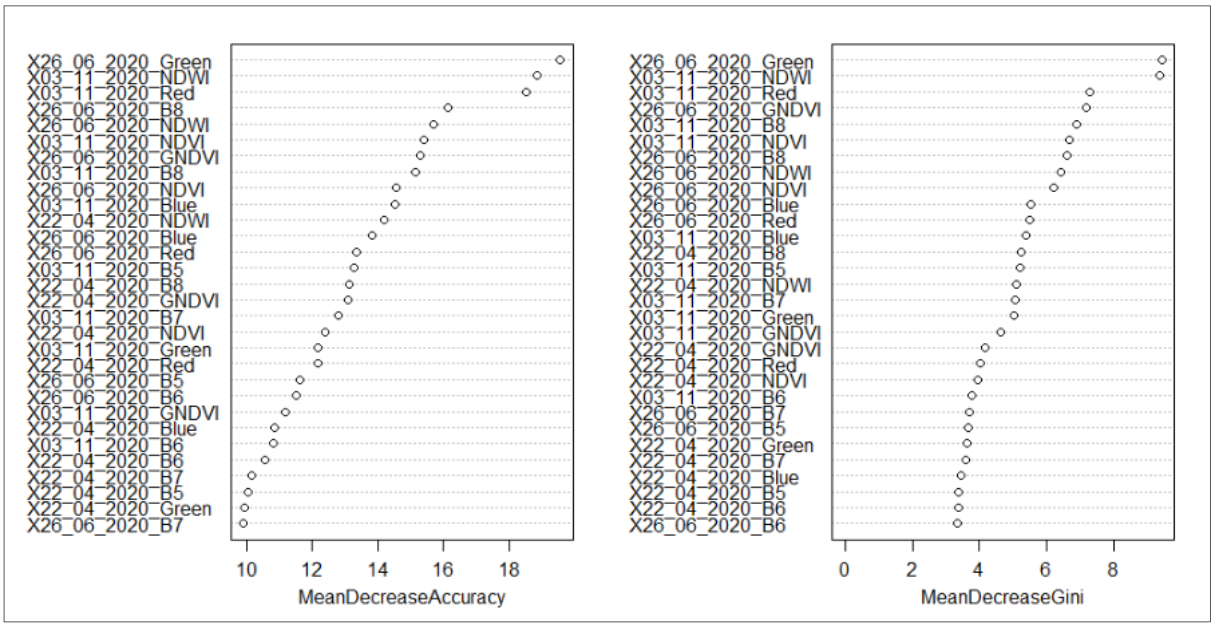

Figure 22. Variable Importance plot for Sentinel-2, produced while using additional UAV-obtained samples to classify the imagery using RF

For SuperView-1 classified using only field samples (*Figure 23*), the plot shows that the NIR layer of the 04-04-2020 imagery has both the highest MDA and MDG values. Whereas the red layer of the same date has the lowest MDA and MDG values.

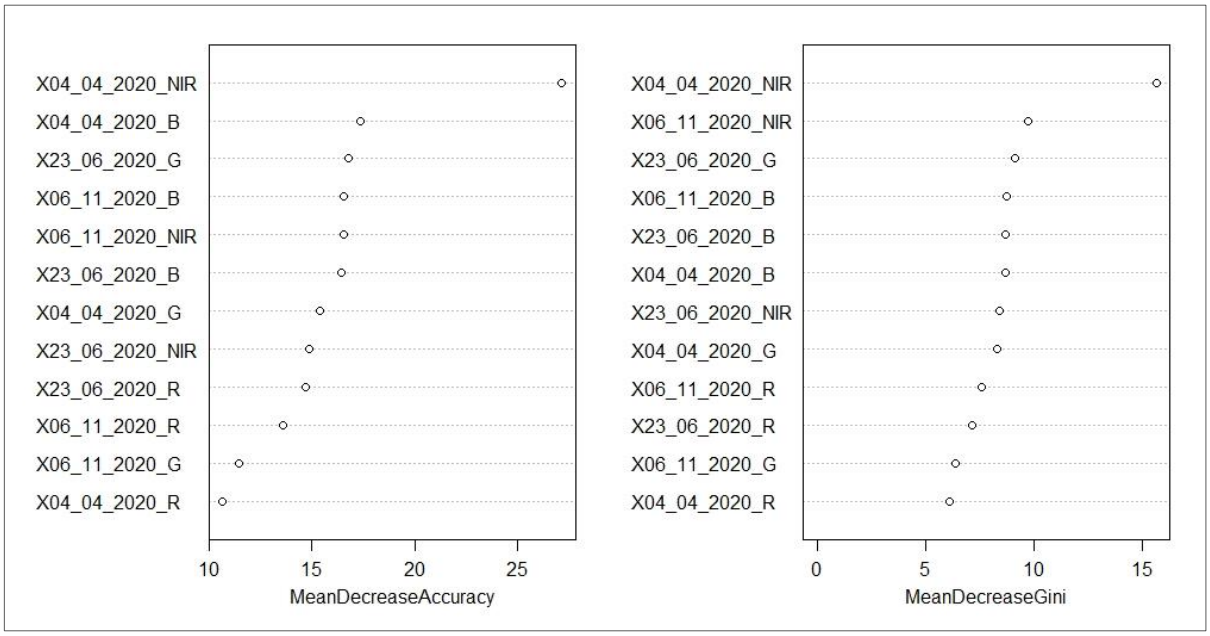

Figure 23. Variable Importance plot for SuperView-1, produced while using only field samples to classify the imagery using RF

In the case of SuperView-1 classified using additional UAV obtained samples (*Figure 24*), follows the same pattern, where the NIR layer for 04-04-2020 has the highest MDA and MDG values and the red layer of the same date has the lowest.

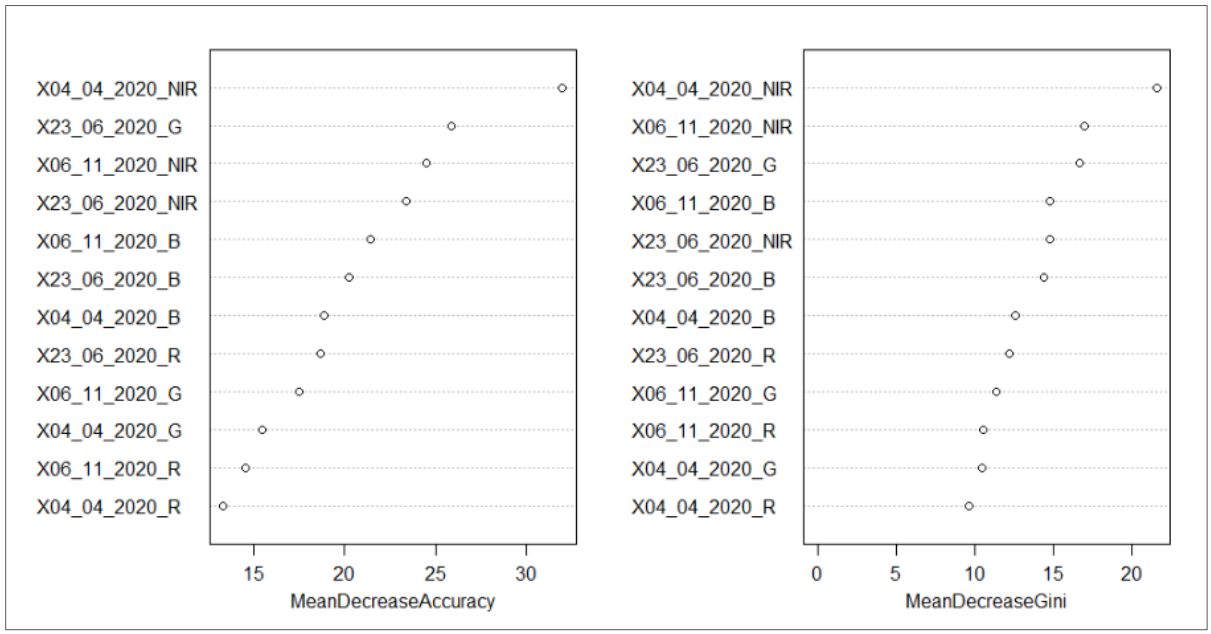

Figure 24. Variable Importance plot for SuperView-1, produced while using additional UAV obtained samples to classify the imagery using RF

Additional Analysis

The error matrices for the classification results for the additional analysis performed for Sentinel-2 are presented in the following tables. The error matrix for the classification done using only field samples is presented in *Table 18* and the one with additional UAV obtained samples is presented in *Table 19*. The error matrices with the original values (before rounding off) for all 11 classes (before merging the others) are presented in Appendix VII.

User Class/Samples	*Poa an.*	*Phal. au.*	*Juncus e.*	*Phra. as.*	*Carex* s.	*Salix* s.	*Alnus g.*	Others	Sum
Poa annua	4	3	0	0	0	0	7	7	21
Phalaris arundinacea	2	3	2	0	0	0	0	0	7
Juncus effusus	3	4	10	0	0	0	0	0	17
Phragmites australis	1	0	0	6	0	0	0	2	9
Carex spp.	0	0	0	0	4	0	0	2	6
Salix spp.	0	0	0	0	0	5	0	1	6
Alnus glutinosa	0	2	0	0	0	0	5	0	7
Others	2	1	1	4	0	2	0	8	18
Sum	12	13	13	10	4	7	12	20	91
Classes of interest	61%								
Overall Accuracy	49%								
Producer's Accuracy	33%	23%	77%	60%	100%	71%	42%	40%	
User's Accuracy	19%	43%	59%	67%	67%	83%	71%	44%	

Table 18. Error matrix for the classification results for the additional analysis of Sentinel-2 with only field samples, where the shades of green from light to dark indicate grass, shrub and tree life forms respectively

As can be seen in *Table 18*, the ACoI with only field samples is 61%, whereas the OA is 49%. Whereas, with additional UAV obtained samples (*Table 19*) the accuracies improve. The ACoI increases by 9% and OA by 17%. Moreover, the ACoI in this case (70%) is the highest out of all the satellite classification results, including the SuperView-1 results.

User Class/Samples	*Poa an.*	*Phal. au.*	*Juncus e.*	*Phra. as.*	*Carex* s.	*Salix* s.	*Alnus g.*	Others	Sum
Poa annua	5	5	1	0	0	0	1	0	12
Phalaris arundinacea	1	3	3	0	0	0	0	1	8
Juncus effusus	2	5	9	0	0	0	0	0	16
Phragmites australis	0	0	0	6	0	0	0	1	7
Carex spp.	0	0	0	0	4	0	0	1	5
Salix spp.	0	0	0	0	0	5	0	0	5
Alnus glutinosa	0	0	0	0	0	0	11	0	11
Others	4	0	0	4	0	2	0	17	27
Sum	12	13	13	10	4	7	12	20	91
Classes of interest	70%								
Overall Accuracy	66%								
Producer's Accuracy	42%	23%	69%	60%	100%	71%	92%	85%	
User's Accuracy	42%	38%	56%	86%	80%	100%	100%	63%	

Table 19. Error matrix for the classification results for the additional analysis of Sentinel-2 with additional UAV obtained samples, where the shades of green from light to dark indicate grass, shrub and tree life forms respectively

3.3. Comparison of Results

In this section, firstly, the UAV classification results have been compared to the satellite classification results. Secondly, the results of the satellite have been compared with the map in the vegetation report.

3.3.1. Comparison of UAV and Satellite

The classification results of the combined orthomosaic and the satellite imagery have been compared in *Figure 25*. In terms of the level of detail, SuperView-1 results are closer to the UAV results, apparently due to higher spatial resolution. Moreover, the same misclassification can be spotted in the SuperView-1 results, i.e., in the upper left corner (here classified as road), whereas in Sentinel-2 it is correctly classified. Besides that, in the maps classified using only field samples, there is more area classified as *Carex* spp.

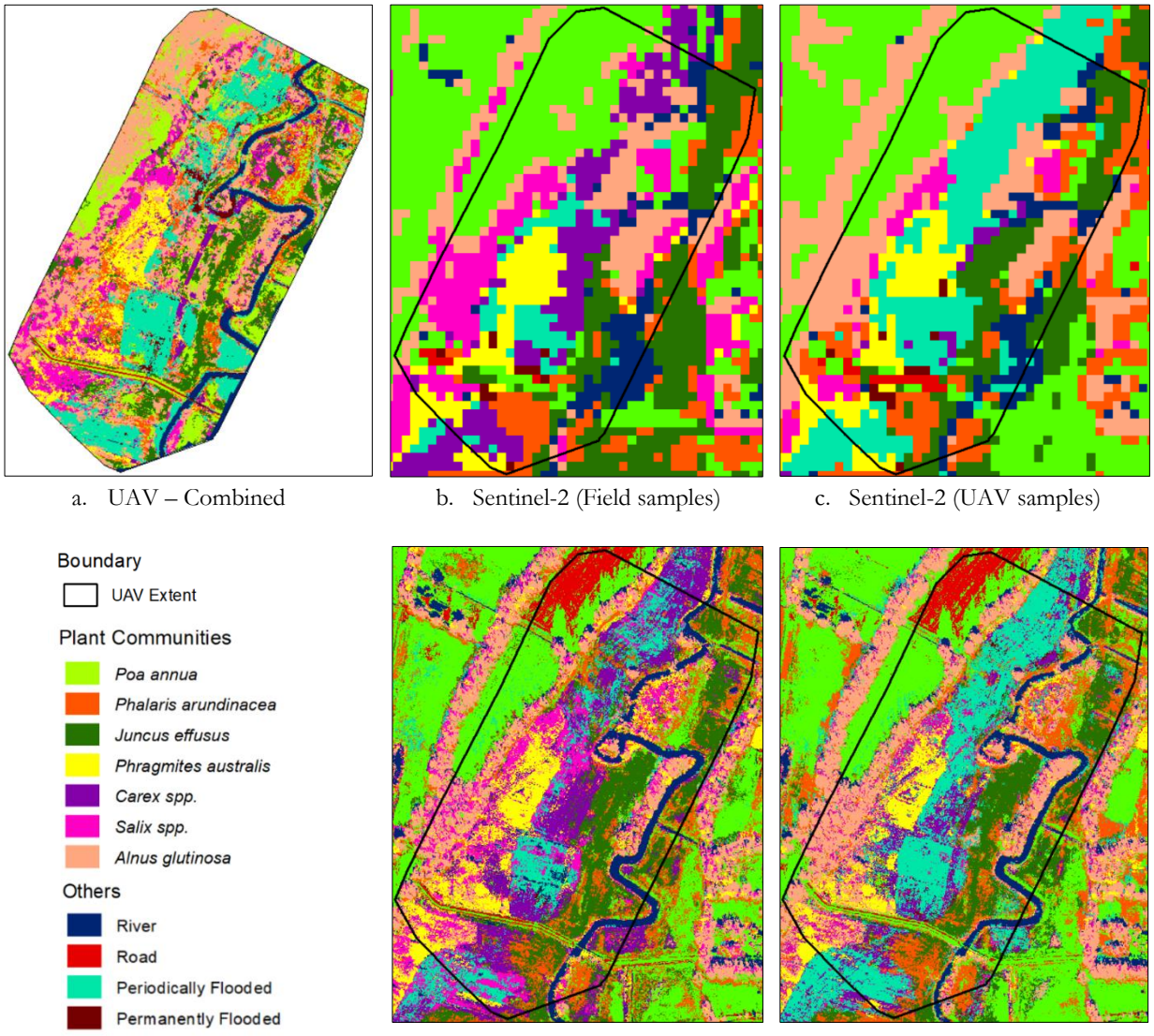

a. UAV – Combined
b. Sentinel-2 (Field samples)
c. Sentinel-2 (UAV samples)
d. SuperView-1 (Field samples)
e. SuperView-1 (UAV samples)

Figure 25. Comparison of the UAV classification results for the combined orthomosaic (winter + spring) with the classified maps for both Sentinel-2 and SuperView-1, along with a common legend for all the classifications

3.3.2. Comparison of Satellite and Vegetation Report Map

To make the satellite classified maps and the vegetation report map comparable, the classes in the satellite results were translated to that of the report as depicted in the legend in *Figure 26*. The 11 classes were merged according to their main life-forms, resulting in a total of four classes for the satellite classification i.e., grasses, shrubs, trees and others.

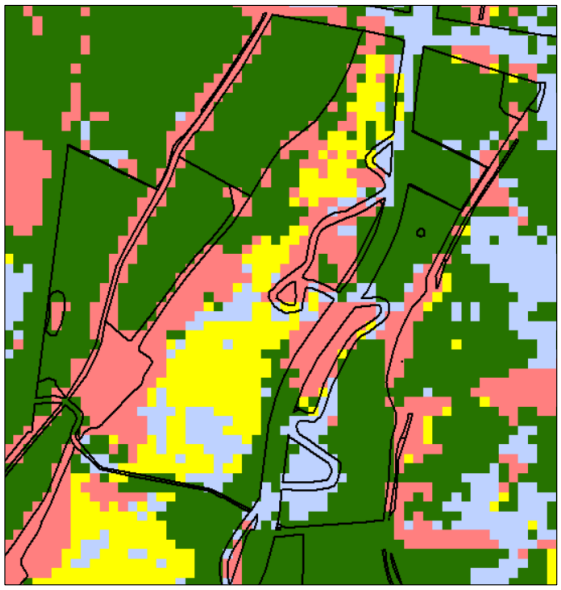

a. Sentinel-2 (only field samples)

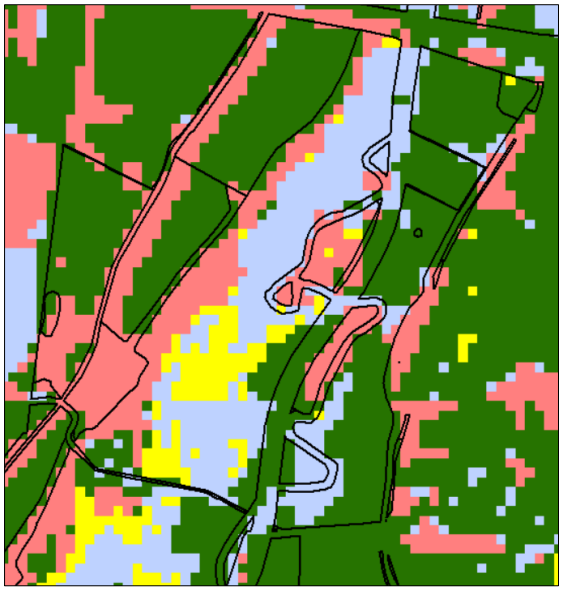

b. Sentinel-2 (additional UAV samples)

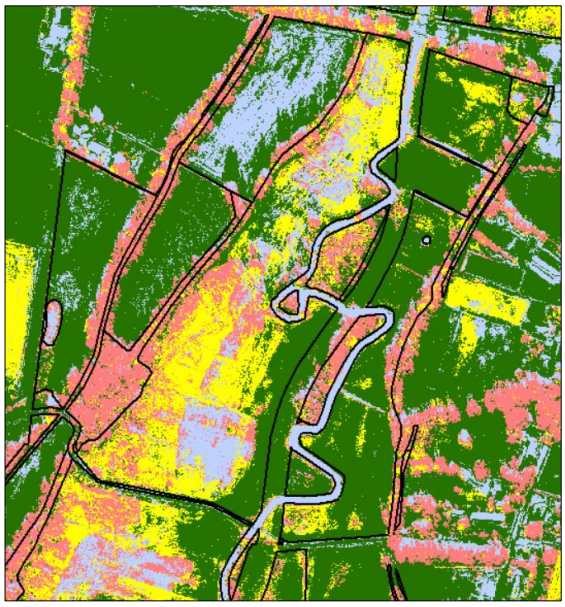

c. SuperView-1 (only field samples)

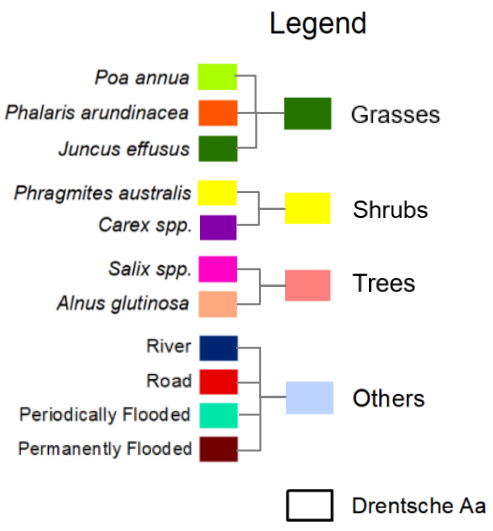

Figure 26. Classes in the satellite classified maps translated to the ones in the Vegetation Report for comparison, along with a new legend representing the newly merged classes (based on the main life-forms of plant communities)

For comparison with the already mapped data of Drentsche Aa for the vegetation report, the satellite classification with the highest ACoI i.e., SuperView-1 classified using additional UAV-obtained samples, was selected. *Figure 27* presents a one-on-one comparison of the two.

a. SuperView-1 (additional UAV samples)

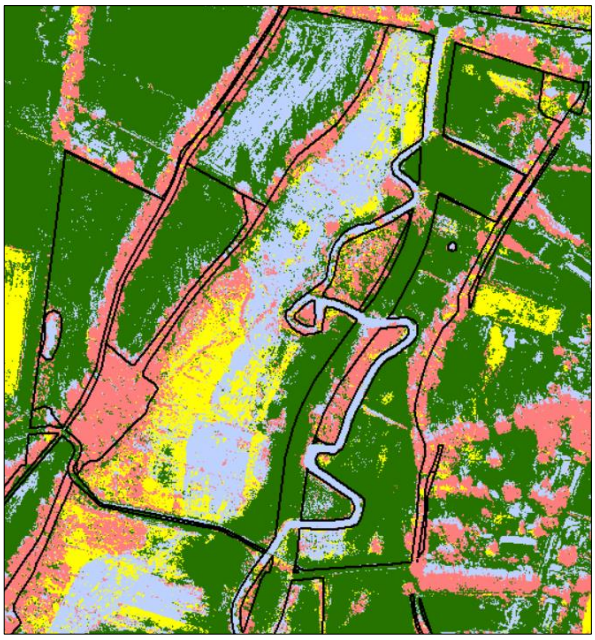

Legend

- Grasses
- Shrubs
- Trees
- Others
- Drentsche Aa boundary

b. Vegetation Report Map

Legend

- *Juncus effusus*
- *Juncus effusus* + *Holcus lanatus* + *Lotus uliginosus*
- *Holcus lanatus*
- Other grasses
- Other grasses + Others
- Sedge species
- *Holpijp*
- *Holpijp*+Sedge species
- Trees
- Others
- Drentsche Aa boundary

Figure 27. Comparison of the classification results of SuperView-1, using additional UAV-obtained samples with the reference map from the Vegetation Report along with their legends

The reference map from the vegetation report has more classes than the SuperView-1 classified map. Some of these additional classes represent communities that had just started to flourish in Spring, but their extent did not meet the minimum area cover requirement for this study and consequently, they could not be recorded. These communities mainly flower in the summer months, thus could have possibly flourished after the last field survey was conducted in spring. Therefore, the temporal difference in the field data collection has been kept in mind while qualitatively comparing the results. Also, the blank area in the vegetation report map is the one that was not mapped by the authority. A lot of this area consists of trees, as can be seen in the SuperView-1 classified map.

Merged Error Matrices for the Satellite

As the classes in the classified maps for the satellite imagery were merged to make it comparable to the reference map from the Vegetation Report, the error matrices were merged as well to examine how it influences the accuracies. The following tables represent the newly merged error matrices for all four satellite classification results. In all the descriptions below, the class 'Others' is not considered while discussing the PA and UA.

User Class/Samples	Grasses	Shrubs	Trees	Others	Sum
Grasses	31	0	8	8	47
Shrubs	1	14	2	7	24
Trees	2	0	9	0	11
Others	4	0	0	5	9
Sum	38	14	19	20	91
Classes of interest	81%				
Overall Accuracy	65%				
Producer's Accuracy	82%	100%	47%	25%	
User's Accuracy	66%	58%	82%	56%	

Table 20. Merged error matrix for classification results of Sentinel-2 using only field samples

The ACoI for Sentinel-2 classified using only field samples increased by 21% by merging the error matrix, whereas the OA increased by 16%. As can be seen in *Table 20*, the shrubs have the highest PA of 100%, while the trees have the lowest i.e., 47%. In the case of the UA, the trees have the highest i.e., 82% and the shrubs have the lowest i.e., 58%.

User Class/Samples	Grasses	Shrubs	Trees	Others	Sum
Grasses	34	3	2	1	40
Shrubs	0	7	0	2	9
Trees	0	0	15	0	15
Others	4	4	2	17	27
Sum	38	14	19	20	91
Classes of interest	92%				
Overall Accuracy	80%				
Producer's Accuracy	89%	50%	79%	85%	
User's Accuracy	85%	78%	100%	63%	

Table 21. Merged error matrix for classification results of Sentinel-2 using additional UAV samples

For Sentinel-2 classified using additional UAV-obtained samples, the ACoI increased by 28% and OA increased by 18% by merging the classes, resulting in the new ACoI and OA to be 92% and 80% respectively (*Table 21*). Here, the grasses have the highest PA of 89%, while the lowest is for shrubs i.e., 50%. Whereas for the UA, the trees have the highest i.e., 100%, while the shrubs again have the lowest i.e., 78%.

User Class/Samples	Grasses	Shrubs	Trees	Others	Sum
Grasses	36	1	2	3	42
Shrubs	1	11	0	0	12
Trees	1	1	17	1	20
Others	0	1	0	16	17
Sum	38	14	19	20	91
Classes of interest	91%				
Overall Accuracy	88%				
Producer's Accuracy	95%	79%	89%	80%	
User's Accuracy	86%	92%	85%	94%	

Table 22. Merged error matrix for classification results of SuperView-1 using only field samples

The ACoI and OA in the case of SuperView-1 classified using only field samples increased by 27% and 1% respectively, resulting in the new ACoI to be 91% OA to be 88%, as can be seen in *Table 22*. Grasses have the highest PA of 95%, while the shrubs have the lowest of 79%. However, in the case of the UA, the shrubs have the highest (92%), while the trees have the lowest (85%).

User Class/Samples	Grasses	Shrubs	Trees	Others	Sum
Grasses	38	1	2	4	45
Shrubs	0	10	0	0	10
Trees	0	2	16	0	18
Others	0	1	1	16	18
Sum	38	14	19	20	91
Classes of interest	93%				
Overall Accuracy	88%				
Producer's Accuracy	100%	71%	84%	80%	
User's Accuracy	84%	100%	89%	89%	

Table 23. Merged error matrix for classification results of SuperView-1 using additional UAV obtained samples

For SuperView-1 classified using additional UAV-obtained samples, the ACoI increased by 26% resulting in the new accuracy to be 93%, while OA increased by 20% resulting in the new accuracy to be 88% as can be seen in *Table 23*. Grasses have the highest PA (100%), while the shrubs have the lowest (71%). Whereas for the UA, the shrubs have the highest (100%) and grasses have the lowest (84%).

In conclusion, the accuracies follow the same order as with 11 classes, however the values significantly change. Here, SuperView-1 classified using additional UAV-obtained samples has the highest ACoI (93%), very closely followed by Sentinel-2 classified with additional UAV-obtained samples (92%) and SuperView-1 classified with only field sample (91%). In terms of OA, both the SuperView-1 results have the same accuracy of 88%, which is the highest. While Sentinel-2 classified using only field samples has the lowest ACoI (81%) and OA (65%). Moreover, here also the additional UAV-obtained samples improve the ACoI for both Sentinel-2 and SuperView-1.

4. DISCUSSION

The first part of this section discusses the effect of the seasons and plant life-forms on the classification results. The second and third part discusses about the effect of spatial and spectral resolution, the fourth and the fifth part consists of the discussion related to comparison of results. Finally, the last sections discuss the applicability and limitations of the methods.

4.1. Effect of Seasons and Plant life-forms on the UAV classification results

For the UAV part, two seasons were considered for this study - winter and spring; an additional analysis was done by combining the images from these two seasons to have a bi-seasonal stack. The plant communities were further divided into different plant life-forms namely grass, shrub and tree.

First, in terms of the ACoI, the highest was achieved by the combined orthomosaic (87%), followed by the winter (84%) and the spring orthomosaic (60%). The OA also follows the same order. Moreover, the individual accuracies (both PA & UA) for the combined and the winter orthomosaic are on the higher side compared to the spring orthomosaic, which declines for almost all classes and is the lowest. The reason for low accuracy in spring could be that most of the plant communities in focus were better visible and more distinguishable in winter. *Figure 28* & *Figure 29*, show the seasonal differences affecting the plants present in the study area.

a. Area in winter – 22 December 2020 b. Area in spring – 26 April 2021

Figure 28. A visual comparison of the seasonal differences in the vegetation present at a site in the study area

In winter, the plants have more colour differences and variations which are unique to each plant community, making them more separable. Whereas in spring the plant communities appear to be in the same colour tone i.e., in different shades of brown and a bit of green. The difference in physical form in terms of colour was lost due to the monochromatic appearance of the landscape in spring. Therefore, it led to a lot of misclassifications as there was no clear separation between the classes, which can also be observed in the spring error matrix in Section 3.1.3 (*Table 12*).

a. *Juncus effusus* (w) b. *Juncus effusus* (s) c. *Phalaris arundinacea* (w) d. *Phalaris arundinacea* (s)

Figure 29. Seasonal differences in the physical appearance of Juncus effusus and Phalaris arundinacea in winter (w) and spring (s)

As can be seen in *Figure 29*, the grasses have a more distinctive appearance in winter than in spring. The same was with shrubs. These differences in the phenology of plant communities also influenced the merged accuracies for the dominant plant-life forms (Appendix VIII). In winter, grasses and shrubs have high average accuracies ranging from 89 to 95%, whereas in spring, the accuracies considerably drop, with grasses having the lowest accuracies ranging from 77 to 79%. These seasonal differences can further be visually observed in the orthomosaics (*Figure 30*). In winter, *Juncus effusus* was dark green in colour, *Phalaris arundinacea* had a yellowish appearance, *Poa annua* was light/lime green and the colour of shrubs ranged from dark to light brown as can be seen in *Figure 30*a. This made these communities very distinguishable. Whereas in spring (*Figure 30*b), there was not much contrast in the landscape which caused overlapping among different classes. In the case of trees, they did not have leaves in both the seasons when the UAV images were acquired, but in winter as the rest of the landscape had a more distinctive appearance, trees could still be distinguished (*Figure 30*c). Whereas in spring, the trees had a similar appearance to the rest of the landscape (*Figure 30*d) and hence, classes were not very well separable.

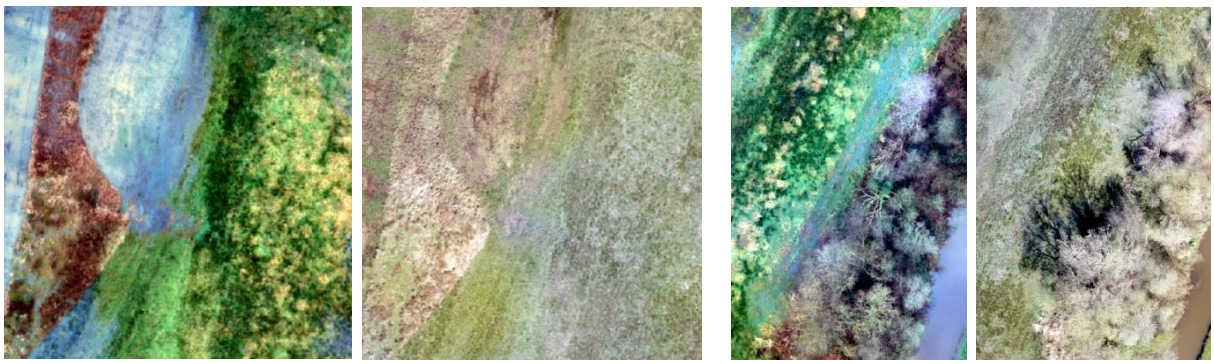

a. Shrubs & grasses in winter b. Shrubs & grasses in spring c. Trees in winter d. Trees in spring

Figure 30. Screenshots from the RGB winter and spring orthomosaics to show the seasonal differences and separability of the plant communities present in the study area, where red, green and blue colours are represented by bands 1, 2 and 3 respectively

Additionally, the spring images were acquired on a sunny day where the trees created shadows too. These shadowed areas could have negatively affected the accuracy, as also shown in a study by Lopatin et al. (2019) where shadows caused interclass variability and led to misclassification which significantly affected

the classification results. Consequently, in spring, the grasses seem to overlap amongst each other and with shrubs and trees as well, for instance, *Juncus effusus* (grass) and *Salix* spp. (tree) seem to overlap as can be seen in the error matrix for the spring results (*Table 12*). This could be because, in spring *Juncus effusus* had a branch-like brownish appearance (*Figure 29*b), which resembled the small branches of *Salix* spp., hence the possible reason for the misclassification. In conclusion, the winter orthomosaic results in better classification of plant communities in the study area than the spring orthomosaic. Besides, this year experienced the coldest spring in 30 years which delayed the vegetation growth and blossoming period (NL Times, 2021), which could have negatively affected the spring results.

Regarding the combined data which has the highest accuracy (both ACoI and OA), a point of discussion is that, if using the spring orthomosaic has any benefits i.e., if combining the two seasons improves the classification results. If analysed in terms of numbers, the ACoI increases by 3% and OA by only 1% for the combined results (in comparison to the winter results). Moreover, the individual accuracies (PA & UA) also seem to be mainly dominated by the winter results. However, the results when visually compared, tell a different story. In the classified map for winter (*Figure 14*) it can be noticed that some parts of the river are misclassified as flooded area and some flooded area as road. Whereas for the combined results (*Figure 16*) these misclassifications cannot be visually detected, due to the information from the spring orthomosaic, where these classes do not overlap as the area was not as flooded. Though these classes were not the focus of this study (were merged as others), they still positively influence the overall classification results. Moreover, another benefit of combining the two seasons is the merged field samples. Additional field samples could be collected for trees in spring as the area was more accessible, which did improve the individual accuracies for the community of trees, where the combined results have the highest PA and UA for trees (Appendix VIII). Thus, the nature of the plant communities of interest with respect to the season when they are more distinctive is crucial to consider while planning the UAV data acquisition.

These results are in line with a previous study by Lu & He (2017) which demonstrates the potential of UAV acquired data to effectively classify species in a heterogeneous grassland. The study also investigates the difference in the classification results for four different months (April, June, July and September) and identifies the month when species are most distinctive or dominant, which differs for each species. The highest accuracy of 86% was produced in the month of June. The study also encourages exploring the optimal spatial resolution and accordingly choosing a reasonable flying height for species classification. For this current study, the resolution of 2.6 cm worked well in classifying the plant communities in the study area. Contrastingly, in a study by Zweig et al. (2015) the resolution of 5 cm was too fine to work with the wetland vegetation. It resulted in a lot of misclassifications due to the similar colour and texture of the communities in focus, making them non-separable which led to high error rates and did not provide satisfactory classification results, until the classes were merged later. Thus, the resolution plays a very important role in determining the results. The importance of resolution, both spatial and spectral is discussed in more detail in the next sections.

4.2. Effect of Spatial and Spectral Resolution on the Satellite classification results

For this study two satellite imageries were used – Sentinel-2 and SuperView-1, both having different spatial and spectral resolutions. Concerning the classification results (in terms of accuracy), the ACoI improves by using additional UAV obtained samples for both the imageries.

In the case of Sentinel-2, the individual accuracies (PA & UA) significantly improve for some classes. However, in the error matrices (*Table 14 & 15*), high overlap can be observed amongst grasses. The additional UAV samples help in reducing the overlap and misclassification of grasses with shrubs and trees, but the confusion within the three grass communities still remains quite apparent. This could be due to the comparatively coarse spatial resolution of Sentinel-2, where one pixel could contain several classes (mixed pixels), making it difficult to assign it to one class. Therefore, the spatial resolution of Sentinel-2 does not allow to accurately separate all the grasses, even with additional UAV samples. On the other hand, the additional UAV samples clearly benefit the classification of trees, whereas shrubs seem to be classified better with only field samples. It could be because of the limited spatial resolution, where the UAV samples instead of providing additional information, confused the classifier in the case of shrubs as they covered smaller areas in comparison to that of trees. Lastly, the accuracy of 'others' significantly improves with additional UAV obtained samples, which also improves the OA (by 13%).

In the case of SuperView-1, the ACoI with only field samples is the same as the ACoI of Sentinel-2 with additional UAV-obtained samples (64%). With additional UAV samples the ACoI further increases, which is the highest out of all four classifications (67%). Grasses seem to be benefitted the most with better spatial resolution and additional UAV obtained samples, especially *Poa annua*. However, in the error matrix (*Table 17*), high overlap can still be observed between the remaining two grass communities (*Phalaris arundinacea* and *Juncus effusus)*. Additionally, *Carex* spp. (shrub) is largely misclassified as *Phragmites australis* (shrub), which caused some overlap between the two shrub communities as well. However, trees are comparatively less misclassified.

The possible reason for this could be that in the study area (as viewed in the satellite), the trees are found in continuous patches, with a distinct texture that makes them easier to be distinguished, as can be seen in *Figure 31*. Shrubs are not as homogeneous and distinct, but the way the management of the area has maintained them in geometric/symmetrical patches makes them somewhat dissociable. However, they are still confused with trees and grasses due to smaller patches and slightly similar physical appearance as perceived by the satellite imageries. On the other hand, grasses are more heterogeneous and found in discontinuous scattered patches, which makes it harder to separate with the given spatial resolution of the satellite imageries. Moreover, as the grasses have the lowest height, the shadow of trees and other larger plants happens to fall on them (*Figure 31*), which creates further problems and causes overlap with other classes. On the whole, trees and shrubs are more separable than grasses with the chosen satellite imageries. These results are in accordance with a study by Kattenborn et al. (2019), which shows that plant

community that occur in large patches and have distinct phenology are easier to classify and map than the ones that occur in scattered/small patches and have similar phenology. It also states that it further affects the visual delineation of classes and the process of collecting samples.

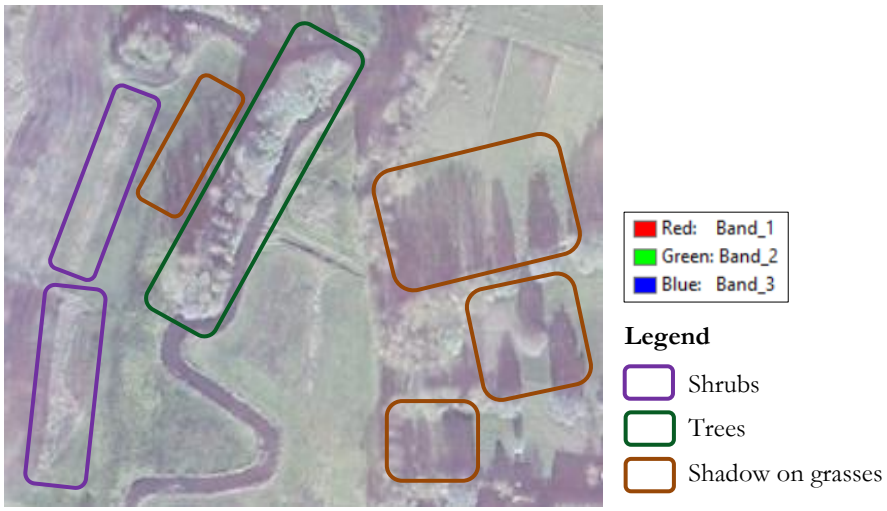

Figure 31. A subset of SuperView-1 imagery (06 November 2020) highlighting some marked areas

In conclusion, the satellite classification results are not satisfactory. The approach of using additional UAV samples does improve the accuracy for some classes but overall, in the end, some classes still remain inseparable. This is largely due to the spatial resolution of the satellite imageries which did not allow clear separation of the fine-scale grass communities. This inference is in congruence with a study by Rapinel et al. (2020) which shows that the plant communities map produced using Sentinel-2 was not accurate enough to be used as reference data, however, integrating it with field methods can be a useful approach and provide valuable information to select areas for further analysis.

The possible reasons for this could be, first, the field samples were collected in a very detailed manner which was more suitable for the UAV classification. Due to a large difference in spatial resolutions, the field samples need to be adjusted or merged to make them more appropriate for the satellite image classification. Nevertheless, these results do give insights on the classes which can and cannot be separated, along with the role the spatial and spectral resolution plays. Second, the field samples were concentrated in the area covered by the UAV, more samples could have been collected from nearby areas to ensure a better distribution for the satellite. Another reason could be the limited temporal information. For this study, the multi-temporal aspect for the satellite included three months, as SuperView-1 only had three good images of the study area for the year 2020. Sentinel-2 had abundant good images available, but they were not used to keep the temporal aspect similar to have a basis for comparison, as the spatial and spectral resolutions differed already. Additional temporal and spectral information could have compensated for the coarser spatial resolution. The results of the additional analysis for Sentinel-2 (*Table 18 & 19*) further verify this argument. The image with additional information layers (60 layers) when classified using the additional UAV obtained samples, significantly improves the accuracy. It produces the

highest ACoI (70%) out of all satellite classifications (including the SuperView-1). However, this image with additional layers when classified using only field samples does not seem to benefit the results. It gives almost the same results as without the additional layers (30 layers). The ACoI only improves by a percent and the OA remains the same. Hence, this not only validates that the additional temporal and spectral information improves the classification but also reemphasizes the benefit of using additional UAV obtained samples. Therefore, it can be concluded that Random Forest performs better with more samples. This is in line with a study by Shang et al. (2018), which also concludes that some of the advanced classifiers perform better and produce more stable results with an increase in sample size.

4.3. Effect of Seasons and Spectral Resolution on the classification results

For this study, satellite imagery from three months was used i.e., April, June and November. Based on the variable importance graphs for Sentinel-2 (*Figure 21 & 22*), the green, red, NDWI, NDVI, GNDVI, NIR (band 8) and Vegetation Red Edge (band 5) layers from June and November influence the accuracy more than band 6 & 7 (Vegetation Red Edge) from June and band 5 from April. For SuperView-1 (*Figure 23 & 24*), the NIR layer for April plays the most important role in classification, whereas the red layer of the same date is the least important. Therefore, for the satellite image classification, there is not one consistent date or month which is the most or least important. Here the different spectral bands or vegetation indices from the same date have varying importance.

On contrary, a study on floodplain grassland plant communities by Rapinel et al. (2019) concludes that the date/season has a higher influence on the accuracy as compared to the spectral bands. The study found out that between spring and early summer (April to June) is the most informative period to discriminate between plant communities. Whereas, between November to February is not suitable as it resulted in the lowest accuracy. The study determines the most suitable period for classification based on vegetation dormancy and senescence. This inference is not in line with the results produced for this current study.

Moreover, to further support this disagreement, the UAV results are discussed as they were the most accurate and detailed out of the ones produced for this study. The plant communities in focus were more distinct and easier to classify and map in winter (December) than in spring (April) as has been discussed in section 4.1. The information from spring only helped with the classification of plant communities in the combined orthomosaic (i.e., when combined with winter), while the winter orthomosaic on its own was more beneficial for discriminating plant communities. Although this is something entirely area and plant community-specific, which could further differ due to the change in climatic conditions or the management of the protected area. Yet, considering the delay in spring this year and assuming that in summer the vegetation in the area would have been at its peak, the following argument is stated. In a scenario like this where the vegetation is in full bloom and the landscape looks visually more similar (is mostly green), the spectral information becomes even more important. Particularly, in the case of the chosen satellite imageries with comparatively limited spatial resolutions. One of the advantages of Remote

Sensing techniques is the additional spectral information and possibility to calculate vegetation indices, which play an important role in classification (as evident in the case of Sentinel-2 for this study). Therefore, the classification of plant communities is also influenced by how distinct the classes are from each other along with the differences in their spectral reflectance, rather than primarily being determined by their peak growth period.

Another point of discussion here is that ideally vegetation surveys are conducted in spring or early summer. At the time when vegetation is usually at its peak, the weather conditions are more ideal to conduct field surveys and good quality satellite data is readily available too. While in winters, the harsh weather conditions could make it difficult to conduct fieldwork. Moreover, it is usually difficult to find good quality satellite imagery. For instance, none of the satellite images of the study area between December to February could be used for the analysis due to extremely high cloud cover. These conditions restrict exploring the information the winter season can offer. Winter could give insight into the habitat characteristics of a region like soil, level of flooding, etc. which could indirectly help in identifying the plant communities. However, the usefulness of this information depends on the nature of plant communities in focus. Nevertheless, it could be very beneficial in some cases, as was for this study. If the analysis relied entirely on satellite imagery, the results could have been completely different. Therefore, UAVs can fill this information gap, by providing good cloud-free data for winter.

4.4. Comparison of UAV and Satellite Results

The UAV imagery classified using OBIA produces the best classification results with the combined orthomosaic, with the highest ACoI of 87%. The individual accuracies are also on the higher side and the error matrix (*Table 13*) has fewer overlaps or misclassifications as compared to the satellite classification results. The UAV imagery with only two seasons provides better classification results than the satellite, which has information from three seasons. The reason is evidently the difference in spatial resolutions, as can be seen in *Figure 32*.

a. Sentinel-2 (03 Nov) b. SuperView-1 (06 Nov) c. UAV (22 Dec)

Figure 32. Screenshots of the same area in the satellite imageries and the orthomosaic at scale 1:250, where red, green and blue colours are represented by bands 1, 2 and 3 respectively

Though, one thing to notice here is that the ACoI for Sentinel-2 (64%) even with a coarser spatial resolution, is not very far away from that of SuperView-1 (67%) which has a comparatively better spatial resolution (both with additional UAV samples). It could be that the higher spectral resolution along with the additional information from the vegetation indices compensated for the coarser spatial resolution (as also shown in the additional analysis).

However, when the results are visually compared, the UAV classified maps have one very evident misclassified area in the upper right corner. The reason for this could be, that in winter, the water in the flooded areas reflected the grey sky as can be seen in *Figure 33*. It could have been confused with the greyish bare branches of trees, due to similar reflectance. Whereas in spring, the plant communities had a similar appearance as has been discussed in section 4.1, hence the reason for the misclassification. These differences were captured in the UAV images and can be seen in the orthomosaics as well (*Figure 11*), which consequently reflected in the classification results.

Figure 33. Water in the flooded area reflecting the grey sky in winter

The satellite imagery seems to have helped with this issue. When comparing the classified maps (*Figure 25*), it can be observed that in the case of Sentinel-2 this misclassification does not occur; the area is correctly classified as *Poa annua* (grass). This could be due to the additional information from the summer imagery, which was not there in the case of UAV. This could also be due to the higher spectral resolution of Sentinel-2. Whereas SuperView-1 only correctly classifies a part of this area, while the remaining area is misclassified as road (others). This could be due to two possible reasons; first the mowing pattern in the summer image (*Figure 34a*) and the slightly hazy winter image with shadows (*Figure 34b*). Moreover, in the study area, *Poa annua* was also found growing along the sides of the narrow strip of road. While reprojecting SuperView-1 in the same coordinate system, even a slight shift could have caused some samples to be on the wrong land cover class.

a. 23 June 2020 (summer) b. 06 November 2020 (winter)

Figure 34. Screenshot of the misclassified patch in two SuperView-1 imageries, where red, green and blue colours are represented by bands 1, 2 and 3 respectively

While comparing the rest of the map, some other differences can also be observed. First of all, the SuperView-1 classified maps visually seem to be closer to the UAV maps, whereas the Sentinel-2 maps are not as detailed. This is largely because of the difference in spatial resolution, but the overall pattern and classification on a coarser scale is still intact for Sentinel-2. However, with the maps classified using only field samples, over-classification can be observed. For both Sentinel-2 (*Figure 25*b) and SuperView-1 (*Figure 25*d) a lot more area is classified as *Carex* spp. (shrub). From knowing the study area, and the way the authority manages some communities, it cannot be that this is due to the information from the summer layer (the spread of these communities would not drastically change). This possibly comes from the limited field samples, which do not cover as many spectral differences representing the communities, as much as the additional UAV samples do. Hence, the satellite maps produced using additional UAV obtained samples visually seem to be closer to the UAV classified map. Therefore, additional UAV samples not only improve the figures/accuracies, but also the classified maps. Now between these two maps, the one with Sentinel-2 (*Figure 25*c) visually seems better, as the map with SuperView-1 (*Figure 25*e) under classifies *Salix* spp. and also has the misclassified upper left corner as road.

4.5. Comparison of Satellite Results with Vegetation Report Map

To compare the satellite classified maps with the vegetation report map, the classes were merged i.e., generalized to the plant life-form level, to link it to the ones in the report. In terms ACoI, it significantly improves for all four classification results, as the misclassification among the overlapping classes reduces. Here also the additional UAV obtained samples produce better classification results as compared to using only field samples. However, here the order slightly changes; the highest ACoI is obtained by Superview-1 with UAV samples (93%), closely followed by Sentinel-2 with UAV samples (92%) and SuperView-1 with field samples (91%).

While visually comparing the classified maps (*Figure 26 & 27*), the only major difference that could be observed is that the maps produced using UAV samples have more area classified as 'others', especially in the middle, which could be due to the flooded area. Other than that, the SuperView-1 maps still consist of the wrongly classified upper right corner (as others). However, for the one-on-one comparison with the vegetation report map (*Figure 27*), the SuperView-1 classified map produced using additional UAV samples was selected, as it has the highest (merged) ACoI. The first thing that comes into notice is that the vegetation report map has some empty spaces that are not mapped, which mainly consists of trees (strips of trees) and some grasses (right-hand side). It could be that this area was not under the management when the vegetation survey was conducted or could have not been mapped due to some other reason. In any case, the classified maps update and fill in this missing information. Besides that, the vegetation report map consists of a few more classes of plant communities. A lot of these communities are the ones that had just started to flourish when the last field samples were collected and as their extent did not match the minimum area requirement for this study, they could not be included in the analysis (these indicative

species are mentioned in section 2.3.4.). These species perhaps could have flourished in the summer months; thus, this difference could be due to the time/seasonal difference in the field survey period. This could also be a reason that *Juncus effusus* is mainly found with other grasses in the vegetation map and only one patch of its pure community is found. *Juncus effusus* was more distinct in winter, when the field samples for this study were collected, while the field survey for the vegetation report was conducted between May and September. Another difference is that the area covered mainly by sedge species in the vegetation map is classified as others and shrubs in the classified map. This again could be due to the seasonal differences, in summer when this area would not be flooded, it could possibly have sedge species. Therefore, the assumption that the differences between the two maps are due to the differences in data, methods and techniques used is most likely true. However, the country did experience two dry summers in 2018 and 2019, which could have had an impact on these communities. The study is a flooded grassland region, where the water table and the soil saturation are important characteristics of the vegetation. On the other hand, it could also be that the plant communities recovered from it last year (2020) as the country experienced a good amount of rainfall as compared to the previous two years. In fact, February 2020 was the wettest February in Dutch history; it was also the second warmest (NL Times, 2020). This could have positively affected the plant communities in the study area and hence a possible reason for no substantial change or shift in their extent. Therefore, it still cannot be assertively concluded if there is any change in the extent of plant communities, or if it is simply because of the differences in the mapping methods.

The final point of discussion is which out of the two satellite imageries is more suitable to classify plant communities in the study area. In terms of numbers, there is only one percent difference between the two highest ACoIs i.e., 93% for SuperView-1 and 92% for Sentinel-2, both classified using additional UAV obtained samples. With respect to the classified maps, the one for Sentinel-2 looks better, majorly due to the correctly classified area (upper left) which even the UAV could not correctly classify. Additionally, Sentinel-2 allows adding more information layers (dates, bands & indices) and increasing the temporal dimension of the analysis, which enhances the possibility of further improving the results (as shown by the additional analysis, *Table 19*). Other than that, SuperView-1 imagery is harder to access and download in comparison to Sentinel-2. It is only available to Dutch nationals and Dutch institutes (Netherlands Space Office, n.d.). In conclusion, the results of this study are more in favour of Sentinel-2 amongst the satellite data for similar applications.

4.6. Applicability of the methods

This study investigates if UAVs can be used to bridge the gap between field methods and satellite imagery to map plant communities for conservation. It tests an approach to see if the benefits of high spatial resolution of UAV imagery can be directed towards the satellite imagery to produce accurate maps covering a larger area. It uses Drentsche Aa as a case study area to test this method. Firstly, the UAV imagery produces very accurate and detailed maps, especially with the combined orthomosaic (winter and

spring). It furthermore revealed the advantage of the winter season over spring to classify the communities in focus, which is contrary to previous studies that claim spring to be the most ideal season for vegetation surveys and related work. Therefore, the UAV imagery successfully classifies plant communities in the study area with high accuracy. It further gives the management of the area scope of detailed mapping in a more efficient way. Secondly, the additional UAV obtained samples improve the classification results and accuracy of the satellite imagery. However, the results and the classified maps are still not as accurate. Nevertheless, when the classes were generalized to the plant life-form level to make it more comparable to the broader scale of the report, the accuracies and the classified maps improved. However, the finer details were lost; there was a trade-off between the number of classes and the accuracy.

This study aimed to bring the satellite classification results closer to the field observations with the help of UAVs, which it successfully does. But it was expected for the accuracy to be higher; nonetheless, it is a good starting point and can act as a road map to integrate UAVs with field methods. It revealed limitations of the data, methods, seasonal differences, nature of the plant communities in focus, etc. which provides a lot of scope of improvement for future work. In terms of the applicability of this method, with some refinements, it can be used to produce more detailed and reliable maps on a larger scale. This method can further be improved and adapted for classifying plant communities in another area or habitat, with necessary adjustments made in the data collection techniques (sampling method, UAV flying heigh, etc.) based on the area requirements. Moreover, if this approach is repeated yearly or with an interval of a few years, it could be used as a technique for a change detection analysis.

In conclusion, UAVs do have the potential to produce results that are close to ground surveys. Though field methods still play an important role in mapping plant communities, integrating them with UAVs can be a promising approach to improve the classification results of the satellite imagery. However, some further research is required to make it more precise on a large scale.

4.7. Limitations of the Research

The following points summarize the limitations of this research: -

- The number of field samples was not evenly distributed among all the plant communities. The study area is a grassland; hence it was majorly covered with grasses, therefore enough samples could be collected for grass communities. Even for trees, there were sufficient samples, as they were found in clusters covering a reasonable area. However, for shrubs it was not the case; they covered a comparatively smaller area. Furthermore, as the training points had to be kept spatially independent from the validation points, it further restricted the number of samples that could be collected. This was especially the case with *Carex* spp. which only had two patches, one of which was not accessible in winter due to flooding. However, in spring a few more samples could be collected, but the total number still remained comparatively low.

- Moreover, the field samples were only collected in the area covered by the UAV. Though the training and validation points were spatially kept independent, but for the satellite imagery, it could have resulted in some spatial autocorrelation. The time restrictions along with the breeding and migration season of birds (in nearby areas) did not allow acquiring more UAV data, which could have been used to collect more samples to classify the satellite imagery.
- GCPs could not be used to improve the positional accuracy of the orthomosaics. The study area did not have many well-distributed natural distinct points. Some natural intersections were found along the river and road, but they were very close to the edges. Theoretically, GCPs should be marked away from the boundary of the area, therefore, the points along the road and river could not be used. Additionally, as the first UAV dataset was acquired in winter, the area was flooded, not only making it harder to access but also not making it possible to place artificial points using checkboards. Due to the same reason, it was also difficult to mark MTPs while combining all the individually processed MS flights. In the end, the positional accuracy of the orthomosaics was visually validated with ArcGIS online, by observing if they fit well with some recognisable or linear features like the road and river.
- The ESP (Estimation of Scale Parameter) tool could not be used to determine the best parameters values for segmentation during OBIA. The processing power of the computer did not allow this tool to successfully work. Therefore, the values were determined by a trial-and-error method.
- The limited data availability for SuperView-1 imagery restricted the multi-temporal dimension for the satellite analysis to only three dates/imageries. Adding more layers to the satellite stack could have allowed exploring the possibilities of improving the results, as has been demonstrated by the additional analysis (*Table 19*).
- The difference between the classified maps and the vegetation map, not only with respect to data type and methods but the seasonal difference of data collection and field survey. Moreover, the UAV data did not have a summer image, when the samples for the vegetation report were mainly collected, therefore, it could not be concluded if there is a change in the extent of the plant communities.

5. CONCLUSION & RECOMMENDATIONS

5.1. Conclusion

This study investigates the potential of UAVs to improve the remote sensing techniques to map plant communities for conservation. It tests a method to combine the benefits of high spatial resolution of UAV imagery with high spatial coverage of satellite imagery to produce accurate maps on a large scale. The final outcomes include the classified maps for plant communities at two scales i.e., UAV and satellite. For the UAV part, the orthomosaics produced detailed maps with high accuracy. OBIA worked well to classify the plant communities in the study area. For the satellite imagery, the additional UAV obtained samples provided better classification results in comparison to using only field samples, but the results were not as accurate. However, when the classes were generalized to the plant life-form level to make the classified maps comparable to the broader scale of the vegetation report map, the accuracies improved. This study aimed to bring the satellite classification results closer to the field observations with the help of UAVs, which it successfully does. But it was expected for the accuracy to be higher. Nonetheless, this approach with some further refinements can emerge as a promising technique to integrate UAVs with field methods to improve the classification results of the satellite imagery. Therefore, drones do have the potential to bridge the gap between field methods and satellite imagery to map plant communities for conservation. However, field methods still remain an integral part of the whole process, but UAVs can complement them and improve the remote sensing techniques of mapping plant communities.

Answer to Research Questions

Based on the findings of this study, the following conclusion can be drawn for the RQs: -

RQ1.1. What is the accuracy of classifying UAV imagery to map plant communities?

- The accuracy of classifying UAV imagery to map plant communities is 87%, which was achieved by combining the images from the two seasons.
  It holds true with the hypothesis which stated that 'the high-resolution UAV imagery would lead to a precise classification of plant communities and high overall accuracy'.

RQ1.2. What is the effect of different seasons on the classification accuracy?

- The ACoI was affected by the seasons, where the winter orthomosaic produced an accuracy of 84%, which dropped to be 60% for the spring orthomosaic. The same pattern could be observed in the case of the individual accuracies (PA & UA) which were on the higher side for the winter results, while it declined in spring for all the classes.
  The hypothesis holds true which stated that 'the seasons would affect the overall as well as the individual accuracies of plant communities'.

RQ1.3. Does combining images from different seasons improve the classification results?

- Yes, combining the images from the two seasons improves the classification results; it resulted in the highest ACoI and OA out of the three UAV classifications i.e., 87%.

  The hypothesis holds true which stated that 'combining images from different seasons will yield higher classification accuracy than single-season imagery'.

RQ1.4. What is the effect of dominant plant life-forms on the classification accuracy?

- The grasses have consistently higher accuracies; it is not the lowest in any season (including the combined orthomosaic). In winter and spring, the PA for grasses is higher than that of shrubs and trees, while the UA for grasses is higher than that of trees. For the combined orthomosaic, trees have the highest PA and UA, followed by grasses and then shrubs.

  The hypothesis which stated that 'the communities dominated by larger plant species like trees and shrubs will be classified with higher accuracy than those of smaller plants, like dwarf shrubs and grasses' does not hold true in this case.

RQ2.1. How do the additional UAV obtained samples affect the classification results of satellite imagery in comparison to using only field samples?

- The additional UAV obtained samples improved the ACoI for Sentinel-2 by 4% and for SuperView-1 by 3%.

  It holds true with the hypothesis which stated that 'the additional samples obtained from visual interpretation of the UAV imagery will result in higher accuracy than the classification with only field samples'.

RQ2.2. What is the effect of different spatial and spectral resolutions on the satellite image classification results?

- The classification results (in terms of ACoI) with a higher spatial resolution (SuperView-1) are slightly better than those with higher spectral resolution (Sentinel-2). Higher spatial resolution improved the accuracy, especially for grasses. However, confusion could still be seen among the grass communities in the error matrices. Overall, the communities of trees and shrubs are more separable than of grasses with the given satellite imageries.

  The hypothesis which stated that 'spatial resolution would be more important for accurate classification of smaller plant life-forms like grasses, whereas the spectral resolution would be more important for classifying plants with similar phenology and spectral properties' holds true only with respect to the spatial resolution aspect, which played a more important role in classifying grasses. However, the hypothesis about spectral resolution is not true. The study area consists of some plant communities that appear distinct (spectrally different) only for a brief period (winter). Whereas the satellite imagery used for the analysis was a multi-temporal stack with information from other seasons too (spring and summer), and in spring the communities

look more similar. Moreover, the most important layers for classification were from summer and winter, and the least important from spring (according to the variable importance graphs). Therefore, it cannot be assertively concluded if spectral resolution played an important role for these similar-looking communities or was it classified better due to the information from the summer and winter layers, where the communities appeared comparatively distinct.

RQ3.1. What differences can be observed between the classified maps and the existing vegetation survey maps?

- The classified maps are updated and fill in the plant communities (classes) for the missing areas in the vegetation report map. The classified maps were more detailed, and the classes had to be merged to match the broad classes of the vegetation report map, which also led to a significant increase in the accuracy.

  It holds true with the hypothesis that 'Integrating UAVs with field methods will improve the quality of the satellite classification results and the classified maps will have more information than the vegetation survey maps'.

5.2. Recommendations

From the problems encountered during the research and limitations of the methods, the following are some recommendations that can be considered to improve future work: -

- A UAV dataset for two more seasons i.e., summer and autumn could be acquired and added to the analysis. It would be interesting to see how the phenology of plant communities changes in these seasons and its influence on the classification results and accuracy.
- More UAV obtained samples could be collected and used for training the classifier. It could be interesting to systematically add the UAV obtained samples to see up to which point these additional samples are beneficial. One can conclude a threshold or maximum range after which these additional samples do not significantly improve the accuracy. This could help in planning the fieldwork accordingly.
- However, if the area is not large enough to collect more samples (as was the case for the current study), then quick additional flights (long strips transecting different communities, instead of a whole area) could be conducted in a nearby area, with the same plant communities. These additional flights then could be used to collect more samples to classify the satellite imagery. It could further provide widely distributed samples for the satellite imagery and can help to deal with spatial autocorrelation.
- Moreover, other outputs of SfM photogrammetric processing like point clouds or Digital Surface Model (DSM) could also be used. It could provide additional information to understand the plant

communities with respect to variations in the height differences and level of flooding. This could be done if one wants to include the habitat and geographic factors in the analysis.

- For segmentation (OBIA) in eCognition, the ESP tool could be used to automatically calculate the best parameter values and settings.
- Data fusion of the satellites could be explored. Different satellite imageries, in this case, Sentinel-2 and SuperView-1 could be fused to combine the advantages of spectral and spatial resolutions.
- The variable importance graphs (RF) could further be explored to perform 'Feature Selection' where variables or layers that do not contribute much to the classification can be systematically removed and its impact on the accuracy could be observed.
- Lastly, if after all these improvements to the methods, it still does not produce satisfactory results, then a sub-pixel classification approach like fuzzy c-means could be used; it might be more appropriate given the spatial resolution of the satellite imageries and the nature of plant communities.

LIST OF REFERENCES

Adelabu, S., Mutanga, O., & Adam, E. (2015). Testing the reliability and stability of the internal accuracy assessment of random forest for classifying tree defoliation levels using different validation methods. *Geocarto International*, *30*(7), 810–821. https://doi.org/10.1080/10106049.2014.997303

Alsadik, B. & Nex, F. (2020). Structure from Motion SfM [PowerPoint slides]. Retrieved from https://canvas.utwente.nl/courses/6078/files/1827889?module_item_id=177434

Assmann, J. J., Kerby, J. T., Cunliffe, A. M., & Myers-Smith, I. H. (2019). Vegetation monitoring using multispectral sensors — best practices and lessons learned from high latitudes. *Journal of Unmanned Vehicle Systems*, *7*(1), 54–75. https://doi.org/10.1139/juvs-2018-0018

Baena, S., Moat, J., Whaley, O., & Boyd, D. S. (2017). Identifying species from the air: UAVs and the very high resolution challenge for plant conservation. *PLOS One*, *12*(11), 1–21. https://doi.org/10.1371/journal.pone.0188714

Beijing Space View Technology Co. Ltd., China. (2020). SuperView-1 Data [TIFF]. Retrieved from https://www.satellietdataportaal.nl/

Belgiu, M., & Drăgu, L. (2016). Random forest in remote sensing: A review of applications and future directions. *ISPRS Journal of Photogrammetry and Remote Sensing*, *114*, 24–31. https://doi.org/10.1016/j.isprsjprs.2016.01.011

Belgiu, M. (2020). Image Analysis: Object-Based Classification [PowerPoint slides]. Retrieved from https://canvas.utwente.nl/courses/5199/files/1610032?module_item_id=160044

Blaschke, T., Lang, S., Lorup, E., Strobl, J., & Zeil, P. (2000). Object-oriented image processing in an integrated GIS/remote sensing environment and perspectives for environmental applications. *Environmental Information for Planning, Politics and the Public*, *2*, 555-570. Retrieved from https://www.researchgate.net/publication/250030480_Object-Oriented_Image_Processing_in_an_Integrated_GISRemote_Sensing_Environment_and_Perspectives_for_Environmental_Applications

Blaschke, T., & Strobl, J. (2001). What's wrong with pixels? Some recent developments interfacing remote sensing and GIS. *Geo-Informations-Systeme*, *14*(6), 12–17. Retrieved from https://www.researchgate.net/publication/216266284_What's_wrong_with_pixels_Some_recent_developments_interfacing_remote_sensing_and_GIS

Brownlee, J. (2020). Train-Test Split for Evaluating Machine Learning Algorithms. Retrieved from https://machinelearningmastery.com/train-test-split-for-evaluating-machine-learning-algorithms/

Copernicus Sentinel Data, European Space Agency. (2020). Sentinel-2 Data [TIFF]. Retrieved from https://scihub.copernicus.eu/dhus/#/home

Corlett, R. T. (2016). Plant diversity in a changing world: Status, trends, and conservation needs. *Plant Diversity*, *38*(1), 10–16. https://doi.org/10.1016/j.pld.2016.01.001

Duffy, J. P., Cunliffe, A. M., DeBell, L., Sandbrook, C., Wich, S. A., Shutler, J. D., Myers-Smith, I. H., Varela, M. R. & Anderson, K. (2018). Location, location, location: considerations when using lightweight drones in challenging environments. *Remote Sensing in Ecology and Conservation*, *4*(1), 7–19. https://doi.org/10.1002/rse2.58

Earth Observing System. (n.d.a). Sentinel-2: Satellite Imagery, Overview, And Characteristics. Retrieved from https://eos.com/find-satellite/sentinel-2/

Earth Observing System. (n.d.b). SuperView-1: Satellite Imagery, Overview, And Characteristics. Retrieved from https://eos.com/find-satellite/superview-1/

Ecologengroep Groningen/EGG consult. (2017). Vegetatie- en Plantensoortkartering, Drentsche Aa 2015-2016 (1164 EGG). Groningen: Staatsbosbeheer.

Einar, G., & Rietz, D. (1931). A Revision of the Classification of Life-forms – The Main Life-form System. In V. Svenska & E. Sallskapet (Eds.), Life-forms of Terrestrial Flowering Plants (pp. 42-83). Retrieved from https://www.diva-portal.org/smash/get/diva2:565457/FULLTEXT01

Fischer, H. S., Michler, B., Ziche, D., & Fischer, A. (2019). Plants as Indicators of Soil Chemical Properties. In N. Wellbrock & A. Bolte (Eds.), *Status and Dynamics of Forests in Germany* (pp. 295-309). https://doi.org/10.1007/978-3-030-15734-0_10

Flora of the Netherlands. (n.d.a). Annual Grass – Poa annua. Retrieved from https://www.floravannederland.nl/planten/straatgras

Flora of the Netherlands. (n.d.b). Reed Grass - Phalaris arundinacea. Retrieved from https://www.floravannederland.nl/planten/rietgras

Flora of the Netherlands. (n.d.c). Pitrus - Juncus effusus. Retrieved from https://www.floravannederland.nl/planten/pitrus

Flora of the Netherlands. (n.d.d). Reed – Phragmites australis. Retrieved from https://www.floravannederland.nl/planten/riet

Flora of the Netherlands. (n.d.e). Black alder - Alnus glutinosa. Retrieved from https://www.floravannederland.nl/planten/zwarte_els

Flora of the Netherlands. (n.d.f). Stripped white bulb – Holcus lanatus. Retrieved from https://www.floravannederland.nl/planten/gestreepte_witbol

Flora of the Netherlands. (n.d.g). Swamp clover – Lotus pedunculatus. Retrieved from https://www.floravannederland.nl/planten/moerasrolklaver

Flora of the Netherlands. (n.d.h). Hollow pipe - Equisetum fluviatile. Retrieved from https://www.floravannederland.nl/planten/holpijp

Gislason, P. O., Benediktsson, J. A., & Sveinsson, J. R. (2006). Random forests for land cover classification. *Pattern Recognition Letters*, *27*(4), 294–300. https://doi.org/10.1016/j.patrec.2005.08.011

Gray, P. C., Ridge, J. T., Poulin, S. K., Seymour, A. C., Schwantes, A. M., Swenson, J. J., & Johnston, D. W. (2018). Integrating drone imagery into high resolution satellite remote sensing assessments of estuarine environments. *Remote Sensing*, *10*(8), 1-23. https://doi.org/10.3390/rs10081257

Hegarty-Craver, M., Polly, J., O'Neil, M., Ujeneza, N., Rineer, J., Beach, R. H., Lapidus, D. & Temple, D. S. (2020). Remote crop mapping at scale: Using satellite imagery and UAV-acquired data as ground truth. *Remote Sensing*, *12*(12), 1–15. https://doi.org/10.3390/rs12121984

Jiménez López, J., & Mulero-Pázmány, M. (2019). Drones for Conservation in Protected Areas: Present and Future. *Drones*, *3*(1), 10-23. https://doi.org/10.3390/drones3010010

Kaneko, K., & Nohara, S. (2014). Review of Effective Vegetation Mapping Using the UAV (Unmanned Aerial Vehicle) Method. *Journal of Geographic Information System*, *6*(6), 733–742. https://doi.org/10.4236/jgis.2014.66060

Kattenborn, T., Lopatin, J., Förster, M., Braun, A. C., & Fassnacht, F. E. (2019). UAV data as alternative to field sampling to map woody invasive species based on combined Sentinel-1 and Sentinel-2 data. *Remote Sensing of Environment*, *227*, 61–73. https://doi.org/10.1016/j.rse.2019.03.025

Kent, M. (2012). *Vegetation Description and Data Analysis: A Practical Approach* (2nd ed.). West Sussex, UK: Wiley-Blackwell.

Koh, L. P., & Wich, S. A. (2012). Dawn of drone ecology: Low-cost autonomous aerial vehicles for conservation. *Tropical Conservation Science*, *5*(2), 121–132. https://doi.org/10.1177/194008291200500202

Lechner, A. M., Fletcher, A., Johansen, K., & Erskine, P. (2012). Characterising Upland Swamps Using Object-Based Classification Methods and Hyper-Spatial Resolution Imagery Derived from an Unmanned Aerial Vehicle. *ISPRS Annals of the Photogrammetry, Remote Sensing and Spatial Information Sciences*, *1*(4), 101–106. https://doi.org/10.5194/isprsannals-I-4-101-2012

Lizzie Harper. (2018). Sedges: An introduction . Retrieved from https://lizzieharper.co.uk/2018/07/sedges-an-introduction/

Lopatin, J., Dolos, K., Kattenborn, T., & Fassnacht, F. E. (2019). How canopy shadow affects invasive plant species classification in high spatial resolution remote sensing. *Remote Sensing in Ecology and Conservation*, *5*(4), 302–317. https://doi.org/10.1002/rse2.109

Lu, B., & He, Y. (2017). Species classification using Unmanned Aerial Vehicle (UAV)-acquired high spatial resolution imagery in a heterogeneous grassland. *ISPRS Journal of Photogrammetry and Remote Sensing*, *128*, 73–85. https://doi.org/10.1016/j.isprsjprs.2017.03.011

Makinde, E. O., Salami, A. T., Olaleye, J. B., & Okewusi, O. C. (2016). Object Based and Pixel Based Classification Using Rapideye Satellite Imager of ETI-OSA, Lagos, Nigeria. *Geoinformatics FCE CTU*, *15*(2), 59–70. https://doi.org/10.14311/gi.15.2.5

Manfreda, S., McCabe, M., Miller, P., Lucas, R., Madrigal, V. P., Mallinis, G., Dor, E. B., Helman, D., Estes, L., Ciraolo, G., Müllerová, J., Tauro, F., De Lima, M. I., De Lima, J. L. M. P., Frances. F., Caylor, Kohv, M., Maltese, A., Perks, M., Ruiz-Pérez, G., Su, Z., Vico, G., & Toth, B. (2018). On the Use of Unmanned Aerial Systems for Environmental Monitoring. *Remote sensing*, *10*(4), 1–20. https://doi.org/10.20944/preprints201803.0097.v1

Martinez-Taboada, F., & Redondo, J. I. (2020). Variable importance plot (mean decrease accuracy and mean decrease Gini). Retrieved from https://doi.org/10.1371/journal.pone.0230799.g002

McFeeters, S. K. (1996). The use of the Normalized Difference Water Index (NDWI) in the delineation of open water features. *International Journal of Remote Sensing*, *17*(7), 1425–1432. https://doi.org/10.1080/01431169608948714

National Park Drentsche Aa. (n.d.a). Home - Drentsche Aa. Retrieved from https://www.drentscheaa.nl/

National Park Drentsche Aa. (n.d.b). Bio plan Drentsche Aa. Retrieved from https://www.drentscheaa.nl/organisatie-beleid/bio-plan-drentsche/

Netherlands Space Office. (n.d.). Satellite data portal – Disclaimer. Retrieved from https://www.spaceoffice.nl/nl/satellietdataportaal/disclaimer/

New World Encyclopedia. (n.d.). Willow. Retrieved from https://www.newworldencyclopedia.org/entry/willow

NL Times. (2020). Wettest February ever, and nearly the warmest on record. Retrieved from https://nltimes.nl/2020/02/27/wettest-february-ever-nearly-warmest-record

NL Times. (2021). Coldest April in 30 years not all bad, says biologist. Retrieved from https://nltimes.nl/2021/04/23/coldest-april-30-years-bad-says-biologist

Parrot Sequoia. (n.d.). Parrot Sequoia – Capture the Invisible. Retrieved from https://www.parrot.com/files/s3fs-public/sequoia_official_documentation_and_specifications_2016_0.pdf

Pesaresi, S., Mancini, A., & Casavecchia, S. (2020). Recognition and Characterization of Forest Plant Communities through Remote-Sensing NDVI Time Series. *Diversity*, *12*(8), 1-19. https://doi.org/10.3390/D12080313

Pix4D. (n.d.). Merging multispectral projects in Pix4Dmapper – Support. Retrieved from https://support.pix4d.com/hc/en-us/articles/360038663932-Merging-multispectral-projects-in-Pix4Dmapper

Pix4D Community (n.d.). Blue and green dots are not together after processing. Retrieved from https://community.pix4d.com/t/blue-and-green-dots-are-not-together-after-processing/6449

Rapinel, S., Mony, C., Lecoq, L., Clément, B., Thomas, A., & Hubert-Moy, L. (2019). Evaluation of Sentinel-2 time-series for mapping floodplain grassland plant communities. *Remote Sensing of Environment*, *223*, 115–129. https://doi.org/10.1016/j.rse.2019.01.018

Rapinel, S., Rozo, C., Delbosc, P., Bioret, F., Bouzillé, J. B., & Hubert-Moy, L. (2020). Contribution of free satellite time-series images to mapping plant communities in the Mediterranean Natura 2000 site: The example of Biguglia Pond in Corse (France). *Mediterranean Botany*, *41*(2), 181–191. https://doi.org/10.5209/MBOT.66535

Reinke, K., & Jones, S. (2006). Integrating vegetation field surveys with remotely sensed data. *Ecological Management and Restoration*, *7*(s1), S18–S23. https://doi.org/10.1111/j.1442-8903.2006.00287.x

Rocchini, D., Balkenhol, N., Carter, G. A., Foody, G. M., Gillespie, T. W., He, K. S., Kark, S., Levin, N., Lucas, K., Luoto, M., Magendra, H., Oldeland, J., Ricotta, C., Southworth, J., & Neteler, M. (2010). Remotely sensed spectral heterogeneity as a proxy of species diversity: Recent advances and open challenges. *Ecological Informatics*, *5*(5), 318–329. https://doi.org/10.1016/j.ecoinf.2010.06.001

Rocchini, D., Foody, G. M., Nagendra, H., Ricotta, C., Anand, M., He, K. S., Amici, V., Kleinschmit, B., Förster, M., Schmidtlein, S., Feilhauer, H., Ghisla, A., Metz, M., & Neteler, M. (2013, January). Uncertainty in ecosystem mapping by remote sensing. *Computers and Geosciences*, *50*, 128–135. https://doi.org/10.1016/j.cageo.2012.05.022

Rocchini, D., Boyd, D. S., Féret, J. B., Foody, G. M., He, K. S., Lausch, A., Nagendra, H., Wegmann, M., & Pettorelli, N. (2016). Satellite remote sensing to monitor species diversity: potential and pitfalls. *Remote Sensing in Ecology and Conservation*, *2*(1), 25–36. https://doi.org/10.1002/rse2.9

Román-Palacios, C., & Wiens, J. J. (2020). Recent responses to climate change reveal the drivers of species extinction and survival. *Proceedings of the National Academy of Sciences of the United States of America*, 117(8), 4211–4217. https://doi.org/10.1073/pnas.1913007117

Rominger, K., & Meyer, S. E. (2019). Application of UAV-Based methodology for census of an endangered plant species in a fragile habitat. *Remote Sensing*, *11*(6), 1–16. https://doi.org/10.3390/rs11060719

Sabat-Tomala, A., Raczko, E., & Zagajewski, B. (2020). Comparison of Support Vector Machine and Random Forest Algorithms for Invasive and Expansive Species Classification Using Airborne Hyperspectral Data. *Remote Sensing*, *12*(3), 1-21. https://doi.org/10.3390/rs12030516

Shang, M., Wang, S. X., Zhou, Y., & Du, C. (2018). Effects of Training Samples and Classifiers on Classification of Landsat-8 Imagery. *Journal of the Indian Society of Remote Sensing*, *46*(9), 1333–1340. https://doi.org/10.1007/s12524-018-0777-z

Sibaruddin, H. I., Shafri, H. Z. M., Pradhan, B., & Haron, N. A. (2018, April 24-25). *Comparison of pixel-based and object-based image classification techniques in extracting information from UAV imagery data.* IOP Conference Series-Earth and Environmental Science: 9th IGRSM International Conference and Exhibition on Geospatial & Remote Sensing, Malaysia. https://doi.org/10.1088/1755-1315/169/1/012098

Strong, C. J., Burnside, N. G., & Llewellyn, D. (2017). The potential of small-Unmanned Aircraft Systems for the rapid detection of threatened unimproved grassland communities using an Enhanced Normalized Difference Vegetation Index. *PLOS One*, *12*(10), 1–16. https://doi.org/10.1371/journal.pone.0186193

Tay, J. Y. L., Erfmeier, A., & Kalwij, J. M. (2018). Reaching new heights: can drones replace current methods to study plant population dynamics? *Plant Ecology*, *219*(10), 1139–1150. https://doi.org/10.1007/s11258-018-0865-8

Tucker, C. J., & Sellers, P. J. (1986). Satellite remote sensing of primary production. *International Journal of Remote Sensing*, *7*(11), 1395–1416. https://doi.org/10.1080/01431168608948944

Tucker, Compton J. (1979). Red and photographic infrared linear combinations for monitoring vegetation. *Remote Sensing of Environment*, *8*(2), 127–150. https://doi.org/10.1016/0034-4257(79)90013-0

Ventura, D., Bonifazi, A., Gravina, M. F., Belluscio, A., & Ardizzone, G. (2018). Mapping and classification of ecologically sensitive marine habitats using unmanned aerial vehicle (UAV) imagery and Object-Based Image Analysis (OBIA). *Remote Sensing*, *10*(9), 1–23. https://doi.org/10.3390/rs10091331

Villoslada, M., Bergamo, T. F., Ward, R. D., Burnside, N. G., Joyce, C. B., Bunce, R. G. H., & Sepp, K. (2020). Fine scale plant community assessment in coastal meadows using UAV based multispectral data. *Ecological Indicators*, *111*, 1-13. https://doi.org/10.1016/j.ecolind.2019.105979

Wulfsohn D. (2010). Sampling Techniques for Plants and Soil. In D. Downey, R. Ehsani, K. Giles, S. Haneklaus, D. Karimi, K. Panten, F. Pierce, E. Schnug, D. Slaughter, S. Upadhyaya & D. Wulfsohn (Eds.), *Advanced Engineering Systems for Specialty Crops: A Review of Precision Agriculture for Water, Chemical, and Nutrient Application, and Yield Monitoring* (pp. 3-30). Retrieved from https://www.researchgate.net/publication/230667530

Zhang, C., Atkinson, P. M., George, C., Wen, Z., Diazgranados, M., & Gerard, F. (2020). Identifying and mapping individual plants in a highly diverse high-elevation ecosystem using UAV imagery and deep learning. *ISPRS Journal of Photogrammetry and Remote Sensing*, *169*, 280–291. https://doi.org/10.1016/j.isprsjprs.2020.09.025

Zweig, C. L., Burgess, M. A., Percival, H. F., & Kitchens, W. M. (2015). Use of Unmanned Aircraft Systems to Delineate Fine-Scale Wetland Vegetation Communities. *Wetlands*, *35*(2), 303–309. https://doi.org/10.1007/s13157-014-0612-4

APPENDICES

Appendix I

FIELD SURVEY FORM
PLANT COMMUNITIES IN DRENTSCHE AA, THE NETHERLANDS

Date:	Time:	Weather:

Relative location:
GPS/Coordinates:

1.	Name of the Indicative or Dominant Species	Scientific	
		English	
		Dutch	
2.	Vegetation Code		
3.	Habitat Code		
4.	Landform		
5.	Soil Type		
6.	Level of flooding		
7.	Total no. of Observations		

Plant Description		Site Description	
Winter	Spring	Winter	Spring
-	-	-	-
-	-	-	-
-	-	-	-
-	-	-	-
-	-	-	-
-	-	-	-

Additional Remarks: _____

_____

_____

Appendix II

i. Change in the default settings in Pix4D during the first step i.e., Initial Processing

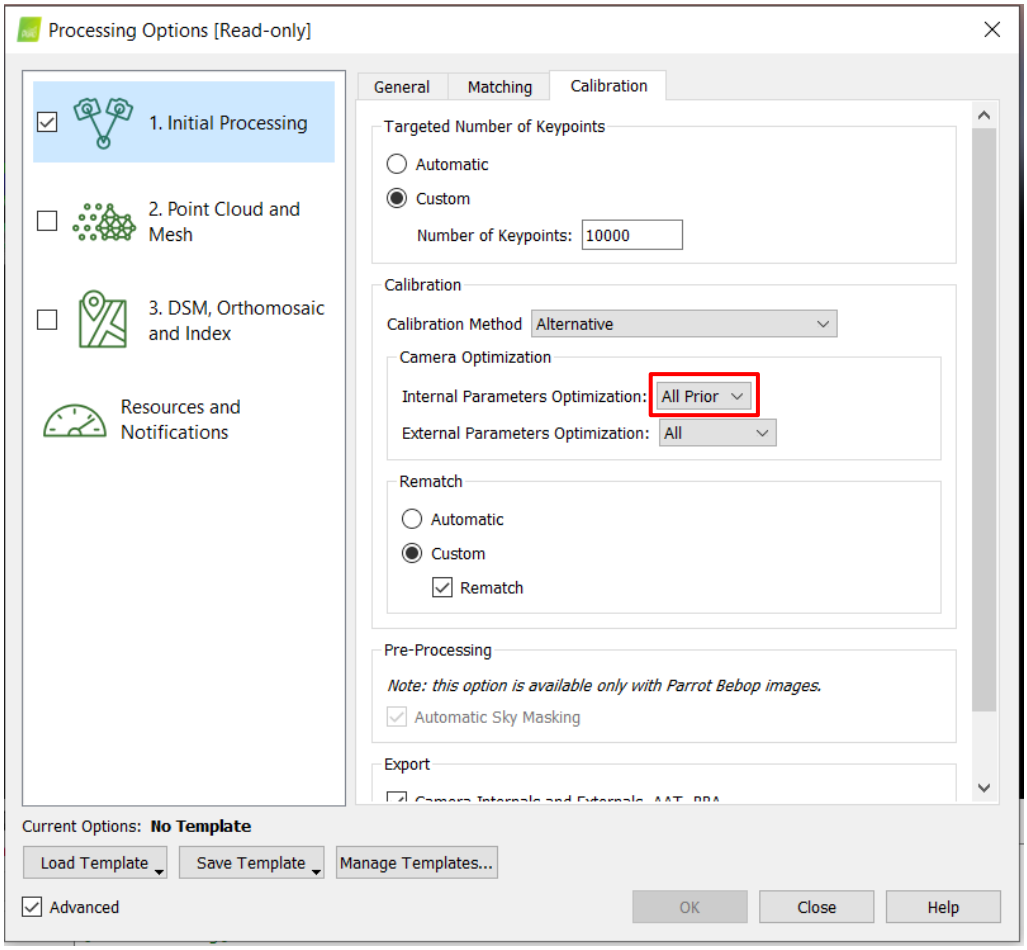

Appendix III

i. Weights assigned to different layers for segmentation in eCognition

Segmentation Settings	
Image Layer weights	2, 1, 2, 0.5, 0.5, 0.5, 3, 3, 3, 2, 2
EVI	2
Green	1
GRVI	2
Layer 5	0.5
Layer 6	0.5
Layer 7	0.5
NDVI	3
NDWI	3
NIR	3
Red	2
RedEdge	2

*Layers 5, 6 & 7 are RGB layers respectively

Appendix IV

i. Overlap of the RGB images for winter (left) and spring (right)

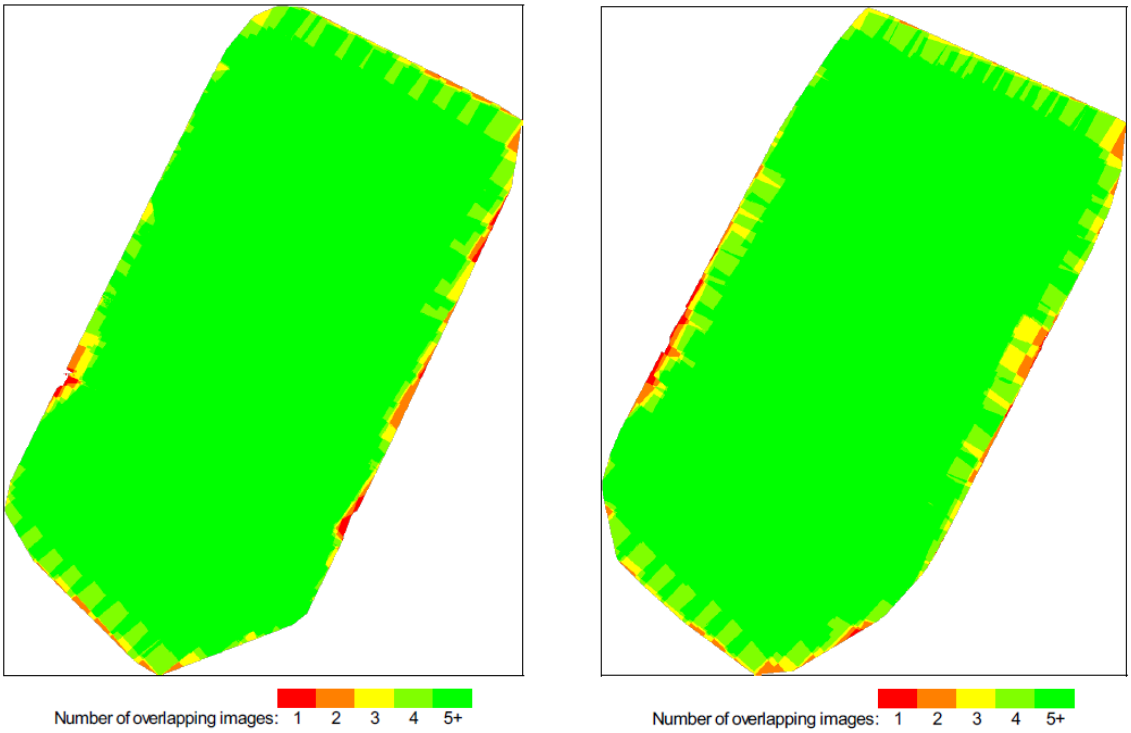

ii. Overlap of the MS images for winter (left) and spring (right)

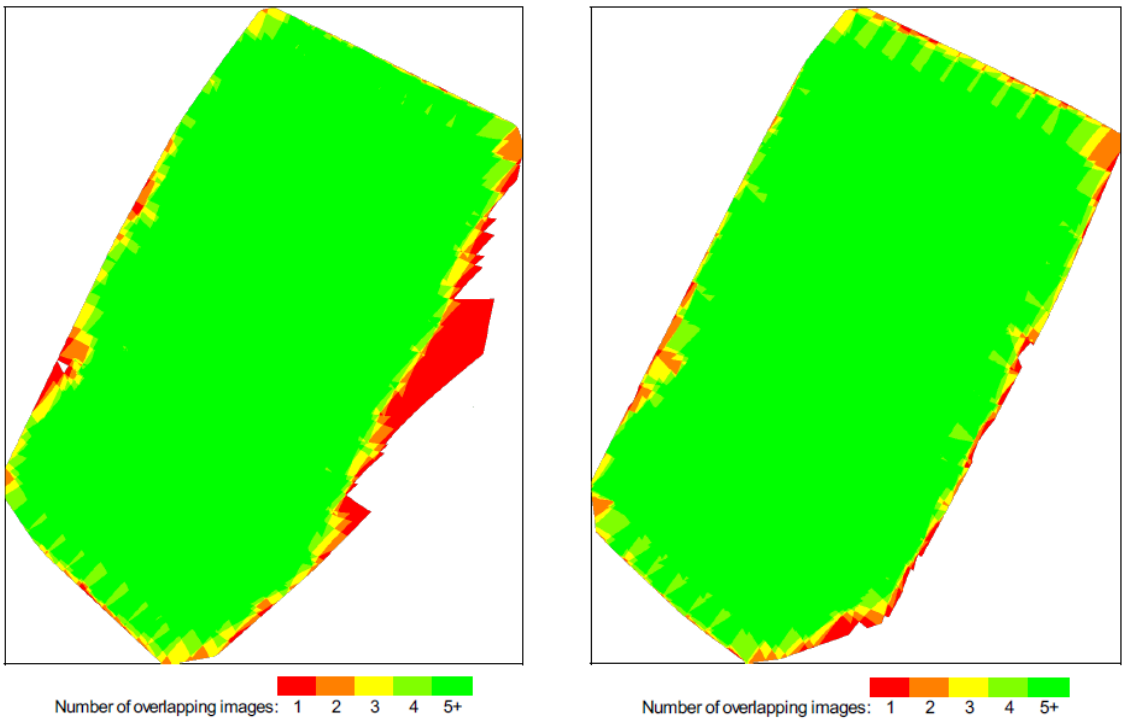

*Green areas indicate a good overlap i.e., over 4 images for every pixel, whereas red, orange and yellow areas indicate low overlap i.e., less than 3 images.

Appendix V

i. Error matrix for the classification results of the winter orthomosaic

User Class/Samples	*Poa an.*	*Phal. au.*	*Juncus e.*	*Phra. as.*	*Carex* s.	*Salix* s.	*Alnus g.*	River	Road	Flooded	Sum
Poa annua	11	1	0	0	0	0	0	0	0	0	12
Phalaris arundinacea	0	10	0	3	0	0	1	0	0	0	14
Juncus effusus	1	1	12	0	0	0	0	0	0	0	14
Phragmites australis	0	0	0	7	0	0	0	0	0	0	7
Carex spp.	0	0	0	0	1	0	0	0	0	0	1
Salix spp.	0	0	0	0	0	4	1	0	0	1	6
Alnus glutinosa	0	1	1	0	0	0	9	0	0	0	11
River	0	0	0	0	0	0	0	4	0	1	5
Road	0	0	0	0	0	0	0	1	4	0	5
Flooded area	0	0	0	0	0	0	0	1	0	3	4
Sum	12	13	13	10	1	4	11	6	4	5	79
Overall Accuracy	82.27%										
Kappa	79.70%										
Producer's Accuracy	91.60%	76.90%	92.30%	70%	100%	100%	81.80%	66.60%	100%	60%	
User's Accuracy	91.60%	71.40%	85.70%	100%	100%	66.60%	81.80%	80%	80%	75%	

ii. Error matrix for the classification results of the spring orthomosaic

User Class/Samples	*Poa an.*	*Phal. au.*	*Juncus e.*	*Phra. as.*	*Carex* s.	*Salix* s.	*Alnus g.*	River	Road	Iron Wt.	Sum
Poa annua	5	2	0	1	0	0	1	0	0	0	9
Phalaris arundinacea	5	8	1	2	0	1	1	0	0	0	18
Juncus effusus	0	1	8	0	0	3	0	0	0	0	12
Phragmites australis	0	1	0	6	1	0	0	0	0	0	8
Carex spp.	0	0	0	1	3	0	0	0	0	2	6
Salix spp.	0	0	3	0	0	3	0	0	0	0	6
Alnus glutinosa	2	1	1	0	0	0	9	0	0	0	13
River	0	0	0	0	0	0	0	6	0	0	6
Road	0	0	0	0	0	0	0	0	6	0	6
Iron-rich Water	0	0	0	0	0	0	0	0	0	1	1
Sum	12	13	13	10	4	7	11	6	6	3	85
Overall Accuracy	64.70%										
Kappa	59.92%										
Producer's Accuracy	41.66%	61.53%	61.53%	60%	75%	42.85%	81.81%	100%	100%	33.33%	
User's Accuracy	55.55%	44.44%	66.66%	75%	50%	50%	69.23%	100%	100%	100%	

iii. Error matrix for the classification results of the combined orthomosaic

User Class/Samples	*Poa an.*	*Phal. au.*	*Juncus e.*	*Phra. as.*	*Carex* s.	*Salix* s.	*Alnus g.*	River	Road	Period F.	Permt. F.	Sum
Poa annua	11	0	0	0	0	0	0	0	0	0	0	11
Phalaris arundinacea	1	10	0	3	0	0	0	0	0	0	0	14
Juncus effusus	0	2	11	0	0	0	0	0	0	0	0	13
Phragmites australis	0	0	0	7	0	0	0	0	0	0	0	7
Carex spp.	0	0	0	0	4	0	1	0	0	0	1	6
Salix spp.	0	0	0	0	0	7	1	0	0	1	0	9
Alnus glutinosa	0	0	1	0	0	0	10	0	0	0	0	11
River	0	0	0	0	0	0	0	6	0	0	0	6
Road	0	0	0	0	0	0	0	0	6	0	0	6
Periodically Flooded	0	0	0	0	0	0	0	0	0	4	0	4
Permanently Flooded	0	1	0	0	0	0	0	0	0	0	2	3
Sum	12	13	12	10	4	7	12	6	6	5	3	90
Overall Accuracy	86.66%											
Kappa	85.08%											
Producer's Accuracy	91.60%	76.90%	91.60%	70%	100%	100%	83.30%	100%	100%	80%	66.60%	
User's Accuracy	100%	71.40%	84.60%	100%	66.60%	77.70%	90.90%	100%	100%	100%	66.60%	

Appendix VI

i. Error matrix for the classification results of Sentinel-2 with only field samples

User Class/Samples	*Poa an.*	*Phal. au.*	*Juncus e.*	*Phra. as.*	*Carex* s.	*Salix* s.	*Alnus g.*	River	Road	Period. F.	Permt. F.	Sum
Poa annua	4	3	0	0	0	0	7	0	4	3	1	22
Phalaris arundinacea	2	3	2	0	0	1	0	0	0	0	0	8
Juncus effusus	3	4	10	0	0	0	0	0	0	0	0	17
Phragmites australis	1	0	0	10	0	2	0	1	2	0	0	16
Carex spp.	0	0	0	0	4	0	0	1	0	2	1	8
Salix spp.	0	0	0	0	0	4	0	0	0	0	0	4
Alnus glutinosa	0	2	0	0	0	0	5	0	0	0	0	7
River	2	1	1	0	0	0	0	4	0	0	0	8
Road	0	0	0	0	0	0	0	0	0	0	0	0
Periodically Flooded	0	0	0	0	0	0	0	0	0	0	1	1
Permanently Flooded	0	0	0	0	0	0	0	0	0	0	0	0
Sum	12	13	13	10	4	7	12	6	6	5	3	91
Overall Accuracy	48.35%											
Kappa	41.69%											
Producer's Accuracy	33.33%	23.07%	76.92%	100%	100%	57.14%	41.66%	66.66%	0%	0%	0%	
User's Accuracy	18.18%	37.50%	58.82%	62.50%	50%	100%	71.42%	50%	0%	0%	0%	

ii. Error matrix for the classification results of Sentinel-2 with additional UAV obtained samples

User Class/Samples	*Poa an.*	*Phal. au.*	*Juncus e.*	*Phra. as.*	*Carex* s.	*Salix* s.	*Alnus g.*	River	Road	Period. F.	Permt. F.	Sum
Poa annua	5	5	1	0	0	0	1	0	0	0	0	12
Phalaris arundinacea	1	3	3	0	0	1	0	1	0	0	0	9
Juncus effusus	2	5	9	0	3	0	0	0	0	0	0	19
Phragmites australis	0	0	0	6	0	0	0	1	1	0	0	8
Carex spp.	0	0	0	0	1	0	0	0	0	0	0	1
Salix spp.	0	0	0	0	0	4	0	0	0	0	0	4
Alnus glutinosa	0	0	0	0	0	0	11	0	0	0	0	11
River	0	0	0	0	0	0	0	4	0	0	0	4
Road	4	0	0	0	0	2	0	0	5	3	1	15
Periodically Flooded	0	0	0	4	0	0	0	0	0	2	2	8
Permanently Flooded	0	0	0	0	0	0	0	0	0	0	0	0
Sum	12	13	13	10	4	7	12	6	6	5	3	91
Overall Accuracy	54.95%											
Kappa	49.41%											
Producer's Accuracy	41.66%	23.07%	69.23%	60%	25%	57.14%	91.66%	67%	83.33%	40%	0%	
User's Accuracy	41.66%	33%	47%	75%	100%	100%	100%	100%	33%	25%	0%	

iii. Error matrix for the classification results of SuperView-1 with only field samples

User Class/Samples	*Poa an.*	*Phal. au.*	*Juncus e.*	*Phra. as.*	*Carex* s.	*Salix* s.	*Alnus g.*	River	Road	Period. F.	Permt. F.	Sum
Poa annua	8	3	1	0	0	0	0	0	0	1	1	14
Phalaris arundinacea	2	3	3	0	0	0	0	0	0	0	0	8
Juncus effusus	0	7	9	0	1	1	1	0	0	1	0	20
Phragmites australis	1	0	0	7	0	0	0	0	0	0	0	8
Carex spp.	0	0	0	1	3	0	0	0	0	0	0	4
Salix spp.	0	0	0	1	0	5	1	0	0	1	0	8
Alnus glutinosa	1	0	0	0	0	1	10	0	0	0	0	12
River	0	0	0	0	0	0	0	6	0	1	0	7
Road	0	0	0	0	0	0	0	0	6	0	0	6
Periodically Flooded	0	0	0	1	0	0	0	0	0	1	2	4
Permanently Flooded	0	0	0	0	0	0	0	0	0	0	0	0
Sum	12	13	13	10	4	7	12	6	6	5	3	91
Overall Accuracy	63.74%											
Kappa	59.17%											
Producer's Accuracy	66.66%	23.07%	69.23%	70%	75%	71.42%	83.33%	100%	100%	20%	0%	
User's Accuracy	57.14%	37.50%	45%	87.5%	75%	62.50%	83.33%	85.71%	100%	25%	0%	

iv. Error matrix for the classification results of SuperView-1 with additional UAV obtained samples

User Class/Samples	*Poa an.*	*Phal. au.*	*Juncus e.*	*Phra. as.*	*Carex* s.	*Salix* s.	*Alnus g.*	River	Road	Period. F.	Permt. F.	Sum
Poa annua	11	2	0	0	0	0	0	0	0	1	1	15
Phalaris arundinacea	1	6	4	0	0	0	0	0	0	1	0	12
Juncus effusus	0	5	9	0	1	1	1	0	0	1	0	18
Phragmites australis	0	0	0	4	0	0	0	0	0	0	0	4
Carex spp.	0	0	0	4	2	0	0	0	0	0	0	6
Salix spp.	0	0	0	1	0	3	0	0	0	0	0	4
Alnus glutinosa	0	0	0	0	1	2	11	0	0	0	0	14
River	0	0	0	0	0	0	0	6	0	0	0	6
Road	0	0	0	0	0	0	0	0	6	0	0	6
Periodically Flooded	0	0	0	1	0	1	0	0	0	2	2	6
Permanently Flooded	0	0	0	0	0	0	0	0	0	0	0	0
Sum	12	13	13	10	4	7	12	6	6	5	3	91
Overall Accuracy	65.93%											
Kappa	61.61%											
Producer's Accuracy	91.66%	46.15%	69.23%	40%	50%	42.85%	91.66%	100%	100%	40%	0%	
User's Accuracy	73.33%	50%	50%	100%	33.33%	75.00%	78.57%	100%	100%	33.33%	0%	

Appendix VII

i. Error matrix for the classification results of the additional analysis of Sentinel-2 with only field samples

User Class/Samples	*Poa an.*	*Phal. au.*	*Juncus e.*	*Phra. as.*	*Carex* s.	*Salix* s.	*Alnus g.*	River	Road	Period. F.	Permt. F.	Sum
Poa annua	4	3	0	0	0	0	7	0	3	3	1	21
Phalaris arundinacea	2	3	2	0	0	0	0	0	0	0	0	7
Juncus effusus	3	4	10	0	0	0	0	0	0	0	0	17
Phragmites australis	1	0	0	6	0	0	0	0	2	0	0	9
Carex spp.	0	0	0	0	4	0	0	0	0	1	1	6
Salix spp.	0	0	0	0	0	5	0	1	0	0	0	6
Alnus glutinosa	0	2	0	0	0	0	5	0	0	0	0	7
River	2	1	1	0	0	0	0	5	0	0	0	9
Road	0	0	0	0	0	2	0	0	1	0	0	3
Periodically Flooded	0	0	0	4	0	0	0	0	0	1	1	6
Permanently Flooded	0	0	0	0	0	0	0	0	0	0	0	0
Sum	12	13	13	10	4	7	12	6	6	5	3	91
Overall Accuracy	48.35%											
Kappa	42.01%											
Producer's Accuracy	33.3%	23%	76.92%	60%	100%	71.42%	41.66%	83.33%	16.66%	20%	0%	
User's Accuracy	19%	42.85%	58.88%	66.66%	66.66%	83.33%	71.42%	55.55%	33.33%	16.66%	0%	

ii. Error matrix for the classification results of the additional analysis of Sentinel-2 with additional UAV obtained samples

User Class/Samples	*Poa an.*	*Phal. au.*	*Juncus e.*	*Phra. as.*	*Carex* s.	*Salix* s.	*Alnus g.*	River	Road	Period. F.	Permt. F.	Sum
Poa annua	5	5	1	0	0	0	1	0	0	0	0	12
Phalaris arundinacea	1	3	3	0	0	0	0	1	0	0	0	8
Juncus effusus	2	5	9	0	0	0	0	0	0	0	0	16
Phragmites australis	0	0	0	6	0	0	0	0	1	0	0	7
Carex spp.	0	0	0	0	4	0	0	0	0	1	0	5
Salix spp.	0	0	0	0	0	5	0	0	0	0	0	5
Alnus glutinosa	0	0	0	0	0	0	11	0	0	0	0	11
River	0	0	0	0	0	0	0	5	0	0	0	5
Road	4	0	0	0	0	2	0	0	5	3	1	15
Periodically Flooded	0	0	0	4	0	0	0	0	0	1	2	7
Permanently Flooded	0	0	0	0	0	0	0	0	0	0	0	0
Sum	12	13	13	10	4	7	12	6	6	5	3	91
Overall Accuracy	59.34%											
Kappa	54.58%											
Producer's Accuracy	41.66%	23%	69.23%	60%	100%	71.42%	91.66%	83.33%	83.33%	20%	0%	
User's Accuracy	41.66%	37.50%	56.25%	85.70%	80%	100%	100%	100%	33.33%	14.28%	0%	

Appendix VIII

i. A summary of the results from all three UAV classifications, along with merged PA and UA for each plant-life form

Seasons	Winter				Spring				Combined			
Classification classes	PA	Merg.	UA	Merg.	PA	Merg.	UA	Merg.	PA	Merg.	UA	Merg.
Poa annua	92%		92%		42%		56%		92%		100%	
Phalaris arundinacea	77%	95%	71%	90%	62%	79%	45%	77%	77%	92%	71%	89%
Juncus effusus	92%		86%		62%		67%		92%		85%	
Phragmites australis	70%	73%	100%	100%	60%	79%	75%	79%	70%	79%	100%	85%
Carex spp.	100%		100%		75%		50%		100%		67%	
Salix spp.	100%	93%	67%	82%	43%	67%	50%	63%	100%	95%	78%	90%
Alnus glutinosa	82%		82%		82%		69%		83%		91%	
Others	93%		100%		87%		100%		90%		95%	
Classes of interest	84%				60%				87%			
Overall Accuracy	86%				65%				87%			

* The shades of green from light to dark indicate grass, shrub and tree life forms respectively